The use of translational profiling for gaining a deeper molecular understanding of memory storage in the brain

A thesis

submitted by

Laurel Drane Conley

In partial fulfillment of the requirements
for the degree of

Doctor of Philosophy

In

Neuroscience

TUFTS UNIVERSITY

Sackler School of Graduate Biomedical Sciences

Date

April, 2016

Advisor: Leon Reijmers, Ph.D.

Abstract

Protein translation is essential to synaptic plasticity and memory storage. Specifically, local protein translation within dendrites provides specific proteins needed at sites of synaptic activation, thereby supporting highly localized synaptic plasticity. Despite this important role for dendritic translation, there is no complete profile of dendritically translated mRNAs. Identifying the types of mRNAs that are translated in dendrites following learning will offer insight into the molecular processes that underlie synaptic plasticity, thereby providing a basis for better understanding how we acquire and store new information.

Here we introduce a novel transgenic mouse that allows for the collection of ribosome-bound mRNAs from defined cell-types. We created a mouse that expresses EGFP-L10a under the tetracycline operator (tetO-TRAP). By crossing this mouse with driver specific tTA mouse lines, EGFP-L10a can be expressed in a cell-type specific manner. Expression of EGFP-L10a then allows for the collection of ribosome-bound mRNA, thereby providing a translational profile of the cell-type of interest. We showed that this mouse can be crossed with the Camk2a-tTA and Fos-tTA driver mice to induce expression of EGFP-L10a in both a cell-type and functionally defined population of neurons, respectively. We show that the Camk2a-TRAP mouse enables successful collection of high quality ribosome-bound mRNA from CA1 pyramidal neurons in the hippocampus.

Using the Camk2a-TRAP mouse line, we created a novel method for collecting ribosome-bound mRNA from *in vivo* neuronal dendrites. By combining this novel

method with RNA-seq analysis, we generated a list of ribosome-bound mRNAs found within neuronal dendrites. This list greatly adds to our understanding of what genes can be locally translated within neuronal dendrites, as well as what genes are regulated during a learning paradigm.

We looked more closely at one of the dendritically translated mRNAs found in our screen. We found that both Med8 mRNA and protein are localized to neuronal dendrites, a surprising finding as the only known function of Med8 protein is within the nucleus of the cell. Besides its well characterized function as part of the transcriptional Mediator complex, we showed that Med8 protein can endogenously incorporate into an E3 ubiquitin ligase. Med8's association with the ubiquitin ligase was most strongly detected in the cytoplasm of brain tissue, and not within other tissues of the body that were examined. This greatly adds to our understanding of where Med8 can function as part of an E3 ubiquitin ligase. Together, our work contributes important new tools to the field of translational profiling, as well as adds to our understanding of local dendritic protein translation and the types of mRNAs that are found within dendrites.

Acknowledgements

During my time at Tufts University, I have been fortunate to come across countless people who have aided in my growth as a person, as well as a scientist. I would like to thank my advisor, Dr. Leon Reijmers, for his ever present encouragement, excitement, and optimism about science. He has not only taught me to be an enthusiastic scientist, but also to keep pushing forward even when experiments don't work. I am thankful for my thesis committee members Dr. Rob Jackson, Dr. Michele Jacob, Dr. Grace Gill, and my external examiner Dr. Joel Richter, for providing a safe and engaging environment for scientific discussion. Their guidance and encouragement were paramount in my graduate school career. I would like to thank the members of the Tufts Neuroscience community, both past and present, who have provided support and fantastic scientific discussion over the years. I am particularly grateful for my phenomenal lab-mates, Josh, Stephanie, Jenny, Alex, Denise, and Patrick, who made the lab a fun and enjoyable place to be. I have learned so much from each and every one of you, thank you.

Outside of Tufts, I would like to thank my parents for their ever present support and love. I would like to thank my husband, Brent, who has loved and encouraged me, and always remained positive during my crazy graduate school adventure. Lastly, I would like to thank my daughter, Charlotte, who has brought me more joy than words can describe.

Table of Contents

List of Figures and Tables

Chapter 1:

Chapter 2:

Chapter 3:

Chapter 4:

Chapter 5:

Chapter 6:

List of Abbreviations

AMPA: α-amino-3-hydroxy-5-methyl-4-isoxazolepropionic acid receptor

BDNF: Brain-derived neurotrophic factor

CA1: Cornus ammonis region 1 of the hippocampus

CA3: Cornus ammonis region 3 of the hippocampus

Camk2a: Calcium/calmodulin-dependent protein kinase II alpha

cAMP: Cyclic adenosine monophosphate

Co-IP: Co-immunoprecipitation

CREB: cAMP response element-binding protein

DAPI: 4' 6-diamidino-2-phenylindole

dCt: Delta cycle threshold

Dox: Standard doxycycline chow

EGFP: Enhanced green fluorescent protein

EGFP-L10a: Enhanced green fluorescent protein fused to the ribosomal protein L10a subunit

ERK: Extracellular signal-regulated kinase

FACS: Fluorescence-activated cell sorting

FC: Fear conditioned

FISH: Fluorescent in situ hybridization

FPKM: Fragments per kilobase per million mapped reads

Gad1: Glutamate Decarboxylase 1

Gfap: Glial fibrillary acidic protein

GFP: Green fluorescent protein

GFP-Trap_A: ChemoTek GFP coated agarose beads

GFP-Trap_M: ChemoTek GFP coated magnetic beads

GKAP: Guanylate kinase-associated protein

GluR: Glutamate receptor

GO: Gene ontology

GTFs: General transcription factors

HC: Home cage

IEG: Immediate early gene

IgG: Immunoglobulin

IP: Immunoprecipitation

LCM: Laser capture microdissection

LTP: Long-term potentiation

MAPK: Mitogen-activated protein kinase

Med8: Mediator subunit 8

mRNA: Messenger ribonucleic acid

MSN: Medium spiny neuron

Naa38: N(Alpha)-Acetyltransferase 38 NatC Auxiliary Subunit

NMDA: N-Methyl-D-aspartate

Nt: Nucleotides

PKA: cAMP-dependent protein kinase

Pkia: cAMP-dependent protein kinase inhibitor alpha

Pol II: RNA polymerase II

PSD: Postsynaptic density

PSD-95: Postsynaptic density protein 95

qPCR: Quantitative real-time polymerase chain reaction

RIN: Ribonucleic acid integrity number

Rps3: Small ribosomal protein S3

RPS6: Small ribosomal protein S6

rRNA: Ribosomal ribonucleic acid

SN: Supernatant

SNP: Single nucleotide polymorphism

tetO: Tetracycline operator

TetTag: Tetracycline controlled tagging

Thy1-YFP: Thy-1 cell surface antigen-yellow fluorescent protein

TRAP: Translating ribosome affinity purification

tTA: Tetracycline-transactivator

UPS: Ubiquitin proteasome system

UTR: Untranslated region

WT: Wild type

Chapter 1:

Introduction

1.1 Molecular mechanisms of memory storage

Protein synthesis in memory consolidation

Memory formation is a critical, adaptive process in which changes in synaptic strength underlie our ability to create and store new information. Research using protein synthesis inhibitors has indicated that *de novo* protein synthesis underlies the neural mechanisms supporting learning and memory (Davis & Squire, 1984). Memory formation begins with a labile, short-term memory phase lasting for seconds to minutes (Alberini, Milekic, & Tronel, 2006). Short-term memory formation is a protein synthesis independent process that relies on electrical activity and post-translational modifications to existing proteins. The transition of labile short-term memories into stable long-term memories starts during the first hours after learning, and is known as consolidation (Schafe, Nader, Blair, & LeDoux, 2001). Memory consolidation is a protein synthesis dependent process that can be disrupted with trauma (such as electroconvulsive shock), new learning, and protein synthesis inhibitors (Costa-Mattioli, Sonenberg, & Richter, 2009). Reactivation of a previously consolidated long-term memory transiently returns the memory to a labile state, where it once again becomes susceptible to modification (Duvarci & Nader, 2004; Schiller et al., 2010). A protein synthesis dependent reconsolidation process is then necessary to re-stabilize the memory for long-term storage (Nader, Schafe, & Le Doux, 2000).

The idea that protein synthesis plays an important role in memory formation gained popularity in the early 1960's, when Flexner et al. showed that the protein synthesis inhibiting antibiotic puromycin caused a loss of memory formation (Flexner,

Flexner, & Stellar, 1963). As application techniques became more precise, it became clear that administration of a protein synthesis inhibitor before the start of a behavioral paradigm did not affect short-term memory formation, but did affect long-term memory formation (Davis & Squire, 1984). Administration of the protein synthesis inhibitor anisomycin 15 minutes before training, or immediately after training revealed an interesting dynamic about the timing of protein synthesis in memory consolidation. Administration of anisomycin 15 minutes before training completely blocked the formation and retention of the memory when tested two and seven days after training. Administration immediately after training, however, was insufficient to block memory retention two days after training, showing that the few minutes of protein synthesis that occurred during the training itself was sufficient to allow for memory formation (Bambah-Mukku, Travaglia, Chen, Pollonini, & Alberini, 2014). Interestingly, although immediate protein translation is required for memory formation, blocking protein synthesis at either 12 or 24 hours after training impairs memory retention seven days after training (Bambah-Mukku et al., 2014; Bekinschtein et al., 2007). This shows that additional waves of protein synthesis at both 12 and 24 hours are required for memory maintenance and persistence.

Anisomycin has been widely used to inhibit protein synthesis in memory studies. It inhibits protein synthesis by blocking the formation of peptide bonds between amino acids during the translation process, thereby inhibiting elongation (Hernandez & Abel, 2008). However, off-target effects of anisomycin, as well as other protein synthesis inhibitors, adds confounding variables to studies using them to assess learning and memory, as the off-target effects could also affect learning and memory (Hernandez &

Abel, 2008). To circumvent these issues, researchers have used genetic manipulations to block protein synthesis and assess memory formation. For example, activity at the synapse (the junction between two neuronal cells) activates mitogen-activated protein kinase/extracellular signal-regulated kinase (MAPK/ERK) signaling that leads to gene transcription and translation, and ultimately synaptic plasticity (a strengthening or weakening of synaptic connections) and memory formation. Researchers showed that genetic inhibition of ERK signaling through expression of a dominant-negative form of an upstream component MEK1, led to a decrease in memory retention, and a decrease in the protein synthesis dependent phase of long-term potentiation (LTP; a persistent increase in the strength of a synapse after stimulation) (Kelleher, Govindarajan, Jung, Kang, & Tonegawa, 2004). Additionally, GCN2 is a protein kinase that regulates protein translation by phosphorylating the initiation factor eIF2α. eIF2α, once phosphorylated, stimulates the translation of ATF4. The ATF4 protein is a transcriptional modulator that is known to inhibit CREB-mediated LTP. Knock-out of GCN2 caused a decrease in ATF4, and thereby increased CREB activity and synaptic plasticity triggered by a weak stimulus (Costa-Mattioli et al., 2005). In agreement with this finding, blocking phosphorylation of eIF2α by mutating the phosphorylation site lowers the threshold for LTP (Costa-Mattioli et al., 2007). The use of genetic manipulations to manipulate protein synthesis further demonstrates the importance of protein synthesis in memory formation.

Protein degradation in memory consolidation

In addition to protein synthesis, protein degradation via the ubiquitin-proteasome system (UPS) plays an essential role in synaptic plasticity and memory formation. Protein degradation by the UPS is signaled by the covalent attachment of small 76 amino acid

ubiquitin proteins onto lysine residues of targeted protein substrates (Hershko & Ciechanover, 1998). Attachment of chains ubiquitin proteins, called polyubiquitination, tags the substrate protein for degradation by the 26S proteasome, or targets it to the lysosome depending on ubiquitin branching. A chain of at least four ubiquitin proteins must be attached before the substrate can be recognized and degraded by the proteasome (R. C. Conaway, Brower, & Conaway, 2002). The process of ubiquitination is a highly regulated, three step process involving the identification and attachment of ubiquitin to target substrate proteins via multiple enzymatic reactions (Fioravante & Byrne, 2011; Glickman & Ciechanover, 2002). The enzymatic cascade begins with the ATP-dependent attachment of a ubiquitin protein to an E1 ubiquitin-activating enzyme. Activated ubiquitin is then transferred to an E2 ubiquitin-conjugating enzyme. Ubiquitin is finally targeted to its substrate with the aid of an E3 ubiquitin ligase, which recognizes the protein substrate (Bhat & Greer, 2011) (figure 1.1). Protein ubiquitination is a highly regulated and specific process. The specificity of a ubiquitin ligase is achieved by the E3 ligase. There are over 500 genes encoding E3 ubiquitin ligases (Bhat & Greer, 2011). The large number of E3 ligases allows for great specificity in substrate recognition.

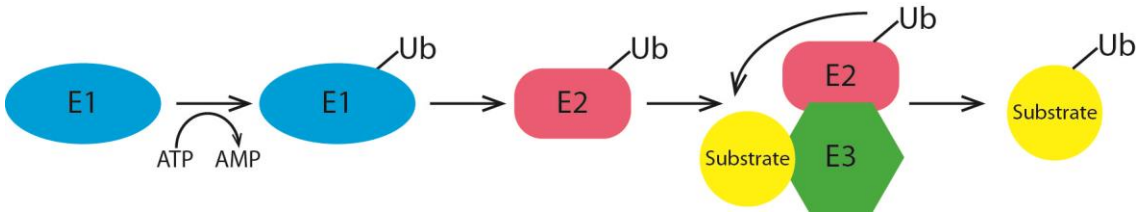

Figure 1.1

The E3 ubiquitin modification pathway. Schematic of the enzymatic ubiquitination cascade.

Introduction of the protein degradation inhibitor, lactacystin, immediately after a learning paradigm disrupts memory consolidation (Artinian et al., 2008; Lopez-Salon et al., 2001). In addition, inhibition of the proteasome using another pharmacological inhibitor, MG132, disrupts late-phase LTP in synapses of the CA1 Shaffer collateral (Karpova, Mikhaylova, Thomas, Knopfel, & Behnisch, 2006). Fear memory reconsolidation, as triggered by memory retrieval, has been shown to increase the amount of polyubiquitination in the synaptosomal fraction of the hippocampus; specifically, increasing polyubiquitinated post-synaptic density (PSD) proteins such as Shank and GKAP (Lee et al., 2008). Protein degradation contributes to synaptic plasticity through removal of inhibitory constraints at the synapse, as well as by regulating the availability of different proteins at the synapse (Cajigas, Will, & Schuman, 2010; Fioravante & Byrne, 2011; A. N. Hegde, Goldberg, & Schwartz, 1993; Merlo & Romano, 2007). For example, the UPS dependent degradation of the ribonucleic acid (RNA) binding protein MOV10 at the synapse releases translationally repressed messenger RNAs (mRNAs) and allows for activity-regulated protein translation to occur (Banerjee, Neveu, & Kosik,

2009). In Aplysia, synaptic stimulation induces degradation of the cAMP-dependent protein kinase (PKA) regulatory subunit, thereby allowing PKA signaling to exert its positive function over long-term memory formation (Chain, Schwartz, & Hegde, 1999). It is now thought that synaptic plasticity occurs through a balance of both protein synthesis and protein degradation (Jarome & Helmstetter, 2014).

BC-box containing E3 ubiquitin ligases

One class of E3 ubiquitin ligases consists of BC-box containing proteins. The BC-box motif consists of ten amino acids with the consensus sequence of [(A,P,S,T)LxxxCxxx(A,I,L,V)]. Proteins that contain a BC-box motif can interact with the heterodimeric Elongin BC complex. The Elongin BC complex interacts with the RNA polymerase II (Pol II) elongation factor Elongin A to positively stimulate the rate of elongation by Pol II (J. W. Conaway & Conaway, 1999). In addition, Elongins B and C interact with BC-box containing proteins allowing for the assembly of E3 ubiquitin ligases (Brower et al., 2002). In one particular type of E3 ubiquitin ligase, the Elongin BC complex acts as an adaptor linking BC-box containing proteins with the scaffolding protein Cul2, the ring finger protein Rbx1, and the ubiquitin-conjugating enzyme Ubc5 (Okumura, Matsuzaki, Nakatsukasa, & Kamura, 2012). The brain contains a variety of BC-box containing proteins that act to regulate a wide range of functions, including signal transduction and transcription (Petroski & Deshaies, 2005). It is therefore a reasonable assumption that certain BC-box containing proteins contribute to the role of protein degradation in synaptic plasticity and memory storage. During my thesis research, I have studied one such BC-box containing protein: the transcriptional Mediator subunit Med8 (Brower et al., 2002) (figure 1.2).

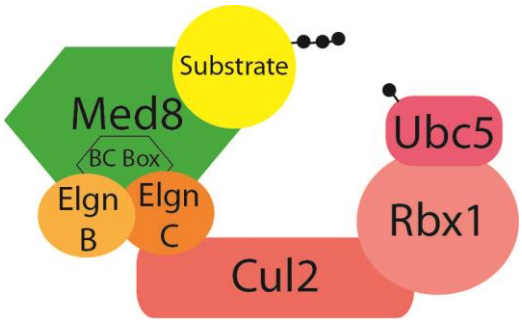

Figure 1.2

The Med8 containing E3 ubiquitin ligase complex. Med8 contains a BC-box binding domain that allows it to interact with Elongins B and C, Cul2, Rbx1, and Ubc5 to form a functioning E3 ubiquitin ligase. (Proteins are not depicted to scale).

Mediator is an essential component of the Pol II transcriptional machinery (R. C. Conaway, Sato, Tomomori-Sato, Yao, & Conaway, 2005). Mediator was first discovered in the budding yeast *Saccharomyces cerevisiae* as a complex containing approximately 20 subunits separated into distinct domains; the head, middle, tail, and kinase (Spahr et al., 2001). To date, approximately 30 mammalian Mediator subunits (22 of which have orthologs in *S. cerevisiae* (Boube, Joulia, Cribbs, & Bourbon, 2002)) have been identified, separated into the same distinct head, middle, tail, and kinase domains (R. C. Conaway et al., 2005; Dotson et al., 2000). Although originally thought to act passively as an adaptor between Pol II and the general transcription factors (GTFs) (Myers & Kornberg, 2000), it is now known that Mediator is actively involved in many aspects of transcription regulation, and can positively and negatively regulate mRNA synthesis based on its subunit composition (Malik & Roeder, 2010; Napoli, Sessa, Infante, & Casamassimi, 2012). Although Mediator is predominantly known to be involved in transcription and localized to the nucleus, the Med8 subunit has been shown to assemble

with Elongins B and C, Cul2, and Rbx1 to form an E3 ubiquitin ligase complex (Brower et al., 2002). An *in vitro* ubiquitination assay in insect cells revealed that Med8 and Rbx1 along with the E2 ubiquitin-conjugating enzyme Ubc5, the E1 ubiquitin-activating enzyme Uba1, GST-ubiquitin, and ATP could form polyubiquitin conjugates (Brower et al., 2002). Although this strongly suggests that the Med8 containing ubiquitin ligase complex is functional, Rbx1 has been shown to activate E2s to form nonspecific polyubiquitin chains without E3 specific substrate recognition (Brower et al., 2002).

Med8 is part of the head domain of the Mediator complex, and is conserved from yeast to humans (Cai et al., 2010; Imasaki et al., 2011; Tsai et al., 2014). The head module directly interacts with Pol II and the GTFs to regulate basal transcription (Lariviere et al., 2006; Malik & Roeder, 2010). In all organisms, Med8 is essential for viability (Lariviere et al., 2006; Myers & Kornberg, 2000). Within the head domain, Med8 binds to the Med18 and Med20 subunits to positively regulate transcription (Lariviere et al., 2006). The Med8/18/20 complex interacts with Med17, the core protein within the head module, without which there is abolishment of all mRNA transcription (Lariviere et al., 2006).

Although Med8 is conserved across species, its BC-box binding domain is only present within chordates. This means that, although its function as part of the Mediator is highly conserved, its interaction with Elongins BC and subsequent interaction with its ubiquitin ligase complex occurs within higher organisms. Interestingly, despite its specific function in higher organisms, the function of the Med8 ubiquitin ligase complex is not known.

1.2 Local protein regulation

Local protein synthesis within dendrites

For many years it was assumed that all protein synthesis occurred in the cell body of the neuron, and that proteins were trafficked out to distal processes following their synthesis. The realization that neurons also synthesize proteins outside of the soma came about in 1965 when Bodian discovered that some ribosomes localize to the dendrites of neurons (Bodian, 1965) (figure 1.3). In addition, it was found that polyribosomes tend to cluster at the bases of dendritic spines even within distal dendrites (Steward & Levy, 1982). Accordingly, it was found that isolated dendritic or synaptosomal fractions could successfully carry out *de novo* protein translation as seen by the incorporation of radiolabeled amino acids into proteins (Rao & Steward, 1991; Torre & Steward, 1992; Weiler & Greenough, 1991). The functional relevance of dendritic protein synthesis was tested in a preparation where synaptic plasticity was induced in isolated hippocampal dendrites. This synaptic plasticity was blocked by the application of protein synthesis inhibitors, demonstrating the need for dendritic protein synthesis (Kang & Schuman, 1996). Similarly, local introduction of a protein synthesis inhibitor to the dendrites of neurons, but not the soma, was able to block LTP within hippocampal slices (Bradshaw, Emptage, & Bliss, 2003). In agreement with a role for dendritic protein synthesis in synaptic plasticity, synaptic stimulation has been shown to cause a redistribution of polyribosomes from dendritic shafts to dendritic spines (Ostroff, Fiala, Allwardt, & Harris, 2002) (Figure 1.3).

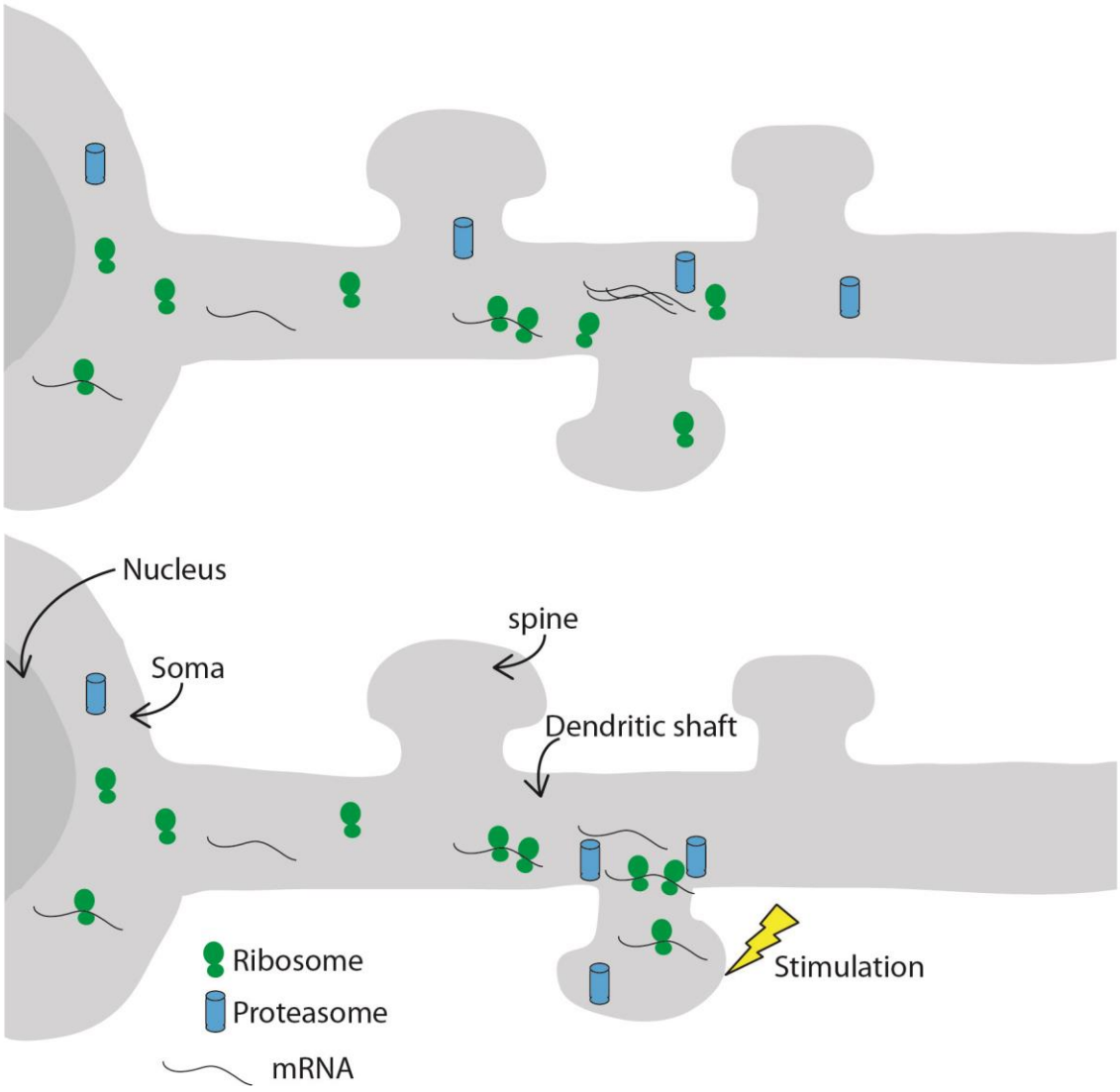

Figure 1.3

Ribosomes and the proteasome localize to dendritic processes. In unstimulated neurons, mRNA, ribosomes, and the proteasome are present within dendrites. Upon stimulation, mRNA, ribosomes, and the proteasome can be seen clustering near dendritic spines (points of synaptic contact between neurons).

The importance of local protein translation in memory consolidation was confirmed in a knockout mouse line. mRNAs contain multiple distinct regions, the protein coding region, flanked by the 5' and 3' non protein coding untranslated regions (UTRs). The 3'UTR of Camk2a has been shown to contain a targeting signal for localization to the dendritic processes (Mayford, Baranes, Podsypanina, & Kandel, 1996). In this mouse line, Camk2a mRNA was mutated so that the protein coding region was kept intact, but the dendritic localization signal was deleted. This caused a marked decrease in the amount of Camk2a protein at postsynaptic densities (PSDs). This mutation caused a reduction in late-phase LTP, as well as disruption in spatial memory, fear conditioning, and object recognition memory (Miller et al., 2002). Although somatic mRNA and protein was left intact, this demonstrated that the local translation of Camk2a was necessary for its proper synaptic localization, subsequent activity-dependent signaling, and normal functioning of the protein.

Direct support for local protein synthesis in neurons has been provided by imaging studies (Aakalu, Smith, Nguyen, Jiang, & Schuman, 2001; Martin et al., 1997; Ouyang, Rosenstein, Kreiman, Schuman, & Kennedy, 1999). In one study, researchers created a green fluorescent protein (GFP) construct flanked by the 5' and 3' untranslated regions (UTRs) of the dendritically translated Camk2a protein. They then showed that stimulation of cultured hippocampal neurons expressing the construct with brain-derived neurotrophic factor (BDNF) resulted in robust local translation of the GFP construct (Aakalu et al., 2001). In addition, in mechanically isolated dendrites, they were able to show that BDNF induced local protein translation of the GFP construct without involvement of the cell body. Another study showed that stimulation of mechanically

isolated dendrites with glutamate caused robust local translation of a transfected GFP construct. In this study, translation "hotspots" were observed where local translation seemed to occur fastest. Immunostaining revealed that these "hotspots" contained an increased density of ribosomes, and were therefore able to produce proteins fastest (Job & Eberwine, 2001). Fluorescent *in situ* hybridization (FISH) studies showed that stimulation causes an unmasking of β-actin mRNA molecules at synaptic sites, allowing for translation and remodeling of the synapse (Buxbaum, Wu, & Singer, 2014). In addition, synaptic stimulation caused an increase in the dendritic translation of a PSD-95-venus fusion protein, showing the importance of local translation of synaptic proteins (Ifrim, Williams, & Bassell, 2015). In summary, the ability of cells to control protein translation in a compartmentalized fashion increases their spatial and temporal control over plasticity, specifically at the synapse (Holt & Schuman, 2013; Martin, Barad, & Kandel, 2000; Zukin, Richter, & Bagni, 2009).

Local protein degradation within dendrites

Along with local protein synthesis, local protein degradation is also necessary for synaptic plasticity. Components of the UPS (both the proteasome and ubiquitin) were discovered to be localized within dendrites, and clustered at the post-synaptic density (Ehlers, 2003; Patrick, Bingol, Weld, & Schuman, 2003) (figure 1.3). Functionally, it has been shown that blocking proteasome activity prevents ubiquitin dependent degradation and remodeling of the synaptic scaffolding protein PSD-95, which in turn prevents the activity-regulated internalization of α-amino-3-hydroxy-5-methyl-4-isoxazolepropionic acid (AMPA) receptors at the synapse (Colledge et al., 2003). In an experiment utilizing a GFP proteasome activity reporter, it was shown that up-regulation of action potentials

by bicuculline (a $GABA_A$ receptor antagonist) caused an increase in the rate of GFP degradation in dendrites of cultured hippocampal neurons, and that the rate of degradation was highest at dendritic spines (Djakovic, Schwarz, Barylko, DeMartino, & Patrick, 2009). In addition, blockade of action potentials by tetrodotoxin (a sodium channel blocker) decreased the local activity of the proteasome (Djakovic et al., 2009). Local stimulation of dendrites causes a physical shift of the proteasome from dendritic shafts into dendritic spines, further supporting a role for the proteasome in localized synaptic plasticity (Bingol & Schuman, 2006). In one study looking at the relationship between protein synthesis and protein degradation, it was shown that inhibition of either protein synthesis or protein degradation disrupted late-phase LTP. However, blocking both protein synthesis and protein degradation at the same time restored late-phase LTP (Fonseca, Vabulas, Hartl, Bonhoeffer, & Nagerl, 2006). This shows that together, both local protein synthesis and local protein degradation work congruently at the synapse to regulate protein availability and synaptic plasticity.

1.3 Gene expression profiling during memory formation

It has been well established that *de novo* protein synthesis is necessary for synaptic plasticity and memory formation (see sections 1.1 and 1.2). The understanding that memory formation relies on protein synthesis raises the following question: which specific proteins need to be synthesized during memory formation? One group of proteins important for synaptic plasticity and memory formation are the immediate early genes (IEGs) such as c-fos, zif268, and Arc (Guzowski, 2002; Okuno, 2011). After synaptic

stimulation, IEGs are the first group of genes to be expressed. Some IEGs, for example Arc, act at the synapse where they interact with other synaptic proteins. Other IEGs, such as c-fos and zif268, act within the nucleus as transcription factors. Since c-fos and zif268 regulate the transcription of a large variety of neuronally expressed genes, it is to be expected that many of these downstream genes are involved in synaptic plasticity and memory. However, to date, a comprehensive list of genes involved in synaptic plasticity and memory formation remains to be compiled.

To discover gene expression changes relevant to memory formation at a genome-wide scale, microarray analysis of brain regions dissected after a memory test has been used. Microarray analysis enables the detection and quantification of a large number of different mRNAs that are present within a sample. In one example, high-density cDNA microarrays containing 8700 cDNA mouse clones were used to look at cerebellar lobe HVI and hippocampal tissue from rabbits trained on an eye blink conditioning paradigm (Cavallaro, Schreurs, Zhao, D'Agata, & Alkon, 2001). This study revealed a greater than two-fold change in gene expression of 79 and 17 genes in the cerebellar lobe HVI and hippocampus respectively. Of these genes, most were seen to be down-regulated after the learning paradigm. A further study using microarrays looking at the hippocampus after passive avoidance training showed 38 differentially expressed genes, with 21 genes down-regulated and 17 genes up-regulated after learning (D'Agata & Cavallaro, 2003). It was also found that the timing of differential gene expression after learning is important. Between 0-2 hours after learning there is an increase in genes involved in transcription. From 0-6 hours after learning there is an increase in synaptic and cytoskeletal genes.

Lastly, at 12 hours after learning there is a decrease in gene expression across all the previously up-regulated groups (O'Sullivan et al., 2007).

Although these first screens identified many genes with a potential memory function (Cavallaro, D'Agata, Manickam, Dufour, & Alkon, 2002; Cavallaro et al., 2001; D'Agata & Cavallaro, 2003; O'Sullivan et al., 2007), they had two important limitations. First, they pooled mRNA from complete brain regions. It is therefore not clear in which cell-types the detected genes expression changes occurred, and changes in sparse cell-types might have been missed. Second, the use of microarrays has some caveats. Microarrays are based on the binding of labeled cDNA samples to a library of predetermined gene primers, each of which are present in the microarray in a set quantity (Heller, 2002). Microarrays therefore do not allow for the unbiased detection of all mRNAs and their splice isoforms. In addition, there is both a threshold and a saturation level for how many copies of each specific mRNA can be detected with a microarray (Wang, Gerstein, & Snyder, 2009). The technical limitations of the early "memory-gene" screens have since been resolved by the advent of new techniques that enable the collection of cell-type specific mRNA samples and their unbiased and highly quantitative analysis using sequencing-based methods.

1.4 Novel techniques for studying gene expression and protein synthesis

Translating Ribosome Affinity Purification

The brain contains a mixture of hundreds of neuronal cell-types. These subtypes can be defined by their morphological, physiological, and molecular makeup. However, the heterogeneity of the brain has obstructed researcher's ability to define many of these cell-types in a molecular manner. Acquiring the gene expression profiles of individual cell-types is imperative for understanding their molecular identities. Although traditionally cell-types are defined by their morphology and functional properties, studies have shown that many sub-classes of neurons can also be distinguished through genome-wide gene expression profiling (Okaty, Sugino, & Nelson, 2011). These studies used various techniques to collect mRNA from defined groups of neurons, including laser capture microdissection (LCM) and fluorescence-activated cell sorting (FACS). However, both LCM and FACS-based methods have various drawbacks. LCM often results in low levels of mRNA, and is prone to contamination from the close proximity of off-target cell-types (Okaty et al., 2011). In addition, LCM requires fixation of the tissue, which alone can increase degradation of nucleic acids. Use of manual cell dissociation techniques can eliminate the off-target contamination seen with LCM. However, this technique can be very time consuming as large numbers of cells must be isolated in order to collect sufficient mRNA quantities. FACS greatly increases the number of cells that can be isolated. However, the harsh conditions of the dissociation and sorting process causes neurons to lose their processes and increases the risk of introducing gene expression artifacts (Okaty et al., 2011). The loss of dendrites and axons during the dissociation of neurons is especially limiting for the detection of mRNA changes that

support synaptic plasticity, given the important role of local protein synthesis (see section 1.2).

Many of the technical limitations of traditional mRNA collection methods can be circumvented with the translating ribosome affinity purification (TRAP) technique (Doyle et al., 2008; Heiman et al., 2008), and other methods based on collecting epitope-tagged ribosomes (Sanz et al., 2009). The TRAP technique utilizes transgenically expressed EGFP-L10a (enhanced green fluorescent protein fused with the ribosomal protein L10a) to affinity purify EGFP-tagged ribosomes from genetically defined cell-types. Through analysis of the co-purified mRNA, it is possible to acquire the translational profile of the cell-type in which EGFP-L10a was expressed. In the paper first describing the TRAP technique, researchers were able to identify gene expression profiles from two morphologically indistinguishable striatal medium spiny neuron (MSN) cell-types: striatonigral and striatopallidal (Heiman et al., 2008). By distinguishing the differences in the gene expression profiles of these MSNs, they were able to identify previously unknown physiological differences that could allow for new pharmacological targets for neurological diseases affecting specific MSNs in the striatum.

TRAP has been applied to cell-types in various mouse tissues including brain (Ainsley, Drane, Jacobs, Kittelberger, & Reijmers, 2014; Doyle et al., 2008; Drane, Ainsley, Mayford, & Reijmers, 2014; Heiman et al., 2008; Schmidt et al., 2012), heart (Fang et al., 2013; Zhou et al., 2013), liver (Wilkins, Gong, & Pack, 2014), and kidney (Liu et al., 2014). In addition to mice, TRAP has been applied in other species such as Drosophila and zebrafish (Huang, Ainsley, Reijmers, & Jackson, 2013; Thomas et al., 2012; Tryon, Pisat, Johnson, & Dougherty, 2013). TRAP has the advantages of being

more high-throughput than LCM without requiring the dissociation of neurons from intact tissue as needed for FACS. In addition, the ribosome-bound mRNA collected through TRAP provides a more accurate representation of potentially translated genes than the total mRNA collected through LCM or FACS (Schwanhausser et al., 2011). Although total mRNA levels are often used as a representation of the protein content of a given sample, it has been shown that total mRNA levels do not give the most accurate read out of actual protein expression (de Sousa Abreu, Penalva, Marcotte, & Vogel, 2009; Maier, Guell, & Serrano, 2009). Collecting ribosome-bound mRNA provides a translational profile that increases the accuracy of predicting changes in protein content. However, it should be noted that not all ribosome-bound mRNA is actively translated, as ribosomes can pause during the initiation and elongation phases (Richter & Coller, 2015).

RNA Sequencing

The TRAP technique allows for great cell-type specificity in the collection of ribosome-bound mRNA from selected brain regions. One way to analyze the resulting mRNA samples is by using microarray technology. However, microarray technology is limited in its ability to unbiasedly profile mRNA samples (see section 1.3). An alternative methodology, next generation sequencing of mRNA (RNA-Seq), allows for unbiased profiling of mRNA samples (Metzker, 2010; Wang et al., 2009). With RNA-Seq, an mRNA sample is converted into a cDNA library that is sequenced in its entirety (Wang et al., 2009). Once sequenced, the resulting sequencing "reads" can be aligned to a reference genome for the identification and quantification of all mRNAs that were present in the sample. In comparison to microarray techniques, RNA-Seq is not limited by a predetermined gene set or primer quantity. In addition, RNA-Seq can reveal

information about differential gene splicing, sequence variations (such as single nucleotide polymorphisms (SNPs)), and critical information about the sequences of the untranslated regions of the RNA.

1.5 Contributions of this thesis

Synaptic plasticity and memory formation depend on a combination of protein synthesis and protein degradation. To better understand this molecular mechanism, it is important to obtain comprehensive lists of proteins that are synthesized during memory formation. To aid future efforts aimed at generating such lists, we created a versatile transgenic mouse model for the spatial and temporal control of EGFP-L10a expression. Our mouse model increases the number of cell-types in the brain that are amenable to TRAP analysis. We achieved this by placing expression of EGFP-L10a under control of the tetO promoter. The tetO promoter is activated by tetracycline transactivator (tTA), which can be temporally suppressed through addition of doxycycline (dox) to the food of the mice (Gossen & Bujard, 1992). As a result, temporally controlled cell-type specific gene expression can be achieved by breeding tetO mouse lines with mouse lines that express tTA under cell-type specific promoters. Here we crossed the tetO-TRAP mouse with both Camk2a-tTA and Fos-tTA driver mice, thereby generating Camk2a-TRAP and Fos-TRAP mice, respectively. We present a characterization of the EGFP-L10a expression patterns in the Camk2a-TRAP mouse, and demonstrate how it can be used to collect ribosome-bound mRNA from hippocampal CA1 neurons. In addition, we demonstrate with the Fos-TRAP mouse how the temporal control conferred by the tTA system enables the expression of EGFP-L10a in neurons activated during a defined time-window.

We used the Camk2a-TRAP mouse to develop a novel method for the collection of ribosome-bound mRNA from *in vivo* dendrites. After dissecting the dendritic layer of the CA1 region of the hippocampus from fresh tissue, we were able to use TRAP to

isolate ribosome-bound mRNA specifically from the dendrites of pyramidal cells in the CA1. Once isolated, we used RNA-Seq in order to unbiasedly characterize the mRNAs present within our samples. Doing so allowed us to acquire a list of ribosome-bound mRNAs from dendrites that include genes previously thought to solely have somatic functions. Fluorescent *in situ* hybridizations were then used to confirm the dendritic localization of the mRNAs. Our findings contribute to our understanding of the types of mRNAs that are locally translated within neuronal dendrites.

Finally, through our screen we identified a locally translated mRNA, Med8, which had previously been thought to only function within the nucleus of the cell. Our findings indicate that Med8 protein is not only present within the cytoplasm and dendrites of neurons, but that it also associates with an E3 ubiquitin ligase (Brower et al., 2002). Interestingly, we discovered that Med8's association with the ubiquitin ligase complex seems to occur in a brain-specific manner. From the creation of a novel mouse model, to its use in a screen, to characterization of a hit from that screen, this work contributes valuable new tools to the field and increases our understanding of the local regulation of proteins that can contribute to synaptic plasticity and memory.

Chapter 2:

Materials and Methods

2.1 Animals

All animal procedures were performed in accordance with the National Institutes of Health Guide for the Care and Use of Laboratory Animals and were approved by the Tufts University Institutional Animal Care and Use Committee. Mice had access to food and water ad libitum and were socially housed prior to the start of any experiment. Mice were kept on a standard 14h/10h light-dark cycle and all experimental manipulations were performed during the light phase. For transferring mice during experiments, mice were handled by the tail. All mice were at least 12 weeks of age at the start of any experiment.

Camk2a-TRAP mice

The Camk2a-TRAP mouse line is heterozygous for two transgenes, a tetracycline transactivator protein (tTA) under control of the Camk2a promoter, and a GFP-L10a fusion protein under the tetracycline operon (tetO). The EGFP-L10a fusion protein coding sequence in a pLD53.SC.EGFP-L10a plasmid was donated by Nathaniel Heintz at Rockefeller University. The plasmid was transformed into One Shot PIR1 Chemically Competent E. coli (Life Technologies #C1010-10) and the EGFP-L10a sequence was obtained and verified using the services of the Tufts University Core Facility. A DNA fragment containing the EGFP-L10a coding sequence was removed by incubating the plasmid with AfeI and BamHI restriction endonucleases. After agarose gel electrophoresis, a ~1.4kb band containing the EGFP-L10a coding sequence was cut from the gel and purified using the PureLink Quick Gel Extraction Kit (Life Technologies #K2100-12). This fragment was treated with T4 DNA Polymerase (NEB #M0203S) to

form blunt ends. The blunt end EGFP-L10a fragment was cloned into pMM400Sfi, a plasmid for transgenic mouse creation containing a tet operon (donated by Mark Mayford at the Scripps Research Institute). pMM400Sfi was digested with the EcoRV restriction endonuclease to create blunt ends and then treated with Calf Intestinal Alkaline Phosphatase (Life Technologies #18009-019) to dephosphorylate the blunt ends and prevent self-ligation. The blunt end EGFP-L10a fragment was cloned into linearized pMM400Sfi by incubating with T4 DNA Ligase (NEB, #M0202S) overnight at 16°C. The correct sequence and insert orientation was verified by DNA sequencing.

Pronuclear microinjection of pMM400Sfi.EGFP-L10a into C57BL/6J embryos was performed at the Tufts Medical Center Transgenic Core Facility. Potential transgenic founder lines were screened for transgene integration using the following genotyping primers: (5'-CAGAACGCACACCGAGAACT-3', 5'-CTTCAAGGACGACGGCAACT-3'). Founders with detectable transgene integration were crossed with C57BL/6J mice to ensure heritability. Offspring carrying the transgene were crossed to Camk2a-tTA transgenic mice (JAX Stock Number 003010) to induce transgene expression in Camk2a-positive neurons in the forebrain. Individual founder lines were screened for strong, specific expression matching the expected spatial pattern and one line was used for all further experiments. Mice were bred and raised on standard chow. Robust expression of the EGFP-L10a transgene can be seen throughout the brain within Camk2a expressing neurons (Drane et al., 2014) (Figures 3.1C and 3.2A-C).

Fos-TRAP mice

The Fos-TRAP mouse line is heterozygous for two transgenes, a tetracycline transactivator protein (tTA) under control of the activity dependent Fos promoter, and a GFP-Fusion protein under control of the tetracycline operon (tetO) (See above section for details on the tetO-EGFP-L10a mouse creation). Mice were bred and raised on standard chow. Upon weaning at 3-4 weeks of age, mice were put on a diet of regular doxycycline chow (40mg/kg dox). Four days prior to experimental fear conditioning, Fos-TRAP mice were removed from dox chow and given standard chow. High dox chow (1g/kg dox) was given immediately following experimental fear conditioning until the following morning when they were returned to regular dox chow. Expression of the EGFP-L10a transgene can be seen throughout the brain (Drane et al., 2014) (Figures 3.1C and 3.2A-C).

Wildtype C57BL6/J mice

Male C57BL6/J mice were purchased from The Jackson Laboratory at 9 weeks of age (Stock #000664). Mice were socially housed until the beginning of each experiment.

2.2 Fear conditioning

To ensure that mice remained in a resting state with minimal neuronal activation prior to fear conditioning, all animals were singly housed and left undisturbed for at least 3 days prior to the start of fear conditioning. This enabled us to control neuronal activation with high temporal specificity. At the beginning of each experiment, mice were transferred from their home cages to a separate room with fear conditioning chambers. At

the start of each experiment, and in between each session, the fear conditioning boxes, grid floors, and trays were wiped down with 70% ethanol. All urine and feces were removed in order to eliminate any cues left from one group to another. At the end of each experimental day the grid floors and trays were washed with soap and water.

Camk2a-TRAP mice

Male and female, 2-3 month old mice were singly housed for at least 3 days prior to behavioral testing. On day 0, mice were submitted to one contextual fear conditioning trial. Fear conditioning trials were performed in a specialized chamber (Coulbourn Instruments; H10-11RTC, 120W x 100D x 120H) and consisted of 500 seconds with 2 second long, 0.7 mA foot shocks administered at 198, 278, 358, and 438 seconds. After the session, mice were returned to their home cages and brought back to their normal housing room.

Fos-TRAP mice

Male and female, 3-4 month mice were singly housed for at least 5 days prior to behavioral testing. On day -3, doxycycline was removed from the food. On day 0, mice were then either left in their cage until tissue dissection (HC), or submitted to three contextual fear conditioning trials (FC) each spaced three hours apart. In between FC sessions, mice were returned to their home cages and brought back to their normal housing room. At the end of the third FC trial, all Fos-TRAP mice (HC and FC) were returned to a diet containing high levels of dox (1g/kg). The day following FC, all animals were returned to a diet containing regular levels of dox (40mg/kg).

2.3 Tissue preparation and immunohistochemistry

Mice were anesthetized with ketamine/xylazine and transcardially perfused with 0.1M phosphate buffer for 1 min at a rate of 15 ml/min followed by ice-cold 4% paraformaldehyde (PFA) in 0.1M phosphate buffer for 5 min at a rate of 15 ml/min. Brains were removed and post-fixed in 4% PFA for 24 hours at 4°C. Brains were transferred to 30% sucrose for 48-72 hours at 4°C, and then snap-frozen in -50°C isopentane for 3 min. Frozen brains were stored wrapped in parafilm in air-tight containers at -20°C until sectioning. Coronal brain sections were sliced at 20µm using a cryostat and immediately placed in 1X PBS at room temperature. Sections were stored at -20°C in a glycerol-based cryoprotectant and protected from light until use.

For immunohistochemistry, free-floating brain sections were washed in a solution of 1X PBS overnight at 4°C to remove any excess cryoprotectant. All washes were done with gentile agitation while protected from light. Sections were rinsed three times for 15 minutes in 1X PBS with 0.25% Triton-X-100 (PBS-T). Sections were then blocked at room temperature for 1 hour in PBS-T containing 10% normal goat or donkey serum. Primary antibodies (Abcam chicken anti-Map2, polyclonal, 1:20,000, ab5392; Santa Cruz goat anti-Med8, polyclonal, 1:50, sc-103619; Aves chicken anti-GFP, polyclonal, 1:500, GFP-1020; Millipore mouse anti-Gad1, monoclonal, 1:10,000, MAB5406; Abcam chicken anti-Gfap, polyclonal, 1:1000, ab4674) were diluted in blocking solution and incubated overnight at 4°C with gentle agitation, while protected from light. Sections were washed three times for 20 min in PBS-T. Secondary antibodies (All from Jackson Immuno research; donkey anti-chicken Alexa 488 1:250; donkey anti-goat DyLight 549 1:500; goat anti-mouse Cy3 1:2,000; goat anti-chicken DyLight 488 1:500; donkey anti-

chicken DyLight 649 1:1500) were diluted in blocking solution and applied to the sections for 2 hours at room temperature. Sections were washed three times for 15 min in 1X PBS. Sections were immersed in 500 µl of DAPI stain (1:20,000 in 1X PBS) for 5 min followed by a 10 min wash in 1X PBS in order to visualize nuclei. Sections were mounted onto slides, coverslipped using Prolong Gold Anti-fade Mounting Media, and stored at 4°C while being protected from light until imaging.

2.4 Microscopy

Widefield microscopy

Images of the Camk2a-TRAP mouse (Figure 3.1) were taken on an inverted Zeiss Axio Observer epi-fluorescent widefield microscope using a 20X Plan-APOCHROMAT air objective (0.8 NA). The microscope used a TissueFAXS Whole Slide Scanning System, allowing for rapid scanning of brain slices across multiple slides. Images were acquired with a PCO monochrome CCD camera 12 bit. Filters used were DAPI (Chroma 49000 ET), Alexa 488/Cy2 (Chroma 49002 ET), and Alexa 568/Cy3 (Chroma 49008 ET). The slide scanner used was located at The Ragon Institute of MGH, MIT, and Harvard.

Confocal microscopy

All other images were acquired using a Nikon A1R confocal laser scanning microscope using 20X air, 40X oil, or 60X oil objectives. Excitation lines were 405 nm, 488 nm, 561 nm, and 639 nm. Band-pass emission filters were used as follows: 425-475 nm (DAPI), 500-550 nm (GFP), 570-620 nm (RFP), and 660-740 nm (far red). 1024 x 1024 resolution images were acquired using an average of 2 line scans with a 1.1 pixel dwell time. Z sections with 1µm step size were taken.

2.5 Tissue and cell culture fractionation

Prior to the start of tissue collection, mice were transferred to a clean cage without food or water. To stimulate activity within the brain, mice were prodded gently with a purple gloved hand. A purple glove was then placed in the cage for 10 minutes prior to tissue collection. Mice were euthanized using inhaled isoflurane. Brains were then extracted and the hippocampus, pre-frontal cortex (PFC), liver, and lung tissue were rapidly dissected. Tissue dissections were immediately snap-frozen in liquid nitrogen and stored at -80°C until further use.

For the collection of cultured cells (Neuro-2a or HEK293T cells), cells were grown on 10cm dishes until approximately 90% confluency. Cells were washed with 10ml of 1X PBS. 2 ml of 0.05% Trypsin-EDTA was added to the cells for 5 min to dissociate the cells. 8 ml of fetal bovine serum containing growth media was added to the plate to stop the trypsin reaction. Cells were then spun down for 5 min at 500 x *g*. The media was removed and the cell pellet was put on ice for immediate fractionation.

Nuclear and cytoplasmic tissue fractionation was performed using the Thermo Scientific NE-PER^{TM} Nuclear and Cytoplasmic Extraction Kit (Product #78833). For cells and tissue, the samples were washed with 500 ml PBS, then spun down for 5 min at 500 x *g*. Depending on the weight of the tissue or size of the cell pellet, the sample was homogenized in the appropriate amount of Cytoplasmic Extraction Reagent I. Samples were vortexed on high for 15 seconds, then incubated on ice for 10 min. Cytoplasmic Extraction Reagent II was then added to the sample which was vortexed on high for 5 seconds, incubated on ice 1 min, then vortexed on high for 5 seconds. Samples were centrifuged 10 min at 15,000 x *g*. The supernatant (the cytoplasmic fraction) was immediately transferred to a clean tube. Nuclear Extraction Reagent was then added to the pelleted sample. Samples were vortexed on high for 15 seconds, and then incubated on ice for 10 minutes. This was repeated for a total of 40 minutes. Samples were then centrifuged at 15,000 x *g* for 10 minutes. The supernatant (nuclear fraction) was immediately transferred to a clean tube. Samples were stored at -80°C until use.

2.6 mRNA isolation and immunoprecipitation

RNA was isolated using a modified version of the translating ribosome affinity purification (TRAP) technique (Doyle et al., 2008; Heiman et al., 2008) that was optimized to remove background (Ainsley et al., 2014). An anti-GFP antibody (HtzGFP-19C8) from the Monoclonal Antibody Core Facility at the Memorial Sloan-Kettering Cancer Center was covalently bound to magnetic epoxy beads (Invitrogen) followed by BSA treatment to reduce non-specific binding.

For whole hippocampal dissections

Immediately following behavioral testing, Camk2a-TRAP mice were anesthetized using inhaled isoflurane. The hippocampi were rapidly dissected and rinsed in ice-cold dissection buffer (1x HBSS, 2.5 mM HEPES-KOH, 35 mM glucose, 4 mM NaHCO3). Each hippocampus was added to 150µl of homogenization buffer (Heiman et al., 2008) and homogenized using an automatic pestle.

For dendritic and somatic tissue punches

Immediately following behavioral testing, Camk2a-TRAP mice were anesthetized using inhaled isoflurane. The brain was rapidly removed in an ice-cold dissection buffer, and then frozen in liquid nitrogen. Coronal sections (~0.5 mm thick) were manually cut using a sterile scalpel and the brain slices were kept frozen in RNAse-free 60% glycerol cooled to -10°C using a cold plate (TCP-2D, Thermoelectrics Unlimited). Tissue punches of CA1 soma or dendrites were collected under a dissection scope with a 30-gauge blunt needle (Hamilton 7762-03). Individual tissue punches were placed in 50 µl homogenization buffer, frozen in liquid nitrogen, and stored at -80°C until RNA isolation. Each brain slice was placed in 4% paraformaldehyde (PFA) overnight, moved to 30% sucrose for one day, and then stained for DAPI. Brain slices were inspected on both sides to ensure accurate placement of each punch in the hippocampus. Dendritic punches were excluded if they touched the CA1 somatic layer at any point, ensuring no contamination with CA1 somatic mRNA in any of the dendritic samples. Accurately placed dendritic or somatic tissue punches from individual mice were pooled before immunoprecipitation.

Once homogenized, the tissue was centrifuged at 15,000 RPM for 10 minutes at 4°C. The lysate was transferred to a clean tube. For each sample, 1000 µg of protein was added to the prepared beads. Samples were incubated with the beads for 1 hour at 4°C with end-over-end rotation. The supernatant (SN) was saved for comparison to the immunoprecipitate (IP). After five washes with 0.5ml of KCl buffer (Heiman et al., 2008), RNA was extracted with Trizol LS. A back extraction was used to improve yield. Organic contaminants were removed with butanol and water-saturated diethyl ether washes (Krebs, Fischaleck, & Blum, 2009). RNA was precipitated using NaOAc, isopropanol, and linear acrylamide overnight at -80°C. After two washes with 80% EtOH, the RNA was re-suspended in 15 µl nuclease-free water.

2.7 Quantitative RT-PCR and bioanalyzer analysis

All mRNA samples were DNase treated to remove any genomic DNA contamination by treatment for 30 minutes with TURBO ^{TM} DNase (Ambion). The DNase was inactivated using a phenol-chloroform extraction. cDNA libraries were prepared using reverse transcription (RT) with Superscript III (Invitrogen) according to the manufacturer's instructions, with the exception that both random hexamers and anchored-oligo dT primers were used during the RT reaction. Quantitative RT-PCR was performed with SYBR Green PCR master mix (Applied Biosystems) on the Mx4000 thermo cycler (Agilent). Primers used are listed in table 2.1. The ΔΔct (ΔΔct = Δct1 – Δct2) was calculated from three biological replicates per primer set where Δct1 represented the normalized supernatant (SN) value to β-actin (Δct1 = gene SN ct – β-

actin SN ct), and Δct2 represented the normalized immunoprecipitate (IP) value to β-actin (Δct2 = gene IP ct – β-actin IP ct). Bioanalyzer analysis was performed using the Agilent Technologies 2100 Bioanalyzer with RNA pico chips according to the manufacturer's instructions.

Table 2.1 qPCR primer sequences

Gene name	Primer sequence
Gad1_F	5'-CACAGGTCACCCTCGATTTTT-3'
Gad1_R	5'-ACCATCCAACGATCTCTCTCATC-3'
Pkia_F	5'-TCGCAGCCACGGGTGAAACG-3'
Pkia_R	5'-TCCAAGCACAGCCCAGGTGA-3'
Gfap_F	5'-CGGAGACGCATCACCTCTG-3'
Gfap_R	5'-AGGGAGTGGAGGAGTCATTCG-3'
Camk2a_F	5'-TTTGAGGAACTGGGAAAGGG-3'
Camk2a_R	5'-CATGGAGTCGGACGATATTGG-3'
Naa38_F	5'-GGCTGTTATTACTTCTGATGGCA-3'
Naa38_R	5'-ACACCACTTGTTCTACTCCCT-3'
β-actin_F	5'-GGCTGTATTCCC CTC CATCG-3'
β-actin_R	5'-CCAGTTGGTAACAATGCCATGT-3'

2.8 Co-immunoprecipitation and western blotting

Co-immunoprecipitation (Co-IP) experiments were all performed using fractionated tissue as described in section 2.5. Protein concentrations for all samples were measured using a Bradford assay compared to a standard BSA curve. Protein concentrations were measured using a BioTek Synergy 2 plate reader set to an absorbance of 595nm, supported by Gen5 software. Before the start of each Co-IP, 25 µg of the sample was removed and used as the input control. For each sample, 500 µg of protein was measured into a clean tube. The total volume was brought to 500 µl using

lysis buffer containing protease inhibitors. Samples were incubated overnight with the appropriate antibody (Santa Cruz goat anti-Med8, polyclonal, sc-103619, 1µg/500µg protein; Abnova mouse anti-Med17 (CRSP6), monoclonal, H00009440-M02, 1µg/500µg protein). The next day, protein A/G magnetic beads (Thermo Scientific, product #88804) were prepared by rinsing 25 µl bead slurry two times with lysis buffer. The sample/antibody mixtures were incubated with the beads for 1h at 4°C while rotating end-over-end. Samples were washed five times with 500 µl of lysis buffer containing protease inhibitors. Between washes 4 and 5, samples were transferred to a clean tube in order to reduce background contamination. The beads were then saturated in 12 µl of sample buffer containing a reducing reagent and boiled for 5 min at 95°C in order to elute the proteins from the beads.

Samples were fractionated by gel electrophoresis using 4-12% Bis-Tris gels (Invitrogen). Samples were run at 140 mA for approximately 45 min. The gels were then transferred to nitrocellulose membranes using the Invitrogen iBlot system (Program 3, 6 min, 40 sec). Membranes were briefly rinsed in Tris buffered saline containing 0.2% tween (TBST). Membranes were blocked in 5% non-fat dried milk (NFDM) in TBST for 1 hour with gentile agitation at room temperature. Membranes were then incubated in primary antibody diluted in 2% NFDM overnight at 4°C with gentile agitation (Sigma rabbit anti-Med8, polyclonal, 1:1000, HPA028377; Abnova mouse anti-Med17 (CRSP6), monoclonal, 1:500, H00009440-M02; BioLegend rabbit anti-Elongin C, polyclonal, 1:500, 613101; Santa Cruz rabbit anti-Elongin B, polyclonal, 1:500, sc-11447; Abcam rabbit anti-Rbx1 (Roc1), monoclonal, 1:1000, ab133565; Santa Cruz rabbit anti-Sp3, polyclonal, 1:200, sc-644; Cell Signaling mouse anti-RPS6, monoclonal, 1:200,

mAB2317; Millipore mouse anti-Gapdh, monoclonal, 1:20,000, MAB374). The following day, membranes were washed three times for 15 min in TBST. Membranes were incubated in secondary antibody for 1 hour with gentile agitation at room temperature in 2% NFDM (All from Jackson Immuno research; Donkey anti-mouse HRP, donkey anti-rabbit HRP). Membranes were washed three times for 20 minutes to remove excess antibody. Immunoblots were incubated for 1 min in Western Lighting® Plus-ECL (PerkinElmer). Proteins were visualized by exposing the blots to Blue Basic Autorad film (GeneMate) for 30 sec - 5 min, and developed using the Mini-Medical 90 film processor from AFP Imaging. Film was then scanned using an Epson Perfection V500 Photo scanner for further analysis.

2.9 Fluorescent in situ hybridization

In situ probe creation

The following primers were used to create the in situ probe using whole hippocampus cDNA as a template: Med8: forward 5'-GACCTGGCCCTCTGTCCT-3' & reverse 5'-CTTGCCGAAAGCCTGTGT-3'. Primers were designed using Primer 3. PCR products were cloned into pCRII-TOPO using the TOPO TA Cloning Kit (Invitrogen). Insert sequences were verified with Sanger sequencing. Based on insert orientation, NotI or SpeI restriction endonucleases (NEB) were used to linearize the vector prior to *in vitro* transcription. Probes were synthesized using digoxigenin-11-UTP (Roche) and T7 or SP6 RNA Polymerase (NEB) according to the manufacturer's instructions. Template DNA was removed with TURBO DNase (Applied Biosystems) according to the manufacturer's instructions.

FISH

Dual FISH and IHC labeling was performed as previously described on Thy1-YFP mice. Brain tissue was prepared as detailed in the Immunohistochemistry section, but under RNase-free conditions. Selected 20 μm brain sections were mounted on HistoBond slides (VWR), desiccated overnight at 42˚C, washed in DEPC-PBS, and then incubated in a Proteinase K wash (50 mM Tris pH 8.0, 25 mM EDTA, 160 mL DEPC-dH20, 200 μg Proteinase K) for 30 minutes at 37˚C. The slides were washed again in DEPC-PBS and transferred to 0.25% acetic anhydride in 0.1M triethanolamine for 10 minutes. Sections were briefly washed in DEPC-PBS and dried at room temperature. The hybridization was performed overnight at 52°C using a humidified, temperature controlled chamber (Boekel Slide Moat Model #240000) in hybridization buffer (50% formamide, 2X SSC, 1X Denhart's solution, 0.25M Tris pH 8.0, 10 mM DTT, 0.5% SDS, 10% dextran sulfate, 265 μg/ml salmon sperm DNA) containing the digoxigenin-labeled probe diluted at 1:50. Slides were washed in 1X SSC, treated with RNase A (Sigma) for 1 hour at 37°C, washed with 1X SSC followed by 0.5X SSC at room temperature, and then washed three times with 0.1X SSC at 65°C.

Tissue was prepared for labeling by incubating for 15 minutes at room temperature in 0.5% hydrogen peroxide and 0.5% Triton X in PBS. Slides were then washed three times in PBS. After a ten minute incubation in maleic acid buffer (100 mM maleic acid, 150 mM NaCl, pH 7.5) at room temperature, tissue was blocked for 10 minutes at room temperature in 1% blocking solution (Roche). Primary antibody (Roche Anti-Digoxigenin-POD 1:100, Invitrogen Rabbit Anti-GFP 1:2000) incubation was performed overnight at 4°C in 1% blocking solution. After three ten minute washes in

PBS, the slides were incubated 30 minutes at room temperature in a biotinylated tyramide solution consisting of 8.25% hydrogen peroxide in PBS (biotinylated tyramide prepared according to Perkin Elmer TSA Biotin kit instructions). After a 30 minute incubation at room temperature, slides were washed 3 times for 10 minutes in PBS at room temperature. Secondary antibody (Invitrogen Alexa-Strep-488 1:500, Jackson Immuno Research Cy3-AffiniPure Goat Anti-Rabbit IgG 1:2000) incubation was performed for 2 hours at room temperature in 1% blocking solution. Slides were washed in PBS for 10 minutes, dried, and then mounted with ProLong Gold with DAPI (Life Technologies).

2.10 Statistical analysis

All data were analyzed using GraphPad Prism 6 software. Error bars represent +/- SEM. Comparisons between groups were done using one-tailed t-tests for normally distributed variables, and differences were considered statistically significant at $P<0.05$.

Chapter 3:

An inducible EGFP-L10a expressing mouse line for cell-type specific gene expression profiling

The content of chapter 3 was originally published in *Frontiers in Molecular Neuroscience*, 2014; 7(82) as "A transgenic mouse line for collecting ribosome-bound mRNA using the tetracycline transactivator system." Authors on the manuscript were Laurel Drane, Joshua Ainsley, Mark Mayford, and Leon Reijmers. Figures and text are published here in accordance with the copyright parameters set by Frontiers (http://www.frontiersin.org/Copyright.aspx).

3.1 Overview

Revealing the molecular identities of individual cell-types through gene expression profiling can contribute to the functional understanding of these cell-types. However, obtaining gene expression profiles of defined neuronal cell-types is challenging, as a significant proportion of neuronal mRNA is located in small processes that are intermingled with other cell-types. This challenge has been resolved with the Translating Ribosome Affinity Purification (TRAP) technique, which enables the collection of epitope-tagged ribosomes and associated mRNA from both the soma and processes of genetically defined neuronal cell-types. We created new mouse lines that expand the number of brain cell types for which gene expression profiles can be acquired using the TRAP method.

3.2 Generation of a mouse line that expresses EGFP-L10a under control of the tetO promoter

In order to better understand the gene expression profiles within individual cell-types, we generated a transgenic mouse expressing the ribosomal protein L10a tagged with enhanced green fluorescent protein (EGFP) under the control of the tetracycline operon (tetO-TRAP) (Figure 3.1A, see methods). After screening multiple founder lines, one line was selected for further use. To test the ability of our tetO-TRAP mouse line to express EGFP-L10a in a tTA-dependent manner, we crossed the tetO-TRAP mouse with a Camk2a-tTA mouse to create a mouse that expresses EGFP-L10a under the Camk2a promoter (Camk2a-TRAP) (Figure 3.1B). Previous work using the same Camk2a-tTA drive line resulted in strong transgene expression in the CA1 region of the hippocampus (but not CA3 or dentate gyrus) as well as strong expression throughout the striatum (Mayford, Bach, et al., 1996). Immunohistochemical analysis of brain sections from 3 month old Camk2a-TRAP mice revealed a similar expression pattern (Figure 3.1C). The CA1 region of the hippocampus showed strong expression of EGFP-L10a, while the CA3 and dentate gyrus did not express EGFP-L10a (Figure 3.2A). Strong EGFP-L10a expression was also observed in the striatum, and appeared restricted to medium spiny neurons that are known to express Camk2a (Figure 3.2B). In addition, analysis of the amygdala revealed sparse EGFP-L10a expression in the basal subdivision, presumably in projection neurons known to express Camk2a (Figure 3.2C). The lack of EGFP-L10a expression in other types of neurons known to express Camk2a is due to a more restricted expression of tTA, presumably due to the genomic integration site of the Camk2a-tTA transgene (Mayford, Bach, et al., 1996). Expression of EGFP-L10a in Camk2a-TRAP

mice was tTA-dependent, as single transgenic tetO-TRAP mice did not express any EGFP-L10a in the brain (data not shown).

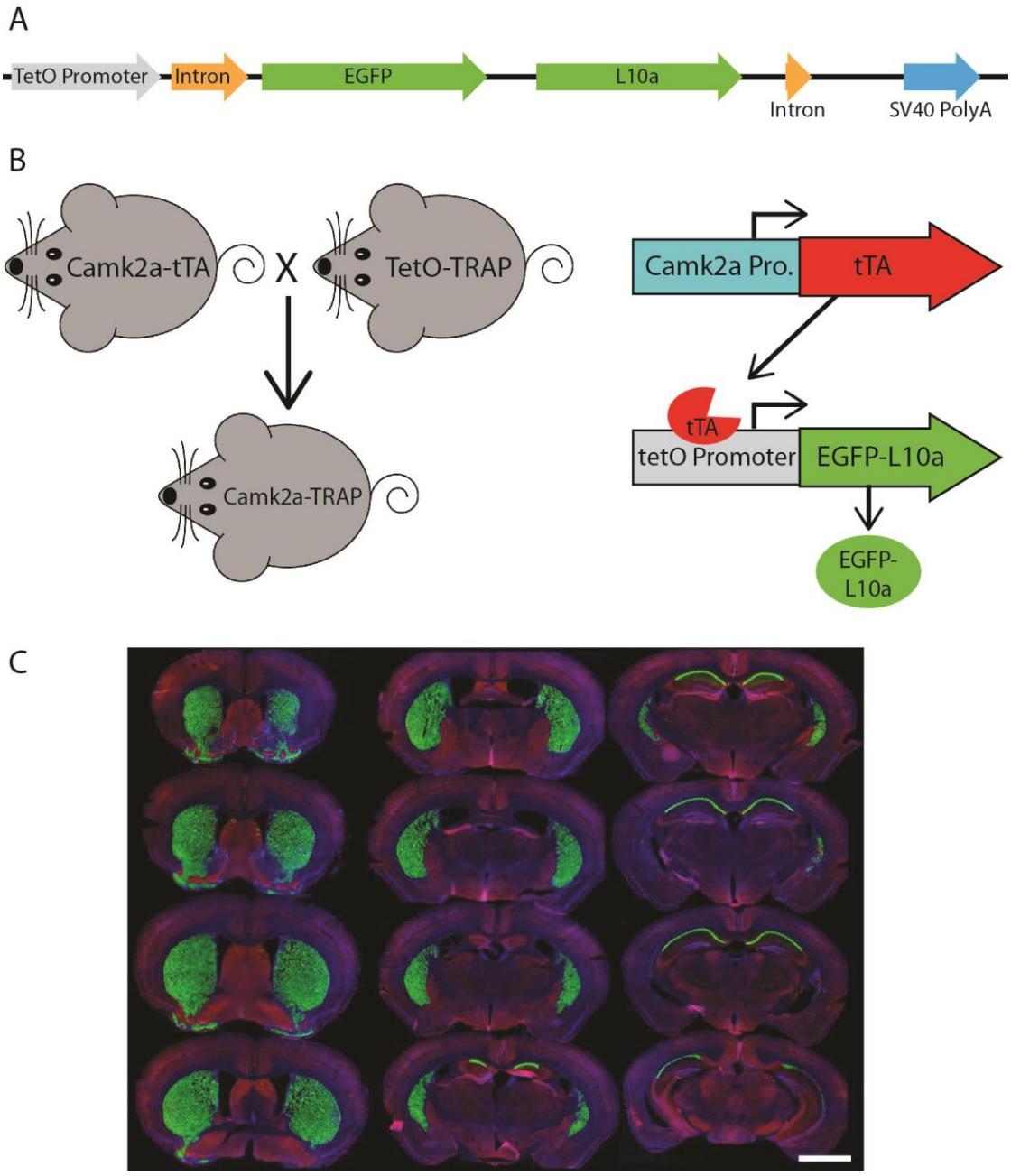

Figure 3.1

Generation of a tetO driven EGFP-L10a transgenic mouse. (A) Construct used to create the tetO-TRAP mouse line. (B) Model of the Camk2a-TRAP mouse. Camk2a-tTA mice were bred with tetO-TRAP mice to create the Camk2a-TRAP mice. Expression of

tTA under control of the Camk2a promoter leads to activation of the tetracycline response element (tetO) to drive expression of EGFP-L10a only in cells expressing Camk2a. (C) EGFP-L10a expression throughout the brain of a 3 month old Camk2a-TRAP mouse kept on food without doxycycline throughout life. Green = EGFP-L10a, red = Gad1, blue = DAPI. Scale bar, 2mm.

In order to confirm the cell-type specificity of EGFP-L10a expression in the Camk2a-TRAP mice, we performed immunostaining for Gad1, a marker of inhibitory interneurons, as well as Gfap, an astrocyte marker. No overlap of EGFP-L10a with either Gad1 or Gfap was seen in the CA1, confirming that the transgene was not expressed in CA1 interneurons or astrocytes (Figure 3.2D-G). In summary, the expression data from Camk2a-TRAP mice confirm cell-type specific tTA-dependent expression of EGFP-L10a, thereby validating proper transgene functioning in the tetO-TRAP mouse line.

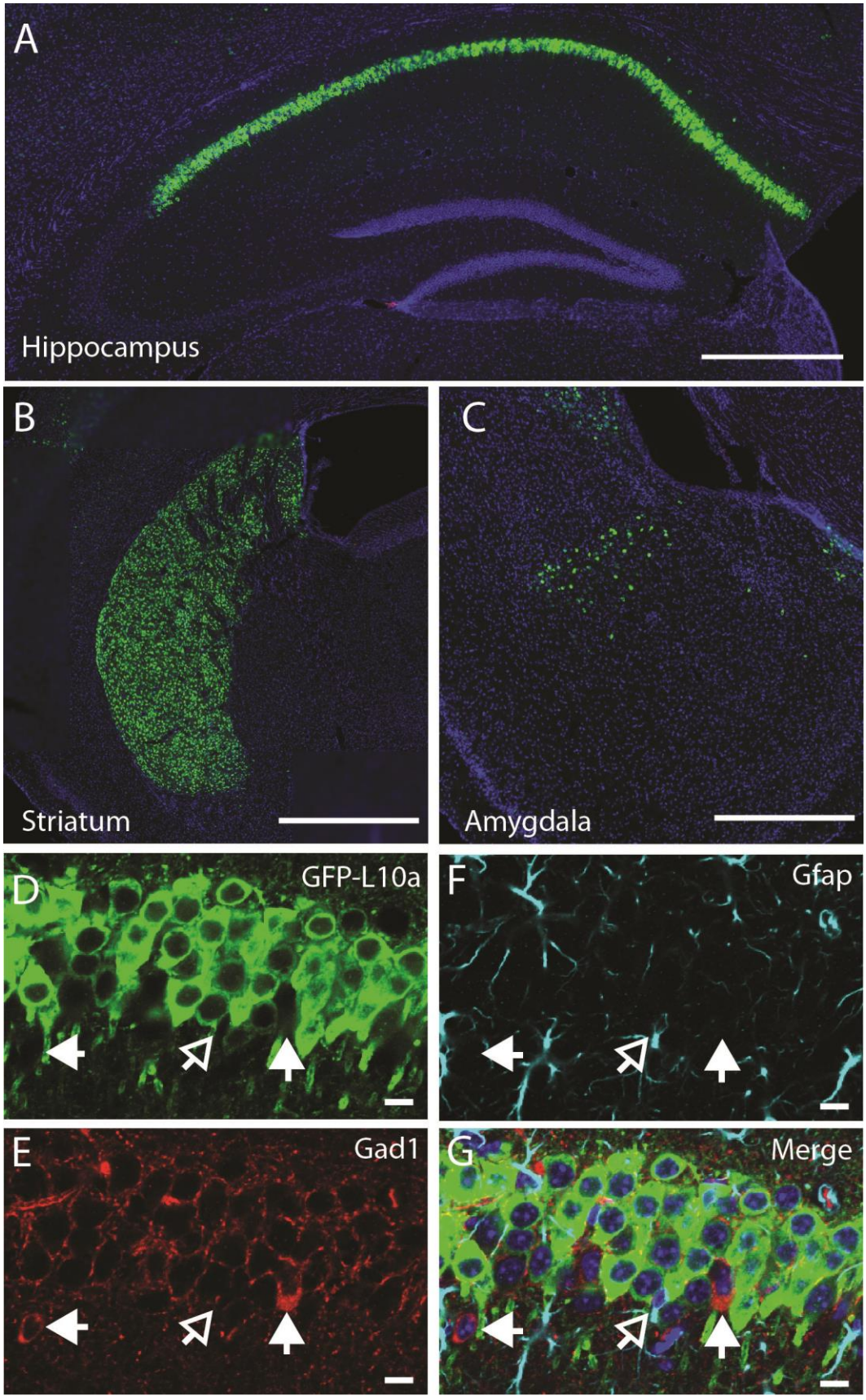
A
Hippocampus
B
Striatum
C
Amygdala
D
GFP-L10a
F
Gfap
E
Gad1
G
Merge

Figure 3.2

EGFP-L10a expression in the Camk2a-TRAP mouse line. (A) EGFP-L10a is highly expressed in pyramidal neurons of the CA1 region of the hippocampus. No EGFP-L10a is seen in the CA3 or dentate gyrus. Scale bar, 0.5mm. (B) EGFP-L10a expression in medium spiny neurons of the striatum. Scale bar, 0.5mm. (C) EGFP-L10a is sparsely expressed in projection neurons of the basal amygdala. Scale bar 0.5mm. (D-G) EGFP-L10a is expressed exclusively in Camk2a expressing pyramidal neurons of the CA1 region of the hippocampus. No overlap of EGFP-L10a was observed with the interneuron marker Gad1, marked by filled in arrows (E), or the astrocyte marker Gfap, marked by the opened arrow (F). (D) EGFP-L10a, (E) Gad1, (F) Gfap, (G) Merge (including DAPI, blue). (D-G) scale bars, 10μm.

3.3 Collection of ribosome-bound mRNA from CA1 pyramidal neurons in the Camk2a-TRAP mouse

To ensure that the EGFP-L10a expressed by Camk2a-TRAP mice integrates into ribosomal complexes, we performed a Co-IP of EGFP-L10a, and probed for a member of the small ribosomal subunit, RPS6. Co-IP of RPS6 would indicate that EGFP-L10a had successfully integrated into the large ribosomal complex, and that this large ribosomal complex was subsequently able to associate with the small ribosomal complex to form a complete ribosome. Immunoprecipitation of EGFP-L10a from whole brain lysate resulted in the Co-IP of RPS6, indicating functional integration of EGFP-L10a into whole ribosomes (Figure 3.3A). RPS6 was not Co-IPed when using a single transgenic animal that did not express EGFP-L10a, confirming the specificity of the Co-IP.

The immunohistochemical analysis of Camk2a-TRAP mice revealed that EGFP-L10a is expressed in excitatory pyramidal cells of the CA1, but not in interneurons or astrocytes in the CA1 or in other subregions of the hippocampus (Figure 3.2). To

determine if this expression pattern enabled the collection of cell-type specific mRNA from CA1 pyramidal neurons, we attempted to collect ribosome-bound mRNA from whole hippocampal lysate of Camk2a-TRAP mice. Neuronal activation increases the association of mRNA with ribosomes (Ainsley et al., 2014; Buxbaum et al., 2014; Job & Eberwine, 2001; Niere, Wilkerson, & Huber, 2012; Weiler & Greenough, 1991, 1993). We therefore subjected all of our animals to a 500 second long contextual fear conditioning trial before tissue collection. The quality of the ribosome-bound mRNA isolated from Camk2a-TRAP mice was analyzed using an RNA Bioanalyzer. Fear conditioned single transgenic Camk2a-tTA animals subjected to the TRAP IP were used as negative controls. Bioanalyzer analysis of Camk2a-TRAP RNA samples revealed the presence of high-quality RNA as indicated by a high RNA Integrity Number (RIN). The RIN value is calculated based on the entire electrophoretic trace of the RNA sample, and takes into account the quantity of RNA degradation (Mueller, Lightfoot, & Schroeder, 2004). No RNA was detected in TRAP IP samples from single transgenic mice, confirming the specificity of our TRAP IP protocol (Figure 3.3B). The Camk2a-TRAP RNA sample contained both rRNA and mRNA. This confirmed that the TRAP IP collected ribosomes (which contain rRNA) bound to mRNA, in agreement with the incorporation of EGFP-L10a into functional translating ribosomes.

Within the hippocampus, EGFP-L10a is only expressed in CA1 pyramidal neurons, so we expected to see an enrichment of transcripts expressed in CA1 pyramidal neurons in the TRAP IP samples, as well as a depletion of genes expressed completely or predominantly outside of CA1 pyramidal neurons. We therefore performed a quantitative real-time polymerase chain reaction (qPCR) analysis of two genes not expressed in CA1

pyramidal neurons (Gad1 and Gfap), one gene expressed predominantly outside of CA1 pyramidal neurons (Pkia), and two genes that are widely expressed in CA1 pyramidal neurons (Camk2a and Naa38) (Figure 3.3C) (Lein et al., 2007). ΔΔct values were calculated using β-actin as a reference gene. Only the two genes known to be widely expressed in CA1 pyramidal neurons were enriched in the IP samples, while the other genes showed a marked depletion (Figure 3.3D). In summary, our data show that Camk2a-TRAP mice enable the cell-type specific collection of ribosome-bound mRNA from CA1 pyramidal neurons.

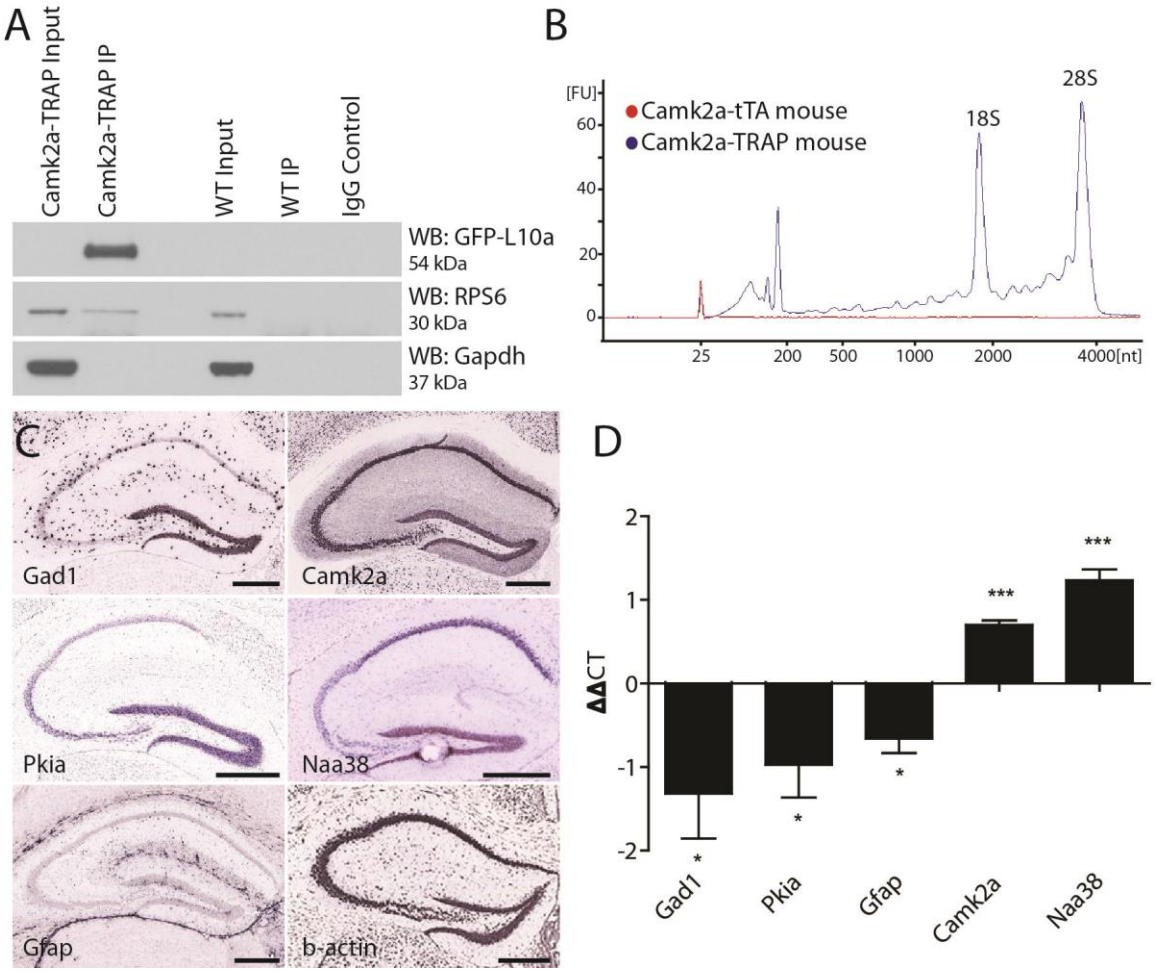

Figure 3.3

Cell-type specific collection of ribosome-bound mRNA using the Camk2a-TRAP mouse. (A) Representative affinity purification of EGFP-L10a and co-immunoprecipitation of the small ribosomal protein RPS6 from whole brain lysate of Camk2a-TRAP animals (N = 6), and wild type littermate controls (WT) (N = 6). 2.5% of each sample was used for input prior to the IP. EGFP-L10a is only visible in the IP lane of the Camk2a-TRAP mice because the IP samples were highly concentrated compared to the input lanes. No RPS6 was co-purified from wild type samples that did not contain EGFP-L10a. The IgG control lane confirms the absence of IgG contamination artifacts. (B) Representative bioanalyzer plot of RNA samples from Camk2a-TRAP (blue; RIN mean ± SEM, 7.48±0.14, N = 7) and single transgenic littermates (red; RIN mean ± SEM, 2.2±1.2, N = 3) indicating successful isolation of ribosome-bound RNA from Camk2a-TRAP mice, but not single transgenic controls. mRNA is represented by the area under the curve between 200nt and 4000nt, with the 18S and 28S peaks representing rRNA present in the affinity purified ribosomes. The peaks between 25-200nt represent small rRNAs and tRNAs, as well as highly degraded mRNA typically seen with Trizol

extraction protocols. (C) *In Situ* hybridization images from the Allan Brain Atlas showing localization of genes used for qPCR analysis. Two negative control genes (Gad1, and Gfap) are not expressed in CA1 pyramidal neurons, and one negative control gene (Pkia) is mainly expressed outside of CA1 pyramidal neurons. Positive control genes (Camk2a and Naa38) are widely expressed in CA1 pyramidal neurons. Beta-actin is expressed in all cell-types throughout the hippocampus and was therefore used as a housekeeping gene for ΔΔCt analysis. Scale bars, 0.42 mm. (Lein et al., 2007). (D) qPCR analysis of mRNA collected with the TRAP protocol from Camk2a-TRAP animals. Negative control genes (Gad1, Pkia, and Gfap) all showed a significant depletion from the IP samples, while positive control genes (Camk2a and Naa38) both showed significant enrichment in the IP samples. (One tailed T-test with mu = 0. *P<0.05, **P<0.01, ***P<0.001) (Gad1 P=0.046, Pkia P=0.045, Gfap P=0.016, Camk2a P=0.0005, Naa38 P=0.001). N = 3.

3.4 Creation of an activity-induced EGFP-L10a mouse line

After validation of the Camk2a-TRAP mouse line, we used the tetO-TRAP mouse to create a second TRAP mouse model that enables the activity-induced expression of EGFP-L10a. For this purpose, we crossed the tetO-TRAP mouse line with a Fos-tTA mouse to drive expression of EGFP-L10a under control of the activity-regulated Fos promoter (Fos-TRAP mouse). Fos is an immediate early gene (IEG) whose promoter is rapidly activated upon neuronal stimulation (Flavell & Greenberg, 2008). Accordingly, the Fos-tTA mouse can trigger expression of tetO-regulated reporter proteins in activated neurons, including activated CA1 pyramidal neurons (Matsuo, Reijmers, & Mayford, 2008; Reijmers, Perkins, Matsuo, & Mayford, 2007; Tayler, Tanaka, Reijmers, & Wiltgen, 2013). The Fos-tTA mouse is also referred to as the TetTag mouse, which stands for “Tet”racycline controlled “Tag”ging. The time-window during which tagging of activated neurons occurs is opened by the removal of doxycycline (dox) from the food, after which Fos-promoter driven tTA can bind to the tetO promoter. The time-window is

closed by adding dox back to the food, after which dox prevents binding of tTA to the tetO promoter (Figure 3.5A).

Successful mRNA isolation by TRAP requires high expression levels of EGFP-L10a, since this fusion protein has to out-compete endogenous L10a for its incorporation into ribosomes. However, the Fos promoter is activated for only a short period of time after neuronal activation. We were concerned that the brief period of Fos promoter activation would not drive sufficient EGFP-L10a expression for successful mRNA isolation using the TRAP technique. A previous study characterizing tetO-driven transgene expression found that mice bred and raised in the absence of dox later showed higher expression levels of the transgene when compared to mice bred and raised in the presence of dox (Bejar, Yasuda, Krugers, Hood, & Mayford, 2002). One explanation for this phenomenon is that the expression of the tetO-driven transgene during brain development might prevent its epigenetic silencing. To prevent potential epigenetic silencing, we bred and raised Fos-TRAP mice in the absence of dox, put the mice on food with dox after weaning, and then waited until all the developmentally expressed EGFP-L10a was degraded. For this, we first needed to determine for how long Fos-TRAP mice had to be kept on food with dox in order to achieve complete degradation of EGFP-L10a. We found that a period of six weeks of dox following high developmental EGFP-L10a expression was sufficient for the complete degradation of EGFP-L10a in Camk2a-TRAP mice (Figure 3.4A-C).

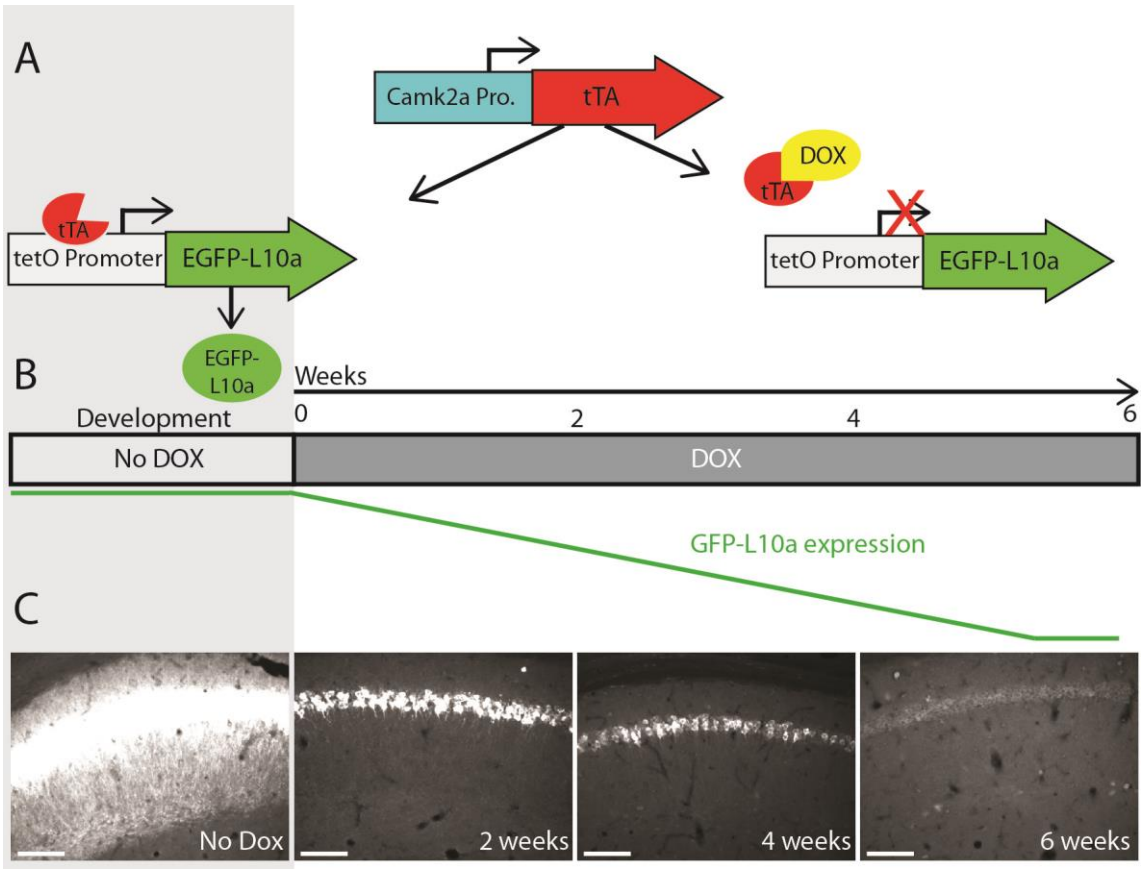

Figure 3.4

Complete degradation of developmentally expressed EGFP-L10a requires six weeks. (A) Schematic representation of dox control over EGFP-L10a expression in the Camk2a-TRAP mouse model. In the absence of dox, tTA is able to bind to the tetO promoter and drive EGFP-L10a expression. In the presence of dox, tTA is no longer able to activate the tetO promoter, thereby preventing any further expression of EGFP-L10a. (B) Experimental design showing the time-points of brain dissection after adding dox, and the anticipated level of EGFP-L10a protein. (C) Images of the CA1 region of the hippocampus show that depletion of high levels of EGFP-L10a takes six weeks of continuous dox. Scale bar, 100 µm. N = 1 for each time-point.

To determine if the Fos-TRAP mouse line can be used for the activity-induced expression of EGFP-L10a, we compared EGFP-L10a expression in home cage (HC) animals versus animals that underwent a fear conditioning trial (FC). Fos-TRAP mice were bred and raised without dox to prevent potential epigenetic silencing, and were kept on dox for at least six weeks following weaning to allow complete degradation of all developmentally expressed EGFP-L10a. We removed dox from the diet of both FC and HC animals on day -3 of the experiment, and subjected the FC group to fear conditioning on day 0 (Figure 3.5A-B). At the end of day 0, both HC and FC mice were put back on dox, and brains were dissected on day 3. Comparison of the HC and FC animals revealed an increase in the number of EGFP-L10a expressing cells in the CA1 of the hippocampus of the FC group as compared with the HC group (Figure 3.5C-E), in agreement with an earlier study that used Fos-tTA x tetO-histoneGFP mice (Tayler et al., 2013). Therefore, the increased neuronal activation in the CA1 caused by FC resulted in the predicted increase in EGFP-L10a expression. In addition, analysis of cell-type specificity of EGFP-L10a expression found no overlap of EGFP-L10a with the interneuron marker Gad1, revealing that EGFP-L10a expression in the CA1 is specific to pyramidal neurons (Figure 3.5F-I). The Fos-TRAP mouse can therefore be used to drive EGFP-L10a expression in CA1 pyramidal neurons that are activated during a behavioral test.

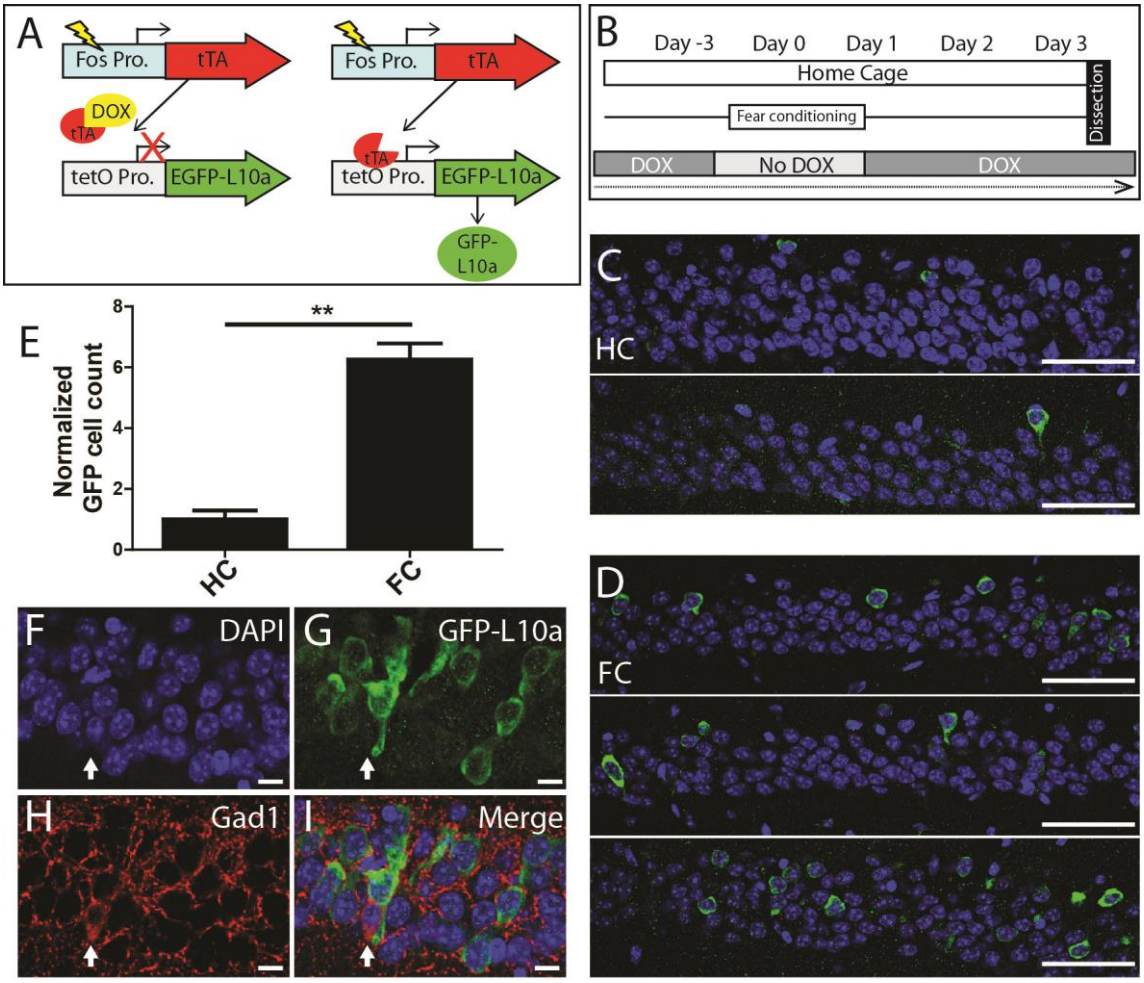

Figure 3.5

Creation and characterization of the Fos-TRAP mouse line. (A) Schematic of the Fos-TRAP mouse model. Activation of the activity-induced Fos promoter induces tTA transcription. When present, dox binds to tTA and prevents it from interacting with the tetO promoter. Removal of dox enables tTA to bind to the tetO promoter and drive expression of EGFP-L10a. (B) Experimental design. Mice were given dox chow for at least six weeks after weaning to enable complete degradation of developmentally expressed EGFP-L10a. On day -3, dox was removed from the diet. FC was done in the absence of dox on day 0 to allow EGFP-L10a expression in activated neurons. Following FC, all animals were put back on dox to prevent further EGFP-L10a transcription. Brains were collected on day 3 to allow time for EGFP-L10a protein accumulation. (C-D) EGFP-L10a expression in pyramidal cells of the CA1 region of the hippocampus in (C) HC (N = 2) and (D) FC (N = 3) Fos-TRAP mice. Scale bar, 50µm. (E) Quantification of EGFP-L10a expressing cells from C-D. The number of EGFP-L10a expressing cells was normalized to the number of DAPI positive cells within the area analyzed. (F-I) EGFP-

L10a expression in the CA1 of Fos-TRAP mice was restricted to pyramidal cells. Mice were bred and raised off dox to allow for maximal EGFP-L10a expression. No overlap of EGFP-L10a was observed with the interneuron marker Gad1, marked by the filled in arrow (H). Scale bars, 10μm. (F) DAPI, (G) EGFP-L10a, (H) Gad1, (I) merge.

Chapter 4:

Screen for locally translated dendritic mRNAs

Figures 4.1-4.5 were adapted from a manuscript originally published in *Nature Communications* 2014; 5 as "Functionally diverse dendritic mRNAs rapidly associate with ribosomes following a novel experience." Authors on the manuscript were Joshua Ainsley, Laurel Drane, Jonathan Jacobs, Kara Kittelberger, and Leon Reijmers. Figures and text are reproduced here in accordance with the copyright parameters set by Nature Publishing Group (http://www.nature.com/reprints/permission-requests.html). My specific contributions included TRAP optimization experiments to test mRNA background binding using different types of beads (figure 4.1). Fear conditioning followed by dendritic dissections (figure 4.2, 4.3 A-B). I performed TRAP IPs for many of the dendritic dissections as well as performing cDNA preparations, and qPCR confirmations. I optimized the FISH protocol as well as created probes and performed FISH experiments (figure 4.5). In addition, I contributed to the scientific discussion in regard to the manuscript, as well as helping with manuscript editing before submission.

4.1 Overview

For this study we were interested in better understanding the subcellular localization and translation of messenger ribonucleic acid (mRNA). In neuronal dendrites, local translation of mRNA provides a rapid and specific mechanism for synaptic plasticity and memory formation. Despite the widely accepted importance of dendritic mRNA translation, little is known about which mRNAs are translated in dendrites *in vivo* and when their translation occurs. Studies have shown that an intact hippocampus is required for contextual fear learning to take place (Anagnostaras, Gale, &

Fanselow, 2002). Within the hippocampus, CA1 pyramidal neurons are a major site of excitatory synaptic activity. We therefore collected ribosome-bound mRNA from the dendrites of CA1 pyramidal neurons in the adult mouse hippocampus. In doing so, we discovered the dendritic presence of various mRNAs that had previously been thought to be limited to the soma.

4.2 Optimization of the TRAP technique

We developed a strategy to collect *in vivo* dendritic mRNA from adult mouse brains using a combination of the translating ribosome affinity purification (TRAP) technique, along with the Camk2a-TRAP mouse line (described in chapter 3). Despite the success of the technique in its original publication (Doyle et al., 2008; Heiman et al., 2008), we decided to re-optimize the TRAP protocol in order to reduce background binding of mRNA. In order to optimize the protocol, we focused on the type of beads used during the immunoprecipitation. Originally, the TRAP protocol used protein G coated beads coupled with a GFP antibody. We compared protein G beads to two other types of beads, protein L beads and a bead with a glycidyl ether (epoxy) reactive group allowing for covalent attachment of the antibody to the bead, in order to try and reduce the amount of background mRNA binding from cell-types that do not express EGFP-L10a that we saw when using the original protocol.

Whole brain lysate from double transgenic Camk2a-TRAP animals and single transgenic tetO-TRAP animals were subjected to a TRAP-IP using protein G, protein L, or epoxy beads. mRNA pull-down was analyzed using a bioanalyzer to measure RNA

quantity. Using Camk2a-TRAP mice, all three beads were able to successfully pull-down ribosome-bound mRNA (Figure 4.1A). When looking at background levels of mRNA pull-down using single transgenic mice, the epoxy beads showed the lowest level of background contamination (Figure 4.1B). In addition to binding the GFP antibody to protein G or L beads ourselves, we tested both ChemoTek GFP-Trap magnetic (GFP-Trap_M) and GFP-Trap agarose (GFP-Trap_A) beads in which the beads come already bound to a GFP antibody. Using double transgenic mice, GFP-Trap_M, GFP-Trap_A, and epoxy beads were all able to successfully isolate ribosome-bound mRNA (Figure 4.1C). When using single transgenic mice to assess background mRNA contamination, the epoxy beads were superior to the other beads in reducing background mRNA contamination (Figure 4.1D). Of the five types of beads tested, the epoxy beads showed the lowest level of background contamination; therefore all experiments going forward were done using epoxy beads.

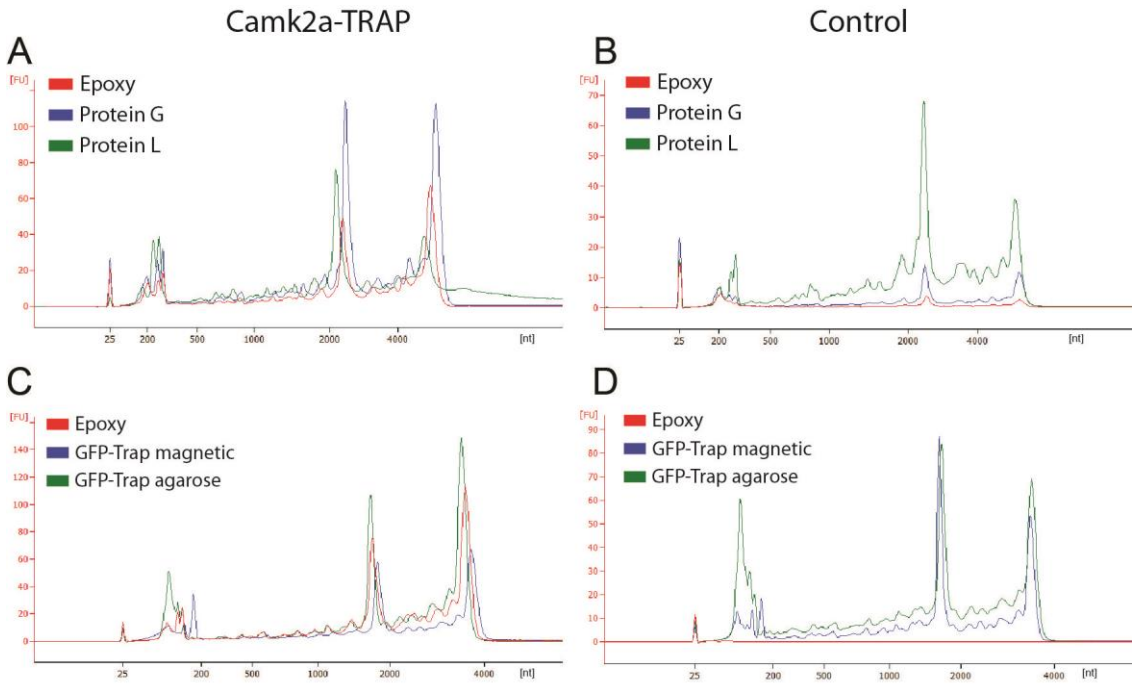

Figure 4.1

Optimization of collection of ribosome-bound mRNA to improve background mRNA immunoprecipitation. Representative Bioanalyzer traces comparing RNA levels for EGFP immunoprecipitation protocols. (A-B) Comparison of EGFP immunoprecipitation protocols either using Protein G or Protein L-coated magnetic beads to bind the anti-GFP antibodies or using a glycidyl ether (epoxy) reactive group to covalently link the antibody to the bead. (A) 10% of a Camk2a-TRAP double transgenic whole brain homogenate was used as input. (B) 10% of a tetO-TRAP single transgenic whole brain homogenate was used as input as a background control. The epoxy beads resulted in the lowest background level. (C-D) Comparison of GFP-Trap magnetic and agarose beads (ChemoTek) with epoxy beads. (C) 10% of a Camk2a-TRAP double transgenic whole brain homogenate was used as input. (D) 10% of a tetO-TRAP single transgenic whole brain homogenate was used as input. The epoxy beads again resulted in the lowest background level.

4.3 Collecting ribosome-bound mRNA from in vivo dendrites

In order to isolate dendritic mRNA without contamination from somatic transcripts, we developed a novel method for collecting ribosome-bound mRNA from *in vivo* dendrites. To do this, we took advantage of the unique architecture of the hippocampal CA1 region, where there are clear somatic and dendritic layers. Flash frozen brain tissue was cut into thin coronal sections. Using a 30-gauge blunt ended needle, tissue punches were collected from either the dendritic or the somatic layers of the CA1 (Figure 4.2A). Although punches taken from the dendritic layer contain the cell bodies of interneurons and glia, the TRAP technique allows for the specific collection of mRNA bound to EGFP-tagged ribosomes which are only expressed in the dendrites of pyramidal neurons in this area (Figure 4.2B). Within the Camk2a-TRAP mice, EGFP-L10a is clearly visible within dendrites of hippocampal CA1 pyramidal neurons (Figure 4.2C). This is in agreement with other studies showing the localization of ribosomes to neuronal dendrites (Ostroff et al., 2002; Steward & Levy, 1982). Since previous studies demonstrated the functional incorporation of EGFP-L10a into functional translating ribosomes (Doyle et al., 2008; Drane et al., 2014; Heiman et al., 2008), the observed dendritic expression pattern of EGFP-L10a suggested the possibility of collecting dendritic mRNA by immunoprecipitating dendritically localized EGFP-tagged ribosomes.

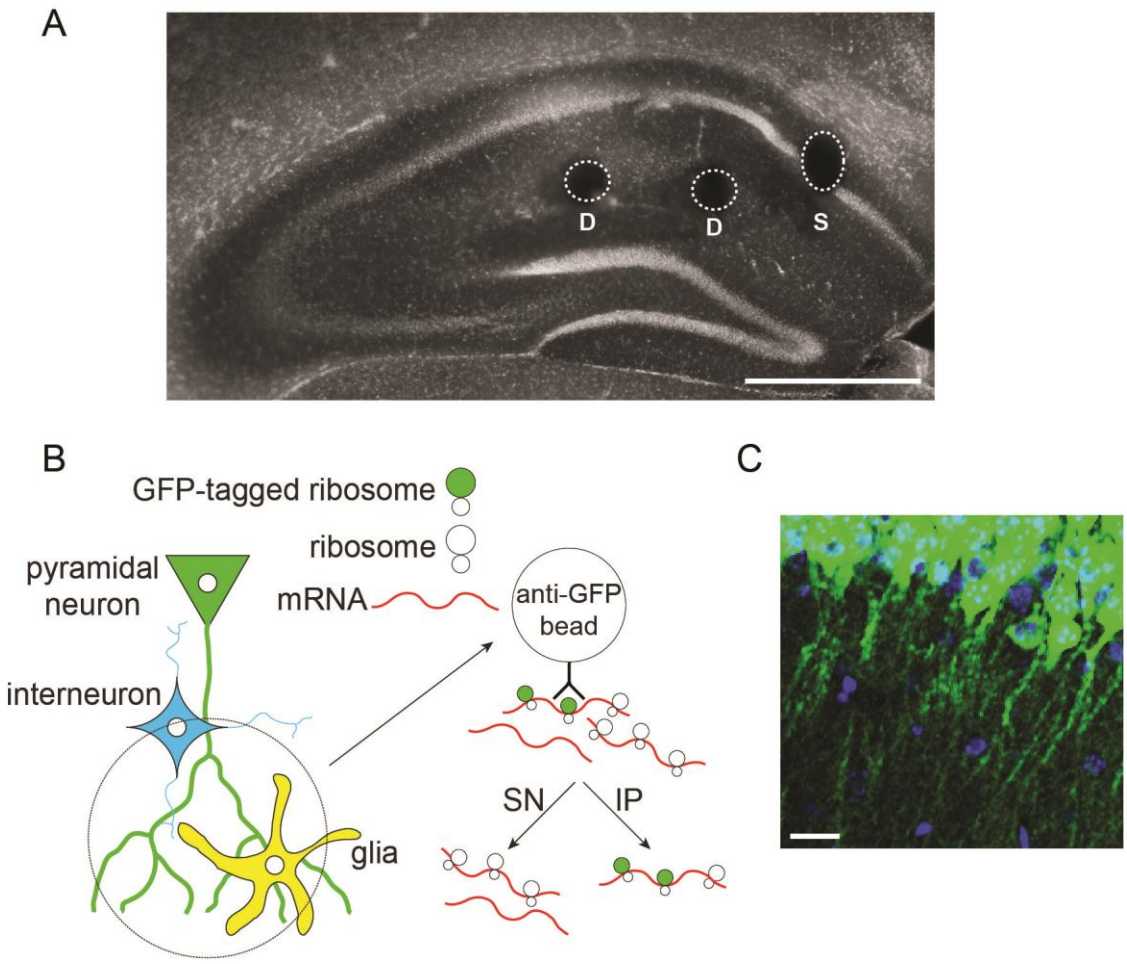

Figure 4.2

A novel method for collecting *in vivo* dendritic mRNA. (A) Representative example of the location of dendritic (D) and somatic (S) punches in the CA1 region of the hippocampus. A DAPI stain was used to visualize nuclei. Scale bar, 0.5 mm. (B) Diagram showing the approach used for collecting ribosome-bound mRNA from *in vivo* dendrites. The immunoprecipitate (IP) will contain mRNA bound to ribosomes in CA1 pyramidal neuron dendrites while the supernatant (SN) will contain mRNA from other sources. (C) EGFP-L10a is present in the dendrites of CA1 pyramidal neurons. Scale bar, 20 µm.

Previous *in vitro* studies have found that the association of dendritic mRNA with ribosomes changes after neuronal activation (Buxbaum et al., 2014; Job & Eberwine, 2001; Kao, Aldridge, Weiler, & Greenough, 2010; Smith, Starck, Roberts, & Schuman, 2005; Weiler & Greenough, 1991, 1993). Therefore, we fear conditioned (FC) all animals prior to mRNA collection. Camk2a-TRAP animals showed normal fear conditioning (Figure 4.3A). In addition, comparison of FC and home cage (HC) animals revealed that there was no difference in the total levels of EGFP-L10a present within hippocampal tissue. This was found by performing a qPCR to look at the amount of EGFP-L10a transcript within dendritic and somatic TRAP IP and SN samples (Figure 4.3B).

To assess the specificity of mRNA isolation from dendritic samples, we looked for the presence of a known dendritic mRNA, Camk2a, along with a glial cell marker, Gfap. In both FC and HC groups, qPCR analysis showed enrichment of Camk2a transcript in the IP fraction, while the glial gene Gfap showed enrichment in the supernatant fraction (Figure 4.3C). This showed that the TRAP-IP was specifically pulling down mRNA from EGFP-L10a containing dendrites, and not from surrounding tissue.

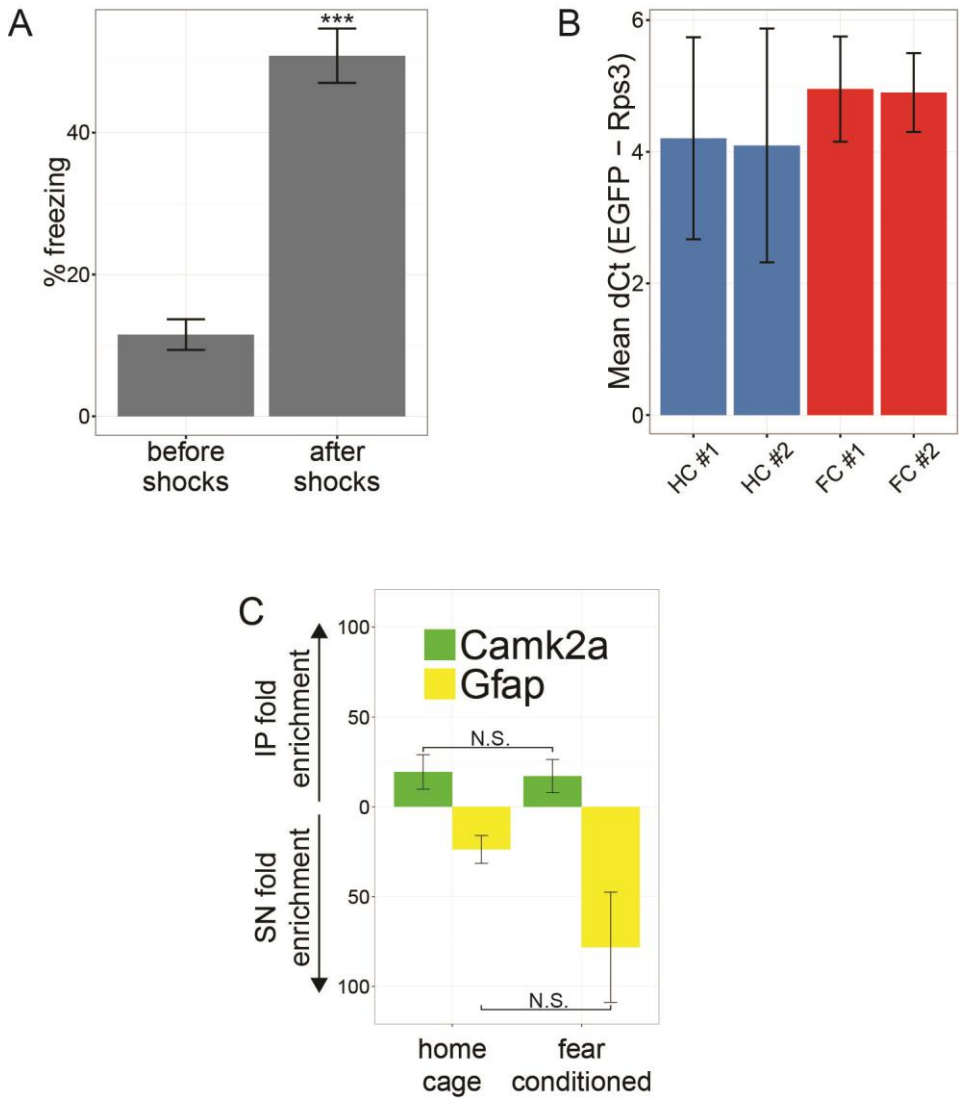

Figure 4.3

Assessment of TRAP protocol and quality. (A) Camk2a-TRAP transgenic mice showed normal fear conditioning. Average percent of time spent freezing for mice before-shocks (minute 2-3 of the protocol) and after-shocks (final 40 seconds of protocol). (n=8, error bars represent SEM, *** = $p<0.0001$ using paired t-test). (B) Home cage and fear conditioned mice had similar EGFP-L10a expression. EGFP-L10a expression was measured with qPCR and normalized to Rps3. Mean delta Ct (dCt) was calculated by averaging the dCt for the dendrite IP, dendrite SN, Soma IP, and soma SN for each individual mouse. Error bars represent SEM. (C) qPCR analysis of dendritic mRNA samples from home cage (n=6) and fear conditioned (n=5) mice confirms the expected IP enrichment of Camk2a and SN enrichment of the astrocyte-specific gene Gfap. Error bars represent SEM. NS = not significant.

4.4 Expected soma-restricted mRNAs can localize to dendrites

Both dendritic and somatic samples were collected from FC mice and subjected to our TRAP protocol in order to collect ribosome-bound mRNA. High-throughput RNA sequencing (RNA-Seq) was utilized in order to identify the mRNAs isolated using TRAP (Metzker, 2010). RNA-Seq was performed using the HiSeq2000. The quality of the sequencing was assessed using FastQC. Reads were aligned to the mm9 UCSC annotation of the mouse genome using STAR (version 2.1.1d) (Dobin et al., 2013). Unique read counts were determined using HTSeq (version 0.5.4p3) (Anders, Pyl, & Huber, 2015) and are annotated in table 4.1 along with the percentage of reads that mapped to the genome.

Mouse	Behavior	Location	Sample	Total Reads	STAR Alignments	STAR Uniques	% Mapped Reads
HC#1	HC	dendrite	IP	8177076	2448748	1445297	29.95
HC#1	HC	soma	IP	8857590	2569133	1638686	29.00
HC#1	HC	dendrite	IP	64774840	22663322	13839586	34.99
HC#1	HC	soma	IP	131280050	42852341	30592880	32.64
HC#2	HC	dendrite	IP	2217975	564322	298102	25.44
HC#2	HC	dendrite	SN	12639045	11777311	7344906	93.18
HC#2	HC	soma	IP	8546990	4763727	2058849	55.74
HC#2	HC	dendrite	IP	214610116	66945555	42993182	31.19
HC#2	HC	dendrite	SN	93163380	87606290	74757988	94.04
HC#2	HC	soma	IP	73420060	41391241	32773341	56.38
FC#1	FC	dendrite	IP	9107338	3614656	2402299	39.69
FC#1	FC	soma	IP	8285494	4566140	3667054	55.11
FC#1	FC	dendrite	IP	108448502	86803138	57233931	80.04
FC#1	FC	soma	IP	77679718	51637767	43115178	66.48
FC#2	FC	dendrite	IP	8874255	3025743	1788058	34.10
FC#2	FC	dendrite	SN	8632308	7966387	4587254	92.29
FC#2	FC	soma	IP	9308237	4525411	2729574	48.62
FC#2	FC	soma	SN	8134420	7646754	3891759	94.00
FC#2	FC	dendrite	IP	149105624	74577311	46498876	50.02
FC#2	FC	dendrite	SN	87811136	87791965	75868211	99.98
FC#2	FC	soma	IP	134445102	82517092	64079881	61.38
FC#2	FC	soma	SN	64056566	62358423	52178497	97.35

Table 4.1

Summary of samples used for RNA-Seq.

Assessment of the RNA-Seq data revealed that samples from fear conditioned mice yielded higher quality sequencing data with a higher percentage of reads that mapped to the genome. We therefore used Gene Ontology (GO) analysis to gain a more

comprehensive understanding of the types of mRNAs that can localize to dendrites in fear conditioned mice. As expected, somatic and dendritic samples showed different gene enrichment profiles (Figure 4.4A). Genes involved in translation and the cytoskeleton were the most enriched in the FC dendritic list, agreeing with previous reports and suggesting the importance of increased local translation and cytoskeleton remodeling in dendrites shortly after neuronal activation (Moccia et al., 2003). Unexpectedly, the dendritic list also showed enrichment in mRNAs encoding proteins known for their functions inside the nucleus, such as those involved in chromosome organization and transcriptional regulation. The list of dendritic mRNAs predicted by our unbiased classification included several gene families with well-known nuclear functions. This included a group of genes that are part of the transcriptional Mediator complex. Out of the 21 detected Mediator mRNAs, seven were predicted to be localized to dendrites. Of the seven found in the dendrites, Med8 was detected in the highest quantities as shown by the fragments per kilobase per million mapped reads (FPKM) values (Figure 4.4B).

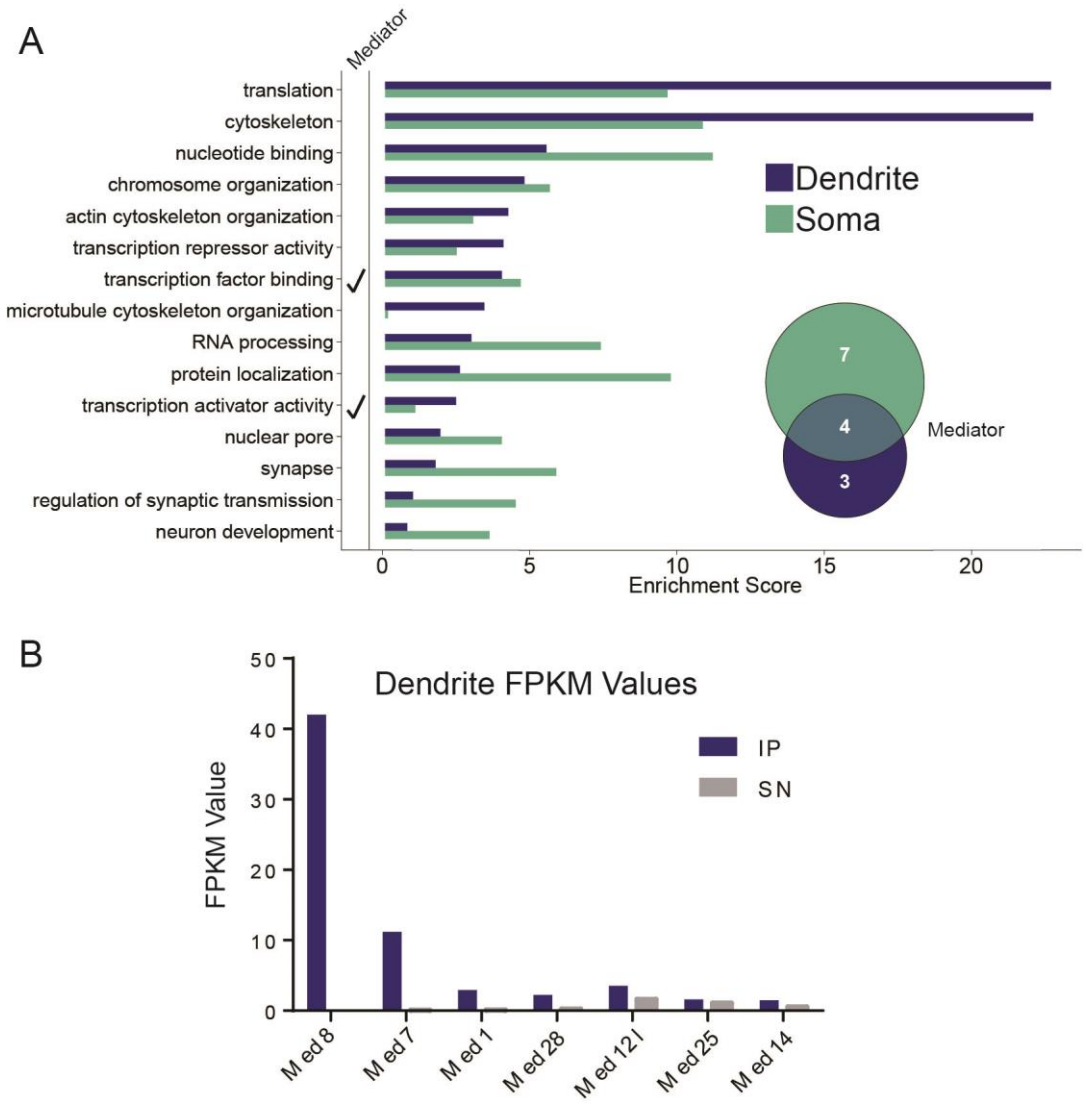

Figure 4.4

Gene ontology enrichment analysis reveals unexpected classes of ribosome-bound dendritic transcripts. (A) Gene ontology (GO) enrichment analysis of dendritic and somatic mRNAs. Dendritic mRNAs were highly enriched in translation and cytoskeleton GO categories. Unexpected GO categories with dendritic mRNA enrichment include chromosome organization and transcription factor binding. Venn diagram insets show the number of unique Mediator mRNAs that were detected in the RNA-Seq data as well as their classification. (B) Fragments per kilobase per million mapped reads (FPKM) values obtained from RNA-Seq showing the relative quantities of all Mediator mRNAs isolated from dendritic IP and SN samples.

In order to confirm the RNA-Seq data, a fluorescent *in situ* hybridization (FISH) of Med8 was performed in order to visualize the localization of dendritic mRNA. Dig-labeled sense and antisense RNA probes were designed against Med8 mRNA. FISH was performed on Thy1-YFP brain tissue where sparsely labeled pyramidal cells within the hippocampal CA1 express YFP protein, making it easy to see the entire outline of the cell. As expected from the RNA-seq data, Med8 mRNA can be seen within both the cell body and dendrites of Thy1-YFP labeled neurons (Figure 4.5). The absence of labeling when using the sense probe confirms the specificity of the FISH protocol.

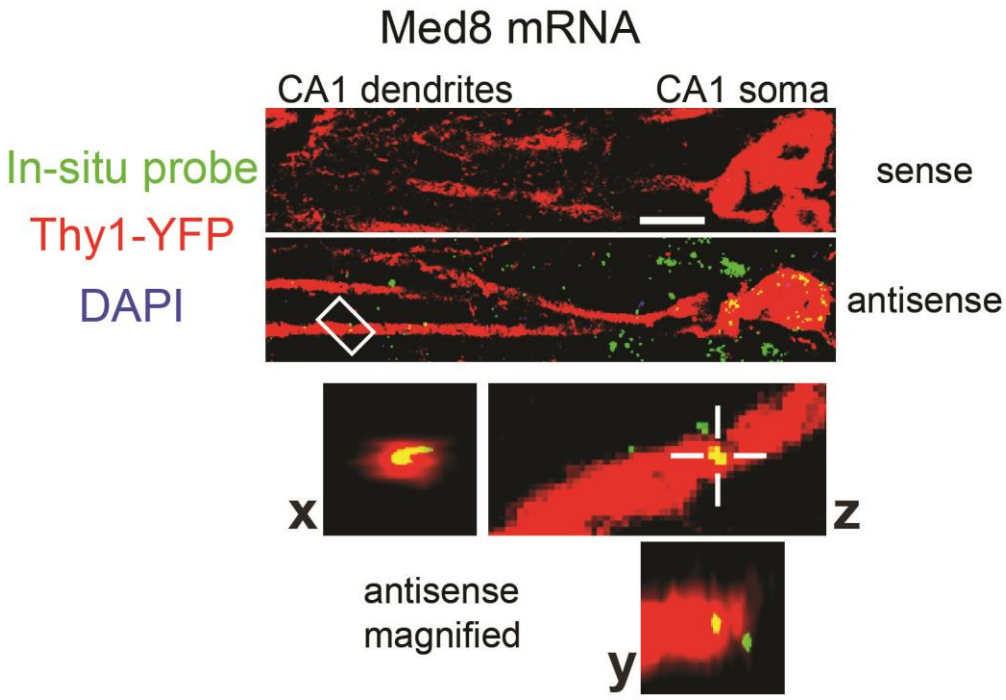

Figure 4.5

Dendritic localization of mRNA encoded by the transcription-associated gene Med8. Fluorescent *In situ* hybridization for Med8 shows puncta within YPF-labeled dendrites with the antisense probe, but not with the sense probe (green = Med8 probe, red = YFP, and blue = DAPI). The bottom panel shows magnified views of the area indicated in the white box. Views from all three angles show colocalization between Med8 mRNA and the YFP-labeled dendrite. Scale bar, 10 µm.

Chapter 5:

Presence of a ubiquitin ligase complex containing the Mediator subunit Med8 in the mouse brain

5.1 Overview

Med8 is a subunit of the Mediator protein complex, which plays an essential role in transcriptional regulation in all eukaryotes. In addition to its highly conserved role within the Mediator complex, Med8 in chordates contains a BC-box domain that enables it to form an E3 ubiquitin ligase complex by interacting with Elongins B and C, Cul2 and Rbx1. The functional significance of the Med8 ubiquitin ligase complex is unclear, because no tissues are known to endogenously contain this complex. We observed the presence of both Med8 mRNA and Med8 protein within the dendritic processes of pyramidal neurons in the mouse hippocampus, suggesting that Med8 might have a function outside of the nucleus. To test the possibility that this extra-nuclear function involves the Med8-ubiquitin ligase complex, we performed co-immunoprecipitation experiments using a Med8 antibody. This revealed that the mouse brain contains an endogenous Med8-ubiquitin ligase complex. The presence of the Med8 ubiquitin ligase complex might be unique to the brain, as we were unable to detect the complex in liver or lung tissue. These findings provide the first demonstration of an endogenous Med8 ubiquitin ligase complex, and indicate a potentially specific function of this complex in the central nervous system of chordates.

5.2 Med8 protein localizes to the dendrites and cytoplasm of neurons

During a screen for dendritic mRNAs, we discovered the presence of Med8 mRNA in the dendrites of pyramidal neurons located in the CA1 region of the hippocampus (Ainsley, Drane, Jacobs, Kittelberger, & Reijmers, 2014) (See chapter 4).

To determine if dendritic Med8 mRNA might give rise to dendritic Med8 protein, we utilized the Thy1-YFP mouse line in which a subset of the CA1 pyramidal neurons express YFP protein, outlining their cell bodies and processes (Feng et al., 2000). Med8 immunohistochemistry performed on a hippocampal slice of a Thy1-YFP mouse confirmed the already known nuclear presence of Med8, but in addition revealed the punctate presence of Med8 protein in the dendritic processes of CA1 pyramidal neurons (Figure 5.1A-C). This indicated that dendritically localized Med8 mRNA could be translated within the dendrite, leading to the dendritic presence of Med8 protein. We wanted to further confirm the extranuclear presence of Med8 protein in the brain, and therefore fractionated hippocampal tissue into nuclear and cytoplasmic fractions followed by western blotting. In agreement with the immunohistochemical detection of Med8 in the hippocampal slice (Figure 5.1A-C), Med8 was predominantly localized in the nuclear fraction (Figure 5.1D). However, Med8 protein was also detected in the cytoplasm (Figure 5.1D). Finally, we determined if Med8 protein can be detected in the dendrites of cultured neurons. We performed Med8 immunohistochemistry on DIV14 cultured cortical neurons that were stained with the somato-dendritic marker Map2. Similar to our hippocampal slice data, we observed the punctate presence of Med8 protein in dendritic processes, in addition to its presence in the nuclear and cytoplasmic regions of the cell body (Figure 5.1E-J). Combined, these data indicated the presence of Med8 protein in the dendrites of neurons, both in the intact brain and in culture.

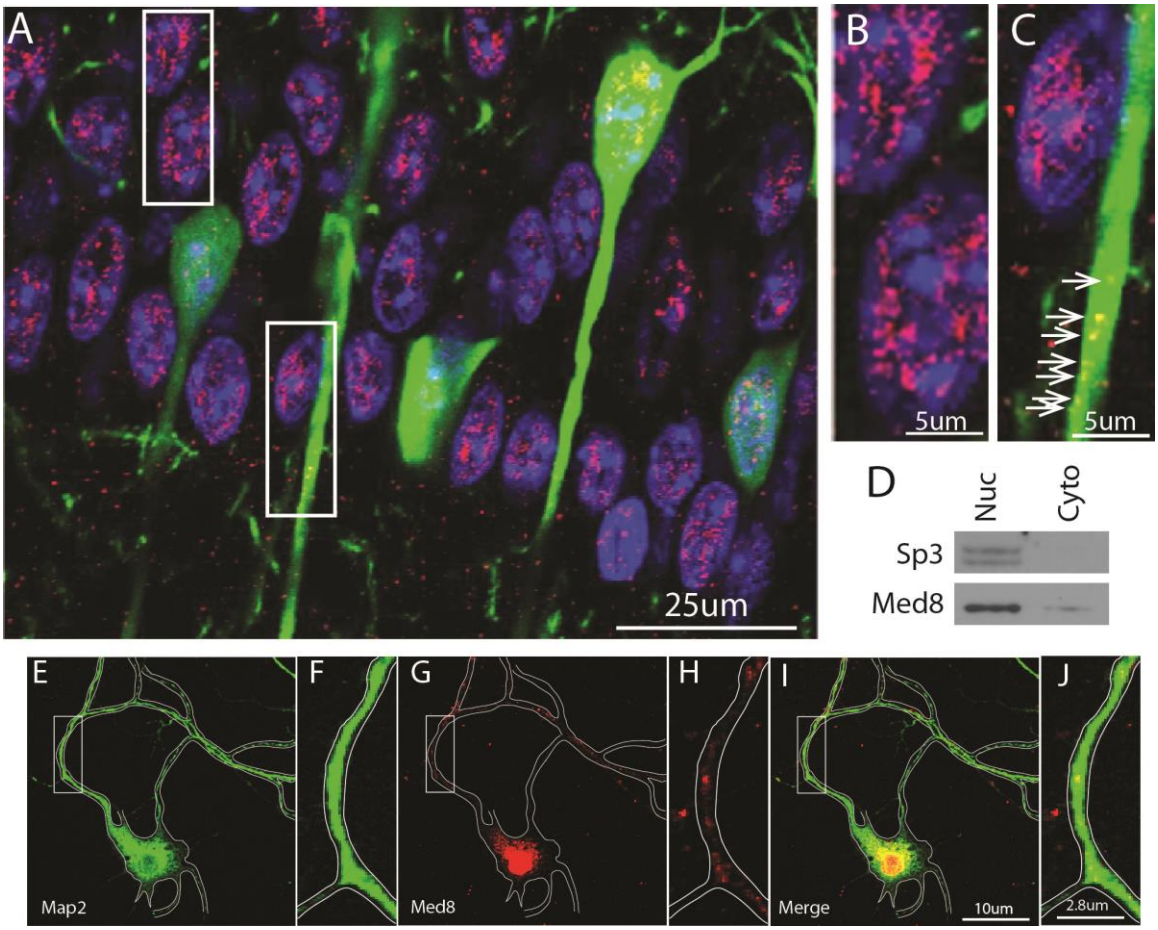

Figure 5.1

Med8 protein localization in neuronal dendrites. (A) Immunohistochemistry of the CA1 region of the hippocampus of a Thy1-YFP mouse. Red: Med8, green: YFP, blue: DAPI. (B-C) Close ups showing Med8 in nuclei (B) and a dendrite (C). Arrows indicate Med8 protein within dendritic processes. Note that within the nucleus Med8 protein mainly localized to euchromatin (weak or no DAPI signal), as expected based on its role in transcription. (D) Nuclear and cytoplasmic fractionation of brain tissue showing Med8 protein in both fractions and the transcription factor Sp3 in just the nuclear fraction. (E-J) Immunohistochemistry of cultured cortical neurons (DIV14) shows Med8 protein localized within the dendritic processes. (E, F) Map2. (G, H) Med8. (I, J) Merge.

5.3 Med8 in the brain can associate with a ubiquitin ligase complex

Med8 has a well-established and highly conserved functional role in the regulation of gene transcription as a member of the nuclear Mediator complex (Figure 5.2A) (R. C. Conaway & Conaway, 2013; R. C. Conaway et al., 2005; Malik & Roeder, 2005, 2010). Our discovery that Med8 protein can localize to the dendrites of neurons, at relatively large distances from the nucleus, suggested two alternative scenarios. First, dendritic Med8 protein translocates to the nucleus to participate in gene transcription as part of the Mediator complex. This would be in agreement with other proteins that have been reported to translocate from neuronal processes to the nucleus as members of signaling pathways (Ch'ng et al., 2012; Crino et al., 1998). Second, dendritic Med8 protein does not translocate to the nucleus, but instead has a second function outside of the nucleus. In search of a possible second function of Med8, we became aware of a paper reporting that Med8 protein can participate in an E3 ubiquitin ligase complex (Brower et al., 2002) (Figure 5.2B). Participation in this complex is made possible by a BC-box motif that is only present in the Med8 protein of chordate species (Figure 5.2C). Despite high conservation of the BC-box motif among chordates, indicating an important function of the Med8 ubiquitin ligase complex, no tissues have been identified that contain this complex. We therefore decided to test if the Med8 ubiquitin ligase complex is present in brain tissue. We fractionated tissue from the prefrontal cortex into nuclear and cytoplasmic fractions, and performed co-immunoprecipitation (Co-IP) of Med8 followed by blotting for either another member of the Mediator complex (Med17, Figure 5.2A) or members of the ubiquitin ligase complex (Elongin B and Elongin C, Figure 5.2B). We chose Med17, as it is an essential core component of the head region of the

Mediator, where it directly interacts with Med8 (Lariviere et al., 2006; Takagi et al., 2006). The Med8 Co-IP experiments revealed that in the mouse brain Med8 associates with members of a ubiquitin ligase complex, and that this complex can be localized outside of the nucleus (Figure 5.2D-G).

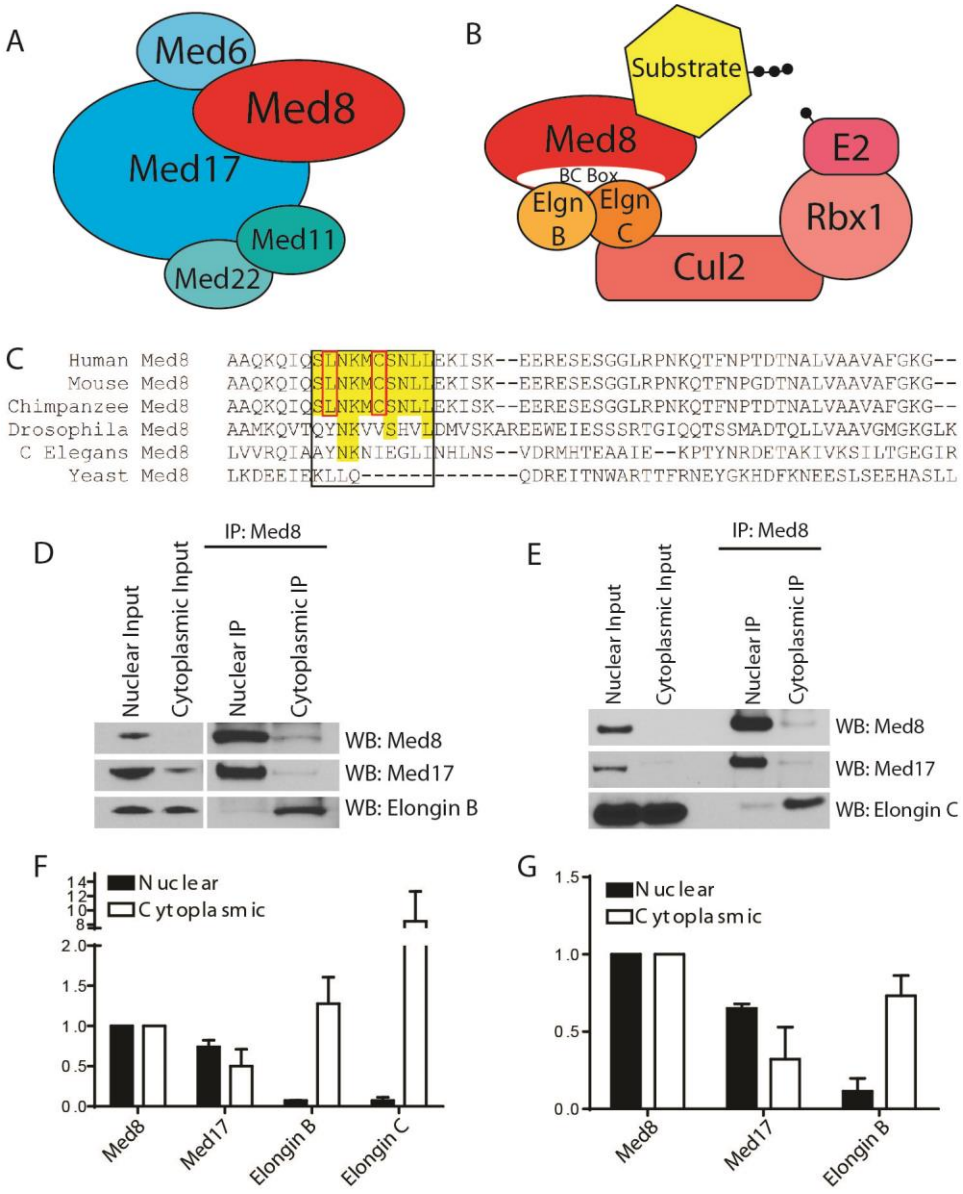

Figure 5.2

Med8's association with a ubiquitin ligase complex. (A) Partial schematic of the head region of the Mediator complex. (B) Schematic of the Med8 containing ubiquitin ligase complex. (In A and B proteins are not depicted to scale). (C) Alignment of Med8 protein sequences from multiple species with the BC box domain circled in black. The BC box domain is conserved within chordata, but not in lower organisms. Essential residues for the binding of the Elongin BC heterodimer are circled in red. (D-E) Representative images of a Med8 Co-IP pulling-down Med17, Elongin B, and Elongin C proteins from mouse prefrontal cortex tissue. Input bands for Med8 and Med17 are visible in the cytoplasmic fraction upon longer exposure (not shown). The nuclear localized

transcription factor Sp3 was used as a control for fractionation efficiency. No nuclear contamination in the cytoplasmic fraction was observed (data not shown). (F) Quantification of the Med8 Co-IP from prefrontal cortex tissue (Med17: N = 6; Elongin B: N=2; Elongin C: N=4; Elongin B and C were done on separate blots). (G) Quantification of the Med8 Co-IP from hippocampal tissue (N=2).

5.4 The Med8 containing ubiquitin ligase complex can be separate from the Mediator complex

It has been hypothesized that the Med8 containing ubiquitin ligase complex might associate with the Mediator complex (Brower et al., 2002). In this situation, as part of the Mediator, the Med8 ubiquitin ligase could ubiquitinate transcription factors as well as other Mediator complex subunits, thereby adding additional layers of transcriptional regulation to that already provided by the Mediator complex. However, since we observed Med8 as part of a ubiquitin ligase complex outside of the nucleus, we decided to further investigate whether the Med8 containing ubiquitin complex could function on its own, without being part of the Mediator. To do this, we immunoprecipitated one of the core Mediator subunits, Med17, and looked for Co-IP of Med8 and two members of the Med8 ubiquitin ligase complex, Elongin C and Rbx1 (Figure 5.2B). In both the nuclear and cytoplasmic fraction, Med17 IP pulled-down Med8, but not Elongin C or Rbx1 (Figure 5.3A-B). This indicated that the Med8 ubiquitin ligase complex does not have to be associated with the Mediator complex.

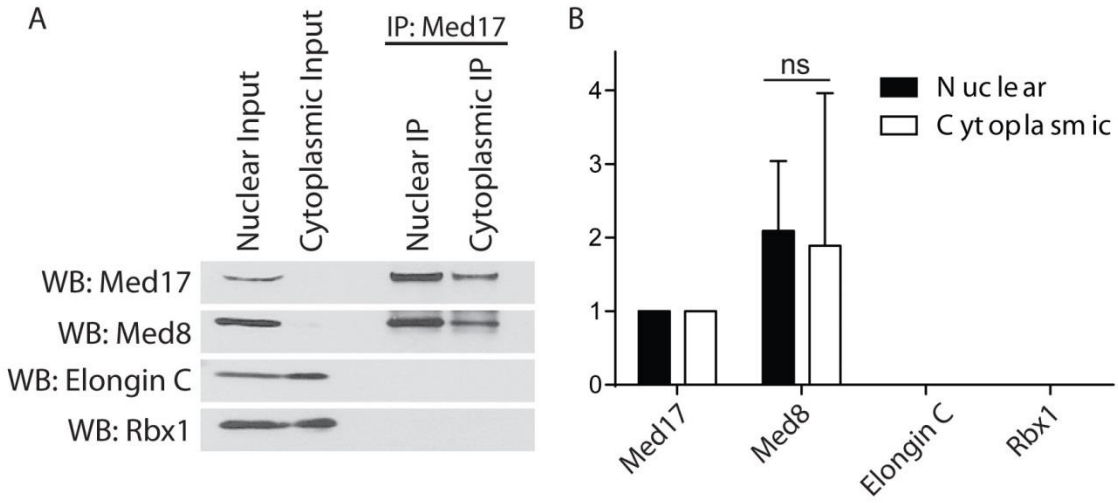

Figure 5.3

Med8's association with a Mediator complex without association with a ubiquitin complex. (A) Representative image of a Med17 Co-IP from hippocampal tissue pulling-down Med8, but not Elongin C, and Rbx1. Input bands for Med17 and Med8 are visible in the cytoplasmic fraction upon longer exposure (not shown). The nuclear localized transcription factor Sp3 was used as a control for fractionation efficiency. No nuclear contamination in the cytoplasmic fraction was observed (data not shown). (B) Quantification of the Med17 Co-IP (N = 5).

5.5 The Med8 ubiquitin ligase complex may be tissue and cell-type specific

After discovering the association of Med8 with its ubiquitin ligase complex in mouse brain tissue, we attempted to detect this complex in other mouse tissues. A previous study suggested the potential presence of the Med8 ubiquitin ligase complex in the liver (Brower et al., 2002). Brower et al. observed co-elution of Med8 with Cul2, Elongin B, and Rbx1 within a fraction obtained through ion-exchange chromatography of a sample obtained from rat liver nuclei. However, they could not detect a direct physical interaction between Med8 and Cul2, Elongin B, or Rbx1. We fractionated fresh mouse liver tissue into nuclear and cytoplasmic fractions. As expected, IP of Med8 resulted in pull-down of Med17 in the nuclear fraction. However, we saw almost no pull-down of Elongin C or Rbx1 from either the nuclear or cytoplasmic fraction of liver tissue (Figure 5.4A). This result suggested that, in liver tissue, Med8 is not associating with members of the ubiquitin ligase complex. The same experiment done in lung tissue gave a similar result. IP of Med8 pulled-down Med17, but very little Elongin C or Rbx1 (Figure 5.4B). In HEK293T cells, again IP of Med8 was able to pull-down Med17, but not Elongin C or Rbx1 (Figure 5.4C-D). Lastly, we looked at Neuro-2a cells, a mouse neuroblastoma cell line, and saw that, in addition to pulling-down Med17, Med8 was able to pull-down Elongin C and Rbx1 in both the nucleus and cytoplasm (Figure 5.4E-F). Combined, these results indicated that Med8 might associate with its ubiquitin ligase in a tissue and cell-type specific manner.

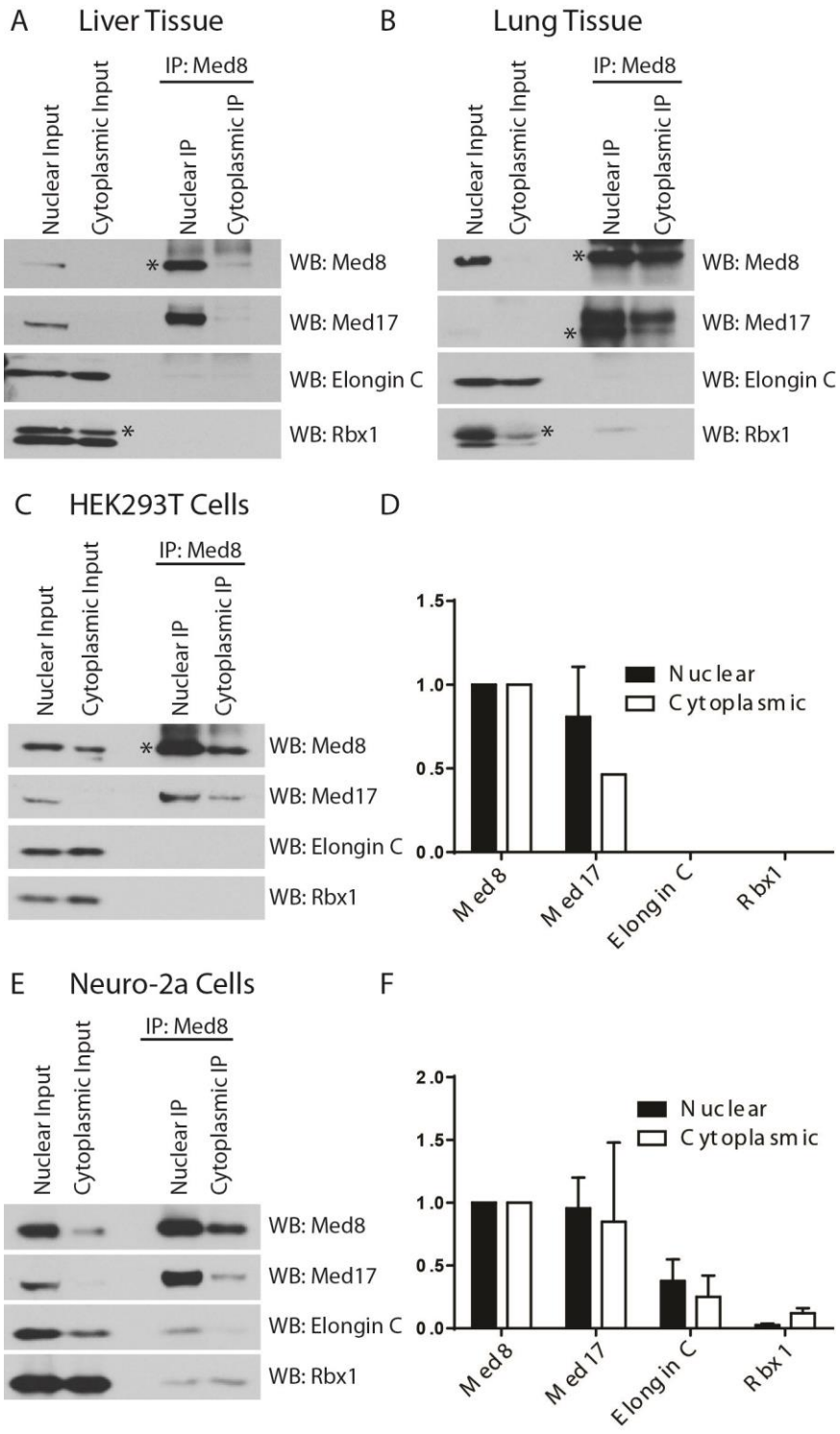

Figure 5.4

Tissue and cell-type specificity of the Med8 ubiquitin ligase complex. (A-C, E) Representative images of Med8 Co-IPs. Input bands for Med8 and Med17 are visible in

the cytoplasmic fraction upon longer exposure (not shown). * indicates the size of the correct band. The nuclear localized transcription factor Sp3 was used as a control for fractionation efficiency. No nuclear contamination in the cytoplasmic fraction was observed (data not shown). (A) Med8 Co-IP from mouse liver tissue. (B) Med8 Co-IP from mouse lung tissue. (C) Med8 Co-IP from HEK293T cells. (D) Quantification of HEK293T cell Co-IP (N = 6). (E) Med8 Co-IP from Neuro-2a cells. (F) Quantification of Neuro-2a cell Co-IP (N = 3).

Chapter 6:

Discussion

6.1 Overview

Chapter 3 of this thesis describes a new mouse model that allows isolation of ribosome-bound mRNA in a cell-type specific manner. By creating a mouse model that expresses EGFP-L10a under control of the tetracycline operator (tetO-TRAP), we were able to cross this mouse with driver specific tTA mice, allowing for cell-type specific expression of the transgene. We crossed the tetO-TRAP mouse with the Camk2a-tTA driver mouse in order to create the Camk2a-TRAP mouse that expresses EGFP-L10a in Camk2a expressing cells. We showed that the expression of EGFP-L10a was specific to Camk2a expressing cells. The patterns of expression throughout the brain followed those of other transgenes expressed using the Camk2a-tTA driver mouse. In addition, EGFP-L10a showed cell-type specificity, as it did not overlap with markers for interneurons or astrocytes. We showed that EGFP-L10a was able to incorporate into functional ribosomes. In addition, we were able to successfully collect ribosome-bound mRNA using the TRAP technique. Finally, we crossed our tetO-TRAP mouse with an activity-regulated tTA driver line (Fos-tTA), and showed that expression of the transgene was regulated in a temporal manner through the addition of dox to the diet. This mouse model adds a valuable tool for translational profiling by increasing the ease of expressing EGFP-L10a in a cell-type specific and time-frame specific manner.

In chapter 4 of this thesis we created a novel method for collecting ribosome-bound dendritic mRNA from excitatory pyramidal cells of the CA1 region of the hippocampus. We began by optimizing the types of beads used from the originally published TRAP protocol in order to decrease background levels of mRNA binding. We showed that our dissection protocol was able to specifically collect tissue with EGFP-

L10a expressing dendrites, and that we could successfully collect ribosome-bound mRNA from this dendritic tissue. Analysis of the ribosome-bound mRNA led to some interesting discoveries, as we were able to detect genes in dendrites that were previously assumed to only have somatic localization and function. In particular, we were able to detect mRNA from a group of Mediator subunits within the dendrites. Using FISH, we confirmed that mRNA from one of the subunits, Med8, is localized to the dendrites of CA1 pyramidal neurons. These data significantly contribute to our understanding of the types of mRNAs that are localized and potentially translated within neuronal dendrites, and provides a starting point for future studies on individual dendritic mRNAs and proteins.

In chapter 5, we looked closely at the role of one dendritically localized mRNA found in our screen, Med8. We found that Med8 protein is localized to neuronal dendrites in both CA1 hippocampal neurons, as well as in cultured cortical neurons. Fractionation revealed that Med8 protein is present in both the nuclear and cytoplasmic fractions of mouse brain tissue. As expected, we found that Med8 in the nucleus was able to interact with subunits of the Mediator complex. In the cytoplasm, however, we found that Med8 preferentially associated with subunits of its ubiquitin ligase complex. We showed that Med8 can be a part of its ubiquitin ligase complex without being a part of the Mediator complex. In addition, we showed that Med8's association with its ubiquitin complex could be brain tissue specific, as we did not detect this interaction in liver tissue, lung tissue, or kidney cells. These data represent the first endogenous isolation of the Med8 containing ubiquitin ligase complex, as well as provide the first indication that the Med8 ubiquitin ligase complex may only exist in the brain.

6.2 A new tool for translational profiling

Creating a new mouse for EGFP-L10a expression

The ability to acquire gene expression profiles in a cell-type specific manner greatly adds to our understanding of how these cell-types function within a system. By creating a mouse model that uses the tetracycline transactivator system we enabled both spatial and temporal control over EGFP-L10a expression. The ability to cross the tetO-TRAP mouse line with various cell-type specific tTA driver lines, such as the Camk2a-tTA line, confers spatial control by restricting EGFP-L10a expression to these cell-types. Though a number of BAC transgenic TRAP mice have been generated for the targeting of various cell-types in the brain (Doyle et al., 2008), our tetO-TRAP mouse significantly expands the number of cell-types that are now amendable to TRAP analysis (Schonig, Bujard, & Gossen, 2010).

The ability to manipulate the timing of EGFP-L10a expression through the use of dox in the food confers temporal control. Temporal control allows the use of activity-induced promoters such as the Fos promoter to tag cells that are activated during a specific time-window, for example when a behavioral task is executed (Reijmers et al., 2007). In addition, temporal control enables more specific expression when using promoters that drive differential expression patterns during different phases of development.

Cell-type specific mRNA collection

In chapter 3, we report a straightforward protocol using the Camk2a-TRAP mouse to collect ribosome-bound mRNA from CA1 pyramidal neurons by dissecting the whole

hippocampus, and subjecting it to homogenization and TRAP IP. By using this protocol, we were able to collect high quality, ribosome-bound mRNA from CA1 pyramidal neurons at a defined time-point immediately following behavioral activation.

To the best of our knowledge, the Camk2a-TRAP mouse is the first reported mouse line that enables the collection of ribosome-bound mRNA from CA1 pyramidal neurons. Given the important role of CA1 pyramidal neurons in learning and memory, we anticipate that future studies will use the Camk2a-TRAP mouse to discover and characterize molecular mechanisms of cognition. As an initial follow up to this study, I propose that mRNA from CA1 pyramidal neurons be collected from multiple time-points after fear conditioning. Analysis of the ribosome-bound mRNAs at each time-point after FC will help to outline the sequence of translational events that occurs during consolidation of a memory within a single defined neuronal cell-type in the hippocampus. The cell-type specificity of this approach would add to a recent study that analyzed translational changes that occur globally within the hippocampus during consolidation of a fear memory (Cho et al., 2015). Additionally, our collection protocol alleviates the need to subtract out potential contaminants from other cell-types in the dendritic layer when the entire hippocampal neuropil is isolated (Cajigas et al., 2012). It will be interesting to analyze translational profiles from different brain regions using the Camk2a-TRAP mouse. In particular, it will be interesting to analyze ribosome-bound mRNAs from the amygdala after fear conditioning, as this brain region plays a central role in fear learning (Duvarci & Pare, 2014).

Temporal control of cell-tagging and mRNA collection

The Fos-TRAP mouse is the first mouse model designed for the collection of ribosome-bound mRNA specifically from neurons that are activated during a behavioral test. Thereby, the Fos-TRAP mouse should make it possible to study protein synthesis in neurons that are functionally defined.

Though our initial data support the feasibility of using the Fos-TRAP mouse for these purposes, two caveats must be addressed in future studies. **First**, the mRNA isolation experiment reported in chapter 3 was done using the Camk2a-TRAP mouse line, which expresses high EGFP-L10a levels throughout its lifetime. In our Fos-TRAP experiment, the animals were fear conditioned three times within a six-hour time-window while off dox, and brains were then collected three days later for analysis of EGFP-L10a expression. This left a six-hour time-window for tTA transcription to occur, followed by three days for tTA translation, EGFP-L10a transcription and translation, and incorporation of EGFP-L10a into functional ribosomes. Although immunohistochemical analysis revealed that this was a sufficient amount of time for the visualization of EGFP-L10a, we do not know whether the EGFP-L10a visualized was incorporated into functional ribosomes that can bind and translate mRNA. Here, Co-IPs of EGFP-L10a can be performed followed by blotting for the small ribosomal subunit RPS6 at different time-points after behavioral activation to figure out when the newly synthesized EGFP-L10a becomes incorporated into functional ribosomes. **Second**, after behavioral activation, we observed sparse labeling of EGFP-L10a throughout the hippocampus. Our successful isolation of ribosome-bound mRNA was done using highly expressed EGFP-L10a from all pyramidal cells within the CA1 of the hippocampus. It therefore remains to

be determined whether the EGFP-L10a expression levels observed in the Fos-TRAP mouse will produce a sufficient number of EGFP-tagged ribosomes to enable successful affinity purification.

Future directions

Once fully optimized, there are many experiments that can be done using the Fos-TRAP mouse line. To begin, collection and analysis of ribosome-bound mRNAs specifically from neurons activated during fear conditioning will give increased specificity to studies looking at gene expression profiles after behavior. This allows for the select isolation of ribosome-bound mRNA from cells involved in a fear memory trace, which will give a more precise read out of the types of mRNAs that are being translated following a behavioral paradigm. In addition, the Fos-TRAP mouse can be used to look at the translational profiles of memory cells during both the reconsolidation and extinction processes (Debiec, LeDoux, & Nader, 2002; Santini, Ge, Ren, Pena de Ortiz, & Quirk, 2004).

Though there are caveats that need to be addressed in future studies, our current data provide an important first validation by showing that EGFP-L10a levels in CA1 pyramidal neurons of Fos-TRAP mice increase after fear conditioning. In addition, the creation of the Fos-TRAP mouse line affirms the versatility of the tetO-TRAP mouse by showing that it can be crossed with different tTA drivers to enable a variety of EGFP-L10a expression patterns (Schonig et al., 2010).

6.3 Dendritic translational profiling

In chapter 4 we developed a novel method for collecting ribosome-bound mRNA from *in vivo* dendrites. We were able to optimize the TRAP technique to decrease the amount of background mRNA, which enabled us to collect ribosome-bound mRNA from dendrites after a behavioral fear conditioning paradigm. Analysis of the mRNAs collected revealed some unexpected findings, as we saw mRNAs encoding proteins that were assumed to only have somatic functions. We verified this finding through FISH to show the localization of one of the unexpected mRNAs, Med8, in *in vivo* dendrites.

Dendritic mRNA collection

Our TRAP-based method for dendritic mRNA collection alleviates the issue of how to isolate *in vivo* dendrites from surrounding tissue. This is an important advance over previous studies that have used either cell culture to look at dendritically localized mRNAs (Eberwine, Belt, Kacharmina, & Miyashiro, 2002; Poon, Choi, Jamieson, Geschwind, & Martin, 2006), or, when using brain tissue, used post-hoc filtering to exclude mRNAs that might have been present in cells immediately surrounding the dendrites (Cajigas et al., 2012). Although our optimized protocol greatly reduced nonspecific binding of mRNA to the beads, it is not possible to eliminate all background binding. We were able to further reduce the impact of nonspecific binding by sequencing both the IP and SN fractions. This allowed us to differentiate mRNAs with high IP/SN ratios versus those with low IP/SN ratios. A high IP/SN ratio is more likely caused by specific binding of a particular mRNA to the beads than a low IP/SN ratio. In addition, we observed that fear conditioning increased the IP/SN ratio of positive control genes

that we expected to see in pyramidal cell dendrites (Ainsley et al., 2014). This not only validated our analysis strategy, but also validated our use of fear conditioning prior to mRNA collection by TRAP. Although we showed an increase in the amount of mRNA isolated after FC, we did not assess the percentage of GFP-tagged ribosomes that are bound to mRNA within our samples. To address this, we could utilize a polysome fractionation technique in order to isolate fractions containing either monosomes or polysomes (Zuccotti & Modelska, 2016). After fractionation, western blotting will be used to assess the amount of GFP-L10a within each fraction. This will give insight into the percentage of GFP-tagged ribosomes that are actively involved in translation within any given sample.

Importance of ribosome-bound mRNA collection

The list of dendritic mRNAs generated from our study can be distinguished from others because it is a list of ribosome-bound mRNAs. This is an important distinction over previous studies that have relied on collection of total mRNA that may or may not have been associated with ribosomes. Isolation of dendritic mRNA with unknown ribosome association leaves open the possibility that the mRNA is never locally translated, and that it is simply a nonfunctional by-product of mRNA diffusion from the soma into proximal dendrites. The ribosome-bound status of the mRNAs collected in this study makes it unlikely that they are nonfunctional. To validate hits from our dendritic mRNA screen, the dendritic localization of the mRNA and the corresponding protein can be confirmed through visualization using FISH and IHC analysis, respectively. In this thesis, I confirmed that Med8 mRNA and protein can have a dendritic localization in hippocampal CA1 pyramidal neurons. Two other dendritic mRNAs from our list

(Pafah1b1, and Hist1h4j) were also confirmed to have dendritic localization (Ainsley et al., 2014). Although the dendritic localization of these three mRNAs was confirmed, it will be important to establish their physiological relevance within dendrites. To test this, knockout of dendritically translated mRNA, without disruption of somatically translated mRNA, through disruption of the dendritic localization signal, will give insight into their physiological properties. It should be noted that the dendritic localization signal for the majority of dendritic mRNAs is unknown. In cases where the dendritic localization of an mRNA can be disrupted, changes in the phenotypic or physiological properties of the cells will give insight into the dendritic function of the mRNA. In addition, a translation run-off assay can be performed in order to establish if the ribosome-bound mRNAs collected are actively being translated, or if they are bound to stalled ribosomes (Darnell et al., 2011). The antibiotic puromycin causes actively translating ribosomes to dissociate from bound mRNAs. By dissociating actively translating ribosomes, followed by a TRAP IP, only mRNAs bound to stalled ribosomes will be isolated. Subtracting the list of mRNAs bound to stalled ribosomes from the list of total ribosome-bound mRNAs collected by TRAP will give insight into what mRNAs are actively being translated at any given time.

Dendritic localization of assumed soma-restricted mRNAs

Our gene ontology analysis showed many known and predicted dendritic mRNAs such as those involved in protein translation and cytoskeleton remodeling, in agreement with previous studies (Moccia et al., 2003; Puthanveettil et al., 2013). This is not surprising, as it is known that synaptic plasticity involves the remodeling of the cytoskeleton at the synapse (Ackermann & Matus, 2003). In addition, translational

machinery is present at the synapse and it is therefore not surprising that new machinery is locally made. However, we also detected dendritically localized mRNAs that encode proteins that so far have only been shown to have a nuclear function. For example, cAMP response element binding protein (CREB) is locally synthesized in dendrites in an activity-dependent manner, and then transported back to the nucleus where it exerts its function as a transcription factor (Crino et al., 1998). We found that multiple subunits of the transcriptional Mediator complex were potentially translated within neuronal dendrites. Further characterization of the subunit Med8 confirmed its dendritic localization through the use of FISH and IHC. At this point we have not determined the exact function of Med8 in the dendrites of neurons; however our investigation into its involvement as part of an E3 ubiquitin ligase suggests a potential role in protein degradation (see section 6.4).

Timing of mRNA collection

For this study, we chose to collect ribosome-bound mRNA immediately following a 500-second long fear conditioning paradigm. The reason for this timing is that we wanted to collect mRNA that already existed within dendrites before activity-induced transcription could lead to changes in the dendritic mRNA population. It is well known that activity at the synapse induces signaling cascades that signal to the nucleus and induce transcription (Abel & Lattal, 2001; Antoine, Serge, & Jocelyne, 2013). Newly synthesized mRNAs are then transported from the nucleus to the dendrites for local translation. By looking at ribosome-bound mRNAs immediately following fear conditioning, we examine a time-point that is too early to include newly transcribed mRNAs (Guzowski, McNaughton, Barnes, & Worley, 1999; Steward, Wallace, Lyford,

& Worley, 1998). This provides a picture of what mRNAs are poised within dendrites and ready for translation immediately upon synapse stimulation. This gives an important first look at what genes are needed immediately upon stimulation for the process of synaptic plasticity, before signaling to the nucleus can lead to changes in dendritic mRNA. When comparing FC and HC TRAP IP data, we saw that up-regulation of translational machinery was one of the first consequences of activity-induced dendritic protein synthesis in CA1 pyramidal neurons. Since short-term memory formation does not rely on *de novo* protein synthesis, it is not surprising that immediate protein synthesis includes genes that are not directly involved in synaptic plasticity, but rather are involved in the process of translation. For future studies, it will be important to expand on the time-points when ribosome-bound mRNA is collected in order to include newly transcribed and trafficked mRNAs. We predict that later time-points will include effector genes that are known to exert their function at the synapse leading to synaptic plasticity and long-term memory formation. Having a time-course of which genes are translated following neuronal activity will help to paint a broader picture of the involvement of protein translation in synaptic plasticity.

Summary

We developed a novel method for collecting ribosome-bound mRNA from *in vivo* dendrites. We provide the first characterization of behavioral induced functional regulation of dendritic mRNAs. This revealed a wide variety of mRNAs that bind to ribosomes within neuronal dendrites, and supports the theory that activity increases the association of mRNAs with ribosomes. Future studies can use this technique in order to create a timeline of dendritically translated mRNAs after neuronal stimulation.

6.4 The Med8 containing ubiquitin ligase

The main finding of chapter 5 is that the Med8 containing ubiquitin ligase complex is present in the mouse brain. Though the potential existence of this complex has been known for quite some time (Brower et al., 2002), it has remained a mystery if and where this complex might exist endogenously. Here, we show that (1) the Med8 protein can be found in the dendrites of both *in vivo* and *in vitro* neurons, (2) within the brain Med8 associates with subunits of a ubiquitin ligase complex, and (3) Med8's association with its ubiquitin ligase complex might occur in a tissue and cell-type specific manner.

Brain specific function of the Med8 ubiquitin ligase

The Med8 protein contains a BC-box binding domain that allows Med8 to interact with Elongins B and C, Cul2, and Rbx1 (Brower et al., 2002). Interestingly, although Med8 is conserved throughout most species, the critical residues within the BC-box domain that allow binding to the Elongin BC complex are only present within chordates. This indicates that the Med8 ubiquitin ligase complex has a function that is specific to more complex organisms. Since we were able to isolate the endogenous Med8 ubiquitin ligase complex from mouse brain tissue and from a brain-derived cultured cell line, Neuro-2a, but not from mouse liver tissue, lung tissue, or a cultured embryonic kidney cell line, HEK-293T, it is possible that this complex plays a specific function within the central nervous system of chordates.

There are several possible ways in which the Med8 ubiquitin ligase could be exerting its function within the brain. Since we see Med8 protein within neuronal

dendrites, one possibility is that the Med8 containing ubiquitin ligase has a role in synaptic regulation through the ubiquitination of synaptic proteins. It has been reported that ubiquitination of synaptic proteins plays a role in synaptic plasticity and consequently learning and memory (Colledge et al., 2003; Ashok N. Hegde, Haynes, Bach, & Beckelman, 2014; Pavlopoulos et al., 2011; Upadhya, Smith, & Hegde, 2004). The ubiquitin-proteasome system (UPS) has been reported to regulate synaptic plasticity in several ways. **First**, glutamate receptor (GluR) trafficking has been shown to control some types of synaptic plasticity, and stimulation with the GluR agonist AMPA is known to induce endocytosis of the receptor. It was found that a proteasome inhibitor administered prior to AMPA stimulation blocks GluR internalization, indicating a role for the UPS in regulating GluR surface expression (Patrick et al., 2003). It is therefore possible that the Med8 containing ubiquitin ligase plays a role in ubiquitinating synaptic proteins to regulate their localization or function. **Second**, activity-regulated changes to the PSD are critical for synapse formation and synaptic plasticity. PSD-95 is ubiquitinated upon NMDA receptor activation and is quickly degraded allowing for changes in surface receptor composition (Colledge et al., 2003). The Med8 containing ubiquitin ligase could exert its function through ubiquitinating scaffolding proteins at the synapse, allowing for the redistribution of synaptic receptors. **Third**, removal of inhibitory constraints on regulatory proteins by the UPS is another way in which the Med8 ubiquitin ligase could exert control over synaptic plasticity. An example of this in *Aplysia* is the UPS dependent degradation of the CREB repressor CREB1b. Removal of the repressor by the UPS allows for gene expression regulation by CREB, and downstream synaptic plasticity to occur (Upadhya et al., 2004).

Alternatively, the Med8 containing ubiquitin complex could help regulate the transport of dendritically synthesized Med8 into the nucleus. In this scenario, sequestering cytoplasmic Med8 into the ubiquitin complex prevents Med8 from entering the nucleus and thereby prevents it from integrating into the Mediator complex (Marchenko et al., 2010). This would add another layer of transcriptional regulation by controlling the assembly of the Mediator itself.

Finally, since we did observe the Med8 ubiquitin ligase complex in the nuclear fraction of Neuro-2a cells, it is possible that this complex has a function inside the nucleus. Though such an intra-nuclear function could involve direct regulation of the Mediator complex by the Med8 ubiquitin ligase complex, we could not confirm a direct association between these two complexes.

Potential activity-dependent regulation of the Med8 ubiquitin ligase complex

In our original screen for ribosome-bound dendritic mRNA, we observed that inducing activity within the neurons prior to TRAP IP by fear conditioning increased the association of mRNA with ribosomes (Ainsley et al., 2014). When comparing TRAP IP data from HC vs. FC animals, we saw an increase in the amount of Med8 mRNA collected in the FC group. This suggested that there could be activity-dependent regulation of dendritic Med8 protein, as well as a potential regulation of Med8's complex association within the dendrites. Since we showed that Med8 preferentially associates with the ubiquitin complex in the cytoplasm of brain tissue, it is possible that neuronal activity could stimulate the association of Med8 with its ubiquitin ligase complex. In a preliminary study, we fear conditioned mice and collected hippocampal tissue at 0, 15,

30, and 60 minutes. We then fractionated the tissue into nuclear and cytoplasmic fractions and performed a Med8 Co-IP to see if we saw differences in its complex association upon neuronal stimulation (data not shown). At this point, the preliminary data were unable to show any differences in Med8's association with its ubiquitin complex or increases in total Med8 protein levels after FC. A follow up study to increase the n will greatly increase our understanding of the dynamics with which the Med8 containing ubiquitin ligase complex functions.

Future directions

The discovery of an endogenous Med8 containing ubiquitin ligase complex in the mouse brain raises a number of important questions that need to be addressed in future studies. First, though the discovery of this complex was precipitated by the finding of Med8 protein in neuronal dendrites, it is not yet known whether the Med8 ubiquitin ligase complex is present specifically in dendrites or more generally in the entire cytoplasmic region of the soma of neurons. One way to answer this question is by using a neuronal cell culture technique that allows for the isolation specifically of dendrites and axons of neurons without their cell bodies (Torre & Steward, 1992). By collecting isolated dendrites from neurons followed by a Med8 Co-IP, we could identify the absence or presence of the Med8 containing ubiquitin ligase.

Second, though our Neuro-2a data indicate the presence of the Med8 ubiquitin ligase complex in neurons, it cannot be excluded at this point that the complex is present in non-neuronal cell-types in the mouse brain (for example glia). To this end, we fractionated cultured astrocytes into nuclear and cytoplasmic fractions followed by a

Med8 Co-IP. We showed that we could, in fact, isolate the Med8 containing ubiquitin ligase complex from cultured astrocytes (figure 6.1). This experiment has an n=1, and we did not confirm the purity of the astrocyte culture by blotting for a neuronal marker to ensure the absence of neuronal cells. In order to ensure that the Med8 containing ubiquitin ligase data collected from brain tissue also contains Med8 ubiquitin ligase from a neuronal cell contribution, a Med8 Co-IP from pure cultured neurons must be performed in order to ensure that the Med8 containing ubiquitin ligase complex exists within neurons.

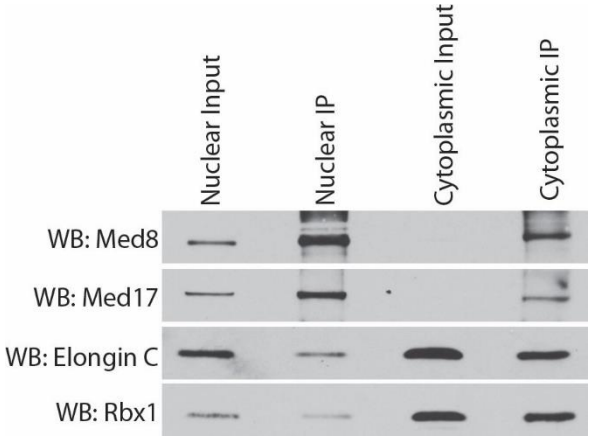

Figure 6.1

Med8 Co-IP on pure cultured astrocytes. Med8 was able to pull-down Med17 from both nuclear and cytoplasmic fractions; this indicated that Med8 can incorporate into the Mediator complex in astrocytes. Med8 was able to pull-down Elongin C and Rbx1, more so from the cytoplasmic fraction than from the nuclear fraction, similar to what was seen using fractionated brain tissue. N = 1.

Third, the Med8 ubiquitin ligase complex has been shown to possess ubiquitin ligase activity (Brower et al., 2002), but its endogenous substrates are still unknown. Future studies will be aimed at further delineating the presence of the Med8 ubiquitin ligase complex within defined cell-types of the brain, and within defined subcellular compartments in those cell-types. More precise spatial localization of the Med8 ubiquitin ligase complex will greatly facilitate the discovery of its endogenous substrates by focusing efforts on candidate substrate proteins that are known to be in close spatial proximity to the complex. Furthermore, precise spatial localization of the Med8 ubiquitin ligase complex could catalyze specific hypotheses on the function of this complex. It should be noted that these functional hypotheses can be tested through the mutation of only two critical BC-box residues within the Med8 protein, as mutating these two residues is sufficient to prevent the incorporation of Med8 into its ubiquitin ligase complex (Brower et al., 2002). One experiment that can be done to give valuable information about the function of the ubiquitin ligase is to knock out endogenous Med8 from cultured hippocampal neurons, and to replace it with a BC-box mutant Med8 that is unable to bind to the ubiquitin ligase complex. Once confirmed that the BC-box mutant Med8 can still associate with Mediator complex subunits, any changes in the phenotypic or physiological properties of the neurons will give insight as to the function of the Med8 ubiquitin ligase.

6.5 Concluding remarks

Our ability to decode the translational profiles of defined cell-types in the brain is paramount in our ability to understand how these cell-types function. The work presented here contributes to the framework of translational profiling by introducing novel mouse lines and techniques for characterizing protein translation with high cellular and subcellular specificity. We conducted a screen by combining one of our novel mouse lines with a dendritic dissection protocol. The results of this screen significantly expand our knowledge base of the types of mRNAs that are associated with ribosomes within neuronal dendrites. In addition, we more deeply characterized one of the locally synthesized proteins, Med8. This led to the discovery of a novel ubiquitin ligase complex with a potentially specific function within the chordate brain. The methods and findings presented in this thesis support a better understanding of how translation is involved in synaptic plasticity and learning and memory.

References

Aakalu, G., Smith, W. B., Nguyen, N., Jiang, C., & Schuman, E. M. (2001). Dynamic visualization of local protein synthesis in hippocampal neurons. *Neuron, 30*(2), 489-502.

Abel, T., & Lattal, K. M. (2001). Molecular mechanisms of memory acquisition, consolidation and retrieval. *Curr Opin Neurobiol, 11*(2), 180-187.

Ackermann, M., & Matus, A. (2003). Activity-induced targeting of profilin and stabilization of dendritic spine morphology. *Nat Neurosci, 6*(11), 1194-1200. doi: 10.1038/nn1135

Ainsley, J. A., Drane, L., Jacobs, J., Kittelberger, K. A., & Reijmers, L. G. (2014). Functionally diverse dendritic mRNAs rapidly associate with ribosomes following a novel experience. *Nature Communications, 5*. doi: 10.1038/ncomms5510

Alberini, C. M., Milekic, M. H., & Tronel, S. (2006). Mechanisms of memory stabilization and de-stabilization. *Cell Mol Life Sci, 63*(9), 999-1008. doi: 10.1007/s00018-006-6025-7

Anagnostaras, S. G., Gale, G. D., & Fanselow, M. S. (2002). The hippocampus and Pavlovian fear conditioning: reply to Bast et al. *Hippocampus, 12*(4), 561-565. doi: 10.1002/hipo.10071

Anders, S., Pyl, P. T., & Huber, W. (2015). HTSeq--a Python framework to work with high-throughput sequencing data. *Bioinformatics, 31*(2), 166-169. doi: 10.1093/bioinformatics/btu638

Antoine, B., Serge, L., & Jocelyne, C. (2013). Comparative dynamics of MAPK/ERK signalling components and immediate early genes in the hippocampus and amygdala following contextual fear conditioning and retrieval. *Brain Struct Funct*. doi: 10.1007/s00429-013-0505-y

Artinian, J., McGauran, A. M., De Jaeger, X., Mouledous, L., Frances, B., & Roullet, P. (2008). Protein degradation, as with protein synthesis, is required during not only long-term spatial memory consolidation but also reconsolidation. *Eur J Neurosci, 27*(11), 3009-3019. doi: 10.1111/j.1460-9568.2008.06262.x

Bambah-Mukku, D., Travaglia, A., Chen, D. Y., Pollonini, G., & Alberini, C. M. (2014). A Positive Autoregulatory BDNF Feedback Loop via C/EBP Mediates Hippocampal Memory Consolidation. *Journal of Neuroscience, 34*(37), 12547-12559. doi: 10.1523/jneurosci.0324-14.2014

Banerjee, S., Neveu, P., & Kosik, K. S. (2009). A coordinated local translational control point at the synapse involving relief from silencing and MOV10 degradation. *Neuron, 64*(6), 871-884. doi: 10.1016/j.neuron.2009.11.023

Bejar, R., Yasuda, R., Krugers, H., Hood, K., & Mayford, M. (2002). Transgenic calmodulin-dependent protein kinase II activation: dose-dependent effects on synaptic plasticity, learning, and memory. *J Neurosci, 22*(13), 5719-5726. doi: 20026537

Bekinschtein, P., Cammarota, M., Igaz, L. M., Bevilaqua, L. R., Izquierdo, I., & Medina, J. H. (2007). Persistence of long-term memory storage requires a late protein synthesis- and BDNF- dependent phase in the hippocampus. *Neuron, 53*(2), 261-277. doi: 10.1016/j.neuron.2006.11.025

Bhat, K. P., & Greer, S. F. (2011). Proteolytic and non-proteolytic roles of ubiquitin and the ubiquitin proteasome system in transcriptional regulation. *Biochim Biophys Acta, 1809*(2), 150-155. doi: 10.1016/j.bbagrm.2010.11.006

Bingol, B., & Schuman, E. M. (2006). Activity-dependent dynamics and sequestration of proteasomes in dendritic spines. *Nature, 441*(7097), 1144-1148. doi: 10.1038/nature04769

Bodian, D. (1965). A suggestive relationship of nerve cell RNA with specific synaptic sites. *Proc Natl Acad Sci U S A, 53*, 418-425.

Boube, M., Joulia, L., Cribbs, D. L., & Bourbon, H. M. (2002). Evidence for a mediator of RNA polymerase II transcriptional regulation conserved from yeast to man. *Cell, 110*(2), 143-151.

Bradshaw, K. D., Emptage, N. J., & Bliss, T. V. (2003). A role for dendritic protein synthesis in hippocampal late LTP. *Eur J Neurosci, 18*(11), 3150-3152.

Brower, C. S., Sato, S., Tomomori-Sato, C., Kamura, T., Pause, A., Stearman, R., . . . Conaway, R. C. (2002). Mammalian mediator subunit mMED8 is an Elongin BC-interacting protein that can assemble with Cul2 and Rbx1 to reconstitute a ubiquitin ligase. *Proc Natl Acad Sci U S A, 99*(16), 10353-10358. doi: 10.1073/pnas.162424199

Buxbaum, A. R., Wu, B., & Singer, R. H. (2014). Single beta-actin mRNA detection in neurons reveals a mechanism for regulating its translatability. *Science, 343*(6169), 419-422. doi: 10.1126/science.1242939

Cai, G., Imasaki, T., Yamada, K., Cardelli, F., Takagi, Y., & Asturias, F. J. (2010). Mediator head module structure and functional interactions. *Nat Struct Mol Biol, 17*(3), 273-279. doi: 10.1038/nsmb.1757

Cajigas, I. J., Tushev, G., Will, T. J., tom Dieck, S., Fuerst, N., & Schuman, E. M. (2012). The local transcriptome in the synaptic neuropil revealed by deep sequencing and high-resolution imaging. *Neuron, 74*(3), 453-466. doi: 10.1016/j.neuron.2012.02.036

Cajigas, I. J., Will, T., & Schuman, E. M. (2010). Protein homeostasis and synaptic plasticity. *EMBO J, 29*(16), 2746-2752. doi: 10.1038/emboj.2010.173

Cavallaro, S., D'Agata, V., Manickam, P., Dufour, F., & Alkon, D. L. (2002). Memory-specific temporal profiles of gene expression in the hippocampus. *Proc Natl Acad Sci U S A, 99*(25), 16279-16284. doi: 10.1073/pnas.242597199

Cavallaro, S., Schreurs, B. G., Zhao, W., D'Agata, V., & Alkon, D. L. (2001). Gene expression profiles during long-term memory consolidation. *Eur J Neurosci, 13*(9), 1809-1815.

Ch'ng, T. H., Uzgil, B., Lin, P., Avliyakulov, N. K., O'Dell, T. J., & Martin, K. C. (2012). Activity-dependent transport of the transcriptional coactivator CRTC1 from synapse to nucleus. *Cell, 150*(1), 207-221. doi: 10.1016/j.cell.2012.05.027

Chain, D. G., Schwartz, J. H., & Hegde, A. N. (1999). Ubiquitin-mediated proteolysis in learning and memory. *Mol Neurobiol, 20*(2-3), 125-142. doi: 10.1007/bf02742438

Cho, J., Yu, N. K., Choi, J. H., Sim, S. E., Kang, S. J., Kwak, C., . . . Kaang, B. K. (2015). Multiple repressive mechanisms in the hippocampus during memory formation. *Science, 350*(6256), 82-87. doi: 10.1126/science.aac7368

Colledge, M., Snyder, E. M., Crozier, R. A., Soderling, J. A., Jin, Y., Langeberg, L. K., . . . Scott, J. D. (2003). Ubiquitination regulates PSD-95 degradation and AMPA receptor surface expression. *Neuron, 40*(3), 595-607.

Conaway, J. W., & Conaway, R. C. (1999). Transcription elongation and human disease. *Annu Rev Biochem, 68*, 301-319. doi: 10.1146/annurev.biochem.68.1.301

Conaway, R. C., Brower, C. S., & Conaway, J. W. (2002). Emerging roles of ubiquitin in transcription regulation. *Science, 296*(5571), 1254-1258. doi: 10.1126/science.1067466

Conaway, R. C., & Conaway, J. W. (2013). The Mediator complex and transcription elongation. *Biochim Biophys Acta, 1829*(1), 69-75. doi: 10.1016/j.bbagrm.2012.08.017

Conaway, R. C., Sato, S., Tomomori-Sato, C., Yao, T., & Conaway, J. W. (2005). The mammalian Mediator complex and its role in transcriptional regulation. *Trends Biochem Sci, 30*(5), 250-255. doi: 10.1016/j.tibs.2005.03.002

Costa-Mattioli, M., Gobert, D., Harding, H., Herdy, B., Azzi, M., Bruno, M., . . . Sonenberg, N. (2005). Translational control of hippocampal synaptic plasticity and memory by the eIF2alpha kinase GCN2. *Nature, 436*(7054), 1166-1173. doi: 10.1038/nature03897

Costa-Mattioli, M., Gobert, D., Stern, E., Gamache, K., Colina, R., Cuello, C., . . . Sonenberg, N. (2007). eIF2alpha phosphorylation bidirectionally regulates the

switch from short- to long-term synaptic plasticity and memory. *Cell, 129*(1), 195-206. doi: 10.1016/j.cell.2007.01.050

Costa-Mattioli, M., Sonenberg, N., & Richter, J. D. (2009). Translational regulatory mechanisms in synaptic plasticity and memory storage. *Prog Mol Biol Transl Sci, 90*, 293-311. doi: 10.1016/s1877-1173(09)90008-4

Crino, P., Khodakhah, K., Becker, K., Ginsberg, S., Hemby, S., & Eberwine, J. (1998). Presence and phosphorylation of transcription factors in developing dendrites. *Proc Natl Acad Sci U S A, 95*(5), 2313-2318.

D'Agata, V., & Cavallaro, S. (2003). Hippocampal gene expression profiles in passive avoidance conditioning. *Eur J Neurosci, 18*(10), 2835-2841.

Darnell, J. C., Van Driesche, S. J., Zhang, C., Hung, K. Y., Mele, A., Fraser, C. E., . . . Darnell, R. B. (2011). FMRP stalls ribosomal translocation on mRNAs linked to synaptic function and autism. *Cell, 146*(2), 247-261. doi: 10.1016/j.cell.2011.06.013

Davis, H. P., & Squire, L. R. (1984). Protein synthesis and memory: a review. *Psychol Bull, 96*(3), 518-559.

de Sousa Abreu, R., Penalva, L. O., Marcotte, E. M., & Vogel, C. (2009). Global signatures of protein and mRNA expression levels. *Mol Biosyst, 5*(12), 1512-1526. doi: 10.1039/b908315d

Debiec, J., LeDoux, J. E., & Nader, K. (2002). Cellular and systems reconsolidation in the hippocampus. *Neuron, 36*(3), 527-538.

Djakovic, S. N., Schwarz, L. A., Barylko, B., DeMartino, G. N., & Patrick, G. N. (2009). Regulation of the proteasome by neuronal activity and calcium/calmodulin-dependent protein kinase II. *J Biol Chem, 284*(39), 26655-26665. doi: 10.1074/jbc.M109.021956

Dobin, A., Davis, C. A., Schlesinger, F., Drenkow, J., Zaleski, C., Jha, S., . . . Gingeras, T. R. (2013). STAR: ultrafast universal RNA-seq aligner. *Bioinformatics, 29*(1), 15-21. doi: 10.1093/bioinformatics/bts635

Dotson, M. R., Yuan, C. X., Roeder, R. G., Myers, L. C., Gustafsson, C. M., Jiang, Y. W., . . . Asturias, F. J. (2000). Structural organization of yeast and mammalian mediator complexes. *Proc Natl Acad Sci U S A, 97*(26), 14307-14310. doi: 10.1073/pnas.260489497

Doyle, J. P., Dougherty, J. D., Heiman, M., Schmidt, E. F., Stevens, T. R., Ma, G., . . . Heintz, N. (2008). Application of a translational profiling approach for the comparative analysis of CNS cell types. *Cell, 135*(4), 749-762. doi: 10.1016/j.cell.2008.10.029

Drane, L., Ainsley, J. A., Mayford, M. R., & Reijmers, L. G. (2014). A transgenic mouse line for collecting ribosome-bound mRNA using the tetracycline transactivator system. *Front Mol Neurosci, 7*. doi: 10.3389/fnmol.2014.00082

Duvarci, S., & Nader, K. (2004). Characterization of fear memory reconsolidation. *J Neurosci, 24*(42), 9269-9275. doi: 10.1523/jneurosci.2971-04.2004

Duvarci, S., & Pare, D. (2014). Amygdala microcircuits controlling learned fear. *Neuron, 82*(5), 966-980. doi: 10.1016/j.neuron.2014.04.042

Eberwine, J., Belt, B., Kacharmina, J. E., & Miyashiro, K. (2002). Analysis of subcellularly localized mRNAs using in situ hybridization, mRNA amplification, and expression profiling. *Neurochem Res, 27*(10), 1065-1077.

Ehlers, M. D. (2003). Activity level controls postsynaptic composition and signaling via the ubiquitin-proteasome system. *Nat Neurosci, 6*(3), 231-242. doi: 10.1038/nn1013

Fang, Y., Gupta, V., Karra, R., Holdway, J. E., Kikuchi, K., & Poss, K. D. (2013). Translational profiling of cardiomyocytes identifies an early Jak1/Stat3 injury response required for zebrafish heart regeneration. *Proc Natl Acad Sci U S A, 110*(33), 13416-13421. doi: 10.1073/pnas.1309810110

Feng, Rebecca H. Mellor, Michael Bernstein, Cynthia Keller-Peck, Quyen T. Nguyen, Mia Wallace, . . . Sanes, a. J. R. (2000). Imaging Neuronal Subsets Neurotechnique.

Fioravante, D., & Byrne, J. H. (2011). Protein degradation and memory formation. *Brain Res Bull, 85*(1-2), 14-20. doi: 10.1016/j.brainresbull.2010.11.002

Flavell, S. W., & Greenberg, M. E. (2008). Signaling mechanisms linking neuronal activity to gene expression and plasticity of the nervous system. *Annu Rev Neurosci, 31*, 563-590. doi: 10.1146/annurev.neuro.31.060407.125631

Flexner, J. B., Flexner, L. B., & Stellar, E. (1963). Memory in mice as affected by intracerebral puromycin. *Science, 141*(3575), 57-59.

Fonseca, R., Vabulas, R. M., Hartl, F. U., Bonhoeffer, T., & Nagerl, U. V. (2006). A balance of protein synthesis and proteasome-dependent degradation determines the maintenance of LTP. *Neuron, 52*(2), 239-245. doi: 10.1016/j.neuron.2006.08.015

Glickman, M. H., & Ciechanover, A. (2002). The ubiquitin-proteasome proteolytic pathway: destruction for the sake of construction. *Physiol Rev, 82*(2), 373-428. doi: 10.1152/physrev.00027.2001

Gossen, M., & Bujard, H. (1992). Tight control of gene expression in mammalian cells by tetracycline-responsive promoters. *Proc Natl Acad Sci U S A, 89*(12), 5547-5551.

Guzowski, J. F. (2002). Insights into immediate-early gene function in hippocampal memory consolidation using antisense oligonucleotide and fluorescent imaging approaches. *Hippocampus, 12*(1), 86-104. doi: 10.1002/hipo.10010

Guzowski, J. F., McNaughton, B. L., Barnes, C. A., & Worley, P. F. (1999). Environment-specific expression of the immediate-early gene Arc in hippocampal neuronal ensembles. *Nat Neurosci, 2*(12), 1120-1124. doi: 10.1038/16046

Hegde, A. N., Goldberg, A. L., & Schwartz, J. H. (1993). Regulatory subunits of cAMP-dependent protein kinases are degraded after conjugation to ubiquitin: a molecular mechanism underlying long-term synaptic plasticity. *Proc Natl Acad Sci U S A, 90*(16), 7436-7440.

Hegde, A. N., Haynes, K. A., Bach, S. V., & Beckelman, B. C. (2014). Local ubiquitin-proteasome-mediated proteolysis and long-term synaptic plasticity. *Front Mol Neurosci, 7*. doi: 10.3389/fnmol.2014.00096

Heiman, M., Schaefer, A., Gong, S., Peterson, J. D., Day, M., Ramsey, K. E., . . . Heintz, N. (2008). A translational profiling approach for the molecular characterization of CNS cell types. *Cell, 135*(4), 738-748. doi: 10.1016/j.cell.2008.10.028

Heller, M. J. (2002). DNA microarray technology: devices, systems, and applications. *Annu Rev Biomed Eng, 4*, 129-153. doi: 10.1146/annurev.bioeng.4.020702.153438

Hernandez, P. J., & Abel, T. (2008). The role of protein synthesis in memory consolidation: progress amid decades of debate. *Neurobiol Learn Mem, 89*(3), 293-311. doi: 10.1016/j.nlm.2007.09.010

Hershko, A., & Ciechanover, A. (1998). The ubiquitin system. *Annu Rev Biochem, 67*, 425-479. doi: 10.1146/annurev.biochem.67.1.425

Holt, C. E., & Schuman, E. M. (2013). The central dogma decentralized: new perspectives on RNA function and local translation in neurons. *Neuron, 80*(3), 648-657. doi: 10.1016/j.neuron.2013.10.036

Huang, Y., Ainsley, J. A., Reijmers, L. G., & Jackson, F. R. (2013). Translational profiling of clock cells reveals circadianly synchronized protein synthesis. *PLoS Biol, 11*(11), e1001703. doi: 10.1371/journal.pbio.1001703

Ifrim, M. F., Williams, K. R., & Bassell, G. J. (2015). Single-Molecule Imaging of PSD-95 mRNA Translation in Dendrites and Its Dysregulation in a Mouse Model of Fragile X Syndrome. *J Neurosci, 35*(18), 7116-7130. doi: 10.1523/JNEUROSCI.2802-14.2015

Imasaki, T., Calero, G., Cai, G., Tsai, K. L., Yamada, K., Cardelli, F., . . . Takagi, Y. (2011). Architecture of the Mediator head module. *Nature, 475*(7355), 240-243. doi: 10.1038/nature10162

Jarome, T. J., & Helmstetter, F. J. (2014). Protein degradation and protein synthesis in long-term memory formation. *Front Mol Neurosci, 7*, 61. doi: 10.3389/fnmol.2014.00061

Job, C., & Eberwine, J. (2001). Identification of sites for exponential translation in living dendrites. *Proc Natl Acad Sci U S A, 98*(23), 13037-13042. doi: 10.1073/pnas.231485698

Kang, H., & Schuman, E. M. (1996). A requirement for local protein synthesis in neurotrophin-induced hippocampal synaptic plasticity. *Science, 273*(5280), 1402-1406.

Kao, D. I., Aldridge, G. M., Weiler, I. J., & Greenough, W. T. (2010). Altered mRNA transport, docking, and protein translation in neurons lacking fragile X mental retardation protein. *Proc Natl Acad Sci U S A, 107*(35), 15601-15606. doi: 10.1073/pnas.1010564107

Karpova, A., Mikhaylova, M., Thomas, U., Knopfel, T., & Behnisch, T. (2006). Involvement of protein synthesis and degradation in long-term potentiation of Schaffer collateral CA1 synapses. *J Neurosci, 26*(18), 4949-4955. doi: 10.1523/jneurosci.4573-05.2006

Kelleher, R. J., 3rd, Govindarajan, A., Jung, H. Y., Kang, H., & Tonegawa, S. (2004). Translational control by MAPK signaling in long-term synaptic plasticity and memory. *Cell, 116*(3), 467-479.

Krebs, S., Fischaleck, M., & Blum, H. (2009). A simple and loss-free method to remove TRIzol contaminations from minute RNA samples. *Anal Biochem, 387*(1), 136-138. doi: 10.1016/j.ab.2008.12.020

Lariviere, L., Geiger, S., Hoeppner, S., Rother, S., Strasser, K., & Cramer, P. (2006). Structure and TBP binding of the Mediator head subcomplex Med8-Med18-Med20. *Nat Struct Mol Biol, 13*(10), 895-901. doi: 10.1038/nsmb1143

Lee, S. H., Choi, J. H., Lee, N., Lee, H. R., Kim, J. I., Yu, N. K., . . . Kaang, B. K. (2008). Synaptic protein degradation underlies destabilization of retrieved fear memory. *Science, 319*(5867), 1253-1256. doi: 10.1126/science.1150541

Lein, E. S., Hawrylycz, M. J., Ao, N., Ayres, M., Bensinger, A., Bernard, A., . . . Jones, A. R. (2007). Genome-wide atlas of gene expression in the adult mouse brain. *Nature, 445*(7124), 168-176. doi: 10.1038/nature05453

Liu, J., Krautzberger, A. M., Sui, S. H., Hofmann, O. M., Chen, Y., Baetscher, M., . . . McMahon, A. P. (2014). Cell-specific translational profiling in acute kidney injury. *J Clin Invest, 124*(3), 1242-1254. doi: 10.1172/jci72126

Lopez-Salon, M., Alonso, M., Vianna, M. R., Viola, H., Mello e Souza, T., Izquierdo, I., . . . Medina, J. H. (2001). The ubiquitin-proteasome cascade is required for mammalian long-term memory formation. *Eur J Neurosci, 14*(11), 1820-1826.

Maier, T., Guell, M., & Serrano, L. (2009). Correlation of mRNA and protein in complex biological samples. *FEBS Lett, 583*(24), 3966-3973. doi: 10.1016/j.febslet.2009.10.036

Malik, S., & Roeder, R. G. (2005). Dynamic regulation of pol II transcription by the mammalian Mediator complex. *Trends Biochem Sci, 30*(5), 256-263. doi: 10.1016/j.tibs.2005.03.009

Malik, S., & Roeder, R. G. (2010). The metazoan Mediator co-activator complex as an integrative hub for transcriptional regulation. *Nat Rev Genet, 11*(11), 761-772. doi: 10.1038/nrg2901

Marchenko, N. D., Hanel, W., Li, D., Becker, K., Reich, N., & Moll, U. M. (2010). Stress-mediated nuclear stabilization of p53 is regulated by ubiquitination and importin-alpha3 binding. *Cell Death Differ, 17*(2), 255-267. doi: 10.1038/cdd.2009.173

Martin, K. C., Barad, M., & Kandel, E. R. (2000). Local protein synthesis and its role in synapse-specific plasticity. *Curr Opin Neurobiol, 10*(5), 587-592.

Martin, K. C., Casadio, A., Zhu, H., Yaping, E., Rose, J. C., Chen, M., . . . Kandel, E. R. (1997). Synapse-specific, long-term facilitation of aplysia sensory to motor synapses: a function for local protein synthesis in memory storage. *Cell, 91*(7), 927-938.

Matsuo, N., Reijmers, L., & Mayford, M. (2008). Spine-type-specific recruitment of newly synthesized AMPA receptors with learning. *Science, 319*(5866), 1104-1107. doi: 10.1126/science.1149967

Mayford, M., Bach, M. E., Huang, Y. Y., Wang, L., Hawkins, R. D., & Kandel, E. R. (1996). Control of memory formation through regulated expression of a CaMKII transgene. *Science, 274*(5293), 1678-1683.

Mayford, M., Baranes, D., Podsypanina, K., & Kandel, E. R. (1996). The 3'-untranslated region of CaMKII alpha is a cis-acting signal for the localization and translation of mRNA in dendrites. *Proc Natl Acad Sci U S A, 93*(23), 13250-13255.

Merlo, E., & Romano, A. (2007). Long-term memory consolidation depends on proteasome activity in the crab Chasmagnathus. *Neuroscience, 147*(1), 46-52.

Metzker, M. L. (2010). Sequencing technologies - the next generation. *Nat Rev Genet, 11*(1), 31-46. doi: 10.1038/nrg2626

Miller, S., Coats, J. K., Yasuda, M., Jones, Y., Martone, M. E., & Mayford, a. M. (2002). Disruption of Dendritic Translation of CaMKII Impairs Stabilization of Synaptic Plasticity and Memory Consolidation. *Neuron, 36*, 507-519.

Moccia, R., Chen, D., Lyles, V., Kapuya, E., E, Y., Kalachikov, S., . . . Martin, K. C. (2003). An unbiased cDNA library prepared from isolated Aplysia sensory neuron processes is enriched for cytoskeletal and translational mRNAs. *J Neurosci, 23*(28), 9409-9417.

Mueller, O., Lightfoot, S., & Schroeder, A. (2004). RNA Integrity Number (RIN) - Standardization of RNA Quality Control. *Agilent Application Note, Publication 5989-1165EN*, 1-8.

Myers, L. C., & Kornberg, R. D. (2000). Mediator of transcriptional regulation. [Review]. *Annu Rev Biochem, 69*, 729-749. doi: 10.1146/annurev.biochem.69.1.729

Nader, K., Schafe, G. E., & Le Doux, J. E. (2000). Fear memories require protein synthesis in the amygdala for reconsolidation after retrieval. *Nature, 406*(6797), 722-726. doi: 10.1038/35021052

Napoli, C., Sessa, M., Infante, T., & Casamassimi, A. (2012). Unraveling framework of the ancestral Mediator complex in human diseases. *Biochimie, 94*(3), 579-587. doi: 10.1016/j.biochi.2011.09.016

Niere, F., Wilkerson, J. R., & Huber, K. M. (2012). Evidence for a fragile X mental retardation protein-mediated translational switch in metabotropic glutamate receptor-triggered Arc translation and long-term depression. *J Neurosci, 32*(17), 5924-5936. doi: 10.1523/jneurosci.4650-11.2012

O'Sullivan, N. C., McGettigan, P. A., Sheridan, G. K., Pickering, M., Conboy, L., O'Connor, J. J., . . . Murphy, K. J. (2007). Temporal change in gene expression in the rat dentate gyrus following passive avoidance learning. *J Neurochem, 101*(4), 1085-1098. doi: 10.1111/j.1471-4159.2006.04418.x

Okaty, B. W., Sugino, K., & Nelson, S. B. (2011). Cell type-specific transcriptomics in the brain. *J Neurosci, 31*(19), 6939-6943. doi: 10.1523/JNEUROSCI.0626-11.2011

Okumura, F., Matsuzaki, M., Nakatsukasa, K., & Kamura, T. (2012). The Role of Elongin BC-Containing Ubiquitin Ligases. *Front Oncol, 2*, 10. doi: 10.3389/fonc.2012.00010

Okuno, H. (2011). Regulation and function of immediate-early genes in the brain: beyond neuronal activity markers. *Neurosci Res, 69*(3), 175-186. doi: 10.1016/j.neures.2010.12.007

Ostroff, L. E., Fiala, J. C., Allwardt, B., & Harris, K. M. (2002). Polyribosomes redistribute from dendritic shafts into spines with enlarged synapses during LTP in developing rat hippocampal slices. *Neuron, 35*(3), 535-545.

Ouyang, Y., Rosenstein, A., Kreiman, G., Schuman, E. M., & Kennedy, M. B. (1999). Tetanic stimulation leads to increased accumulation of Ca(2+)/calmodulin-dependent protein kinase II via dendritic protein synthesis in hippocampal neurons. *J Neurosci, 19*(18), 7823-7833.

Patrick, G. N., Bingol, B., Weld, H. A., & Schuman, E. M. (2003). Ubiquitin-mediated proteasome activity is required for agonist-induced endocytosis of GluRs. *Curr Biol, 13*(23), 2073-2081.

Pavlopoulos, E., Trifilieff, P., Chevaleyre, V., Fioriti, L., Zairis, S., Pagano, A., . . . Kandel, E. R. (2011). Neuralized1 activates CPEB3: a function for nonproteolytic ubiquitin in synaptic plasticity and memory storage. *Cell, 147*(6), 1369-1383. doi: 10.1016/j.cell.2011.09.056

Petroski, M. D., & Deshaies, R. J. (2005). Function and regulation of cullin-RING ubiquitin ligases. *Nat Rev Mol Cell Biol, 6*(1), 9-20. doi: 10.1038/nrm1547

Poon, M. M., Choi, S. H., Jamieson, C. A., Geschwind, D. H., & Martin, K. C. (2006). Identification of process-localized mRNAs from cultured rodent hippocampal neurons. *J Neurosci, 26*(51), 13390-13399. doi: 10.1523/jneurosci.3432-06.2006

Puthanveettil, S. V., Antonov, I., Kalachikov, S., Rajasethupathy, P., Choi, Y. B., Kohn, A. B., . . . Kandel, E. R. (2013). A strategy to capture and characterize the synaptic transcriptome. *Proc Natl Acad Sci U S A, 110*(18), 7464-7469. doi: 10.1073/pnas.1304422110

Rao, A., & Steward, O. (1991). Evidence that protein constituents of postsynaptic membrane specializations are locally synthesized: analysis of proteins synthesized within synaptosomes. *J Neurosci, 11*(9), 2881-2895.

Reijmers, L. G., Perkins, B. L., Matsuo, N., & Mayford, M. (2007). Localization of a stable neural correlate of associative memory. *Science, 317*(5842), 1230-1233. doi: 10.1126/science.1143839

Richter, J. D., & Coller, J. (2015). Pausing on Polyribosomes: Make Way for Elongation in Translational Control. *Cell, 163*(2), 292-300. doi: 10.1016/j.cell.2015.09.041

Santini, E., Ge, H., Ren, K., Pena de Ortiz, S., & Quirk, G. J. (2004). Consolidation of fear extinction requires protein synthesis in the medial prefrontal cortex. *J Neurosci, 24*(25), 5704-5710. doi: 10.1523/jneurosci.0786-04.2004

Sanz, E., Yang, L., Su, T., Morris, D. R., McKnight, G. S., & Amieux, P. S. (2009). Cell-type-specific isolation of ribosome-associated mRNA from complex tissues. *Proc Natl Acad Sci U S A, 106*(33), 13939-13944. doi: 10.1073/pnas.0907143106

Schafe, G. E., Nader, K., Blair, H. T., & LeDoux, J. E. (2001). Memory consolidation of Pavlovian fear conditioning: a cellular and molecular perspective. *Trends Neurosci, 24*(9), 540-546.

Schiller, D., Monfils, M. H., Raio, C. M., Johnson, D. C., Ledoux, J. E., & Phelps, E. A. (2010). Preventing the return of fear in humans using reconsolidation update mechanisms. *Nature, 463*(7277), 49-53. doi: 10.1038/nature08637

Schmidt, E. F., Warner-Schmidt, J. L., Otopalik, B. G., Pickett, S. B., Greengard, P., & Heintz, N. (2012). Identification of the cortical neurons that mediate antidepressant responses. *Cell, 149*(5), 1152-1163. doi: 10.1016/j.cell.2012.03.038

Schonig, K., Bujard, H., & Gossen, M. (2010). The power of reversibility regulating gene activities via tetracycline-controlled transcription. *Methods Enzymol, 477*, 429-453. doi: 10.1016/S0076-6879(10)77022-1

Schwanhausser, B., Busse, D., Li, N., Dittmar, G., Schuchhardt, J., Wolf, J., . . . Selbach, M. (2011). Global quantification of mammalian gene expression control. *Nature, 473*(7347), 337-342. doi: 10.1038/nature10098

Smith, W. B., Starck, S. R., Roberts, R. W., & Schuman, E. M. (2005). Dopaminergic stimulation of local protein synthesis enhances surface expression of GluR1 and synaptic transmission in hippocampal neurons. *Neuron, 45*(5), 765-779. doi: 10.1016/j.neuron.2005.01.015

Spahr, H., Samuelsen, C. O., Baraznenok, V., Ernest, I., Huylebroeck, D., Remacle, J. E., . . . Gustafsson, C. M. (2001). Analysis of Schizosaccharomyces pombe mediator reveals a set of essential subunits conserved between yeast and metazoan cells. *Proc Natl Acad Sci U S A, 98*(21), 11985-11990. doi: 10.1073/pnas.211253898

Steward, O., & Levy, W. B. (1982). Preferential localization of polyribosomes under the base of dendritic spines in granule cells of the dentate gyrus. *J Neurosci, 2*(3), 284-291.

Steward, O., Wallace, C. S., Lyford, G. L., & Worley, P. F. (1998). Synaptic activation causes the mRNA for the IEG Arc to localize selectively near activated postsynaptic sites on dendrites. *Neuron, 21*(4), 741-751.

Takagi, Y., Calero, G., Komori, H., Brown, J. A., Ehrensberger, A. H., Hudmon, A., . . . Kornberg, R. D. (2006). Head module control of mediator interactions. *Mol Cell, 23*(3), 355-364. doi: 10.1016/j.molcel.2006.06.007

Tayler, K. K., Tanaka, K. Z., Reijmers, L. G., & Wiltgen, B. J. (2013). Reactivation of neural ensembles during the retrieval of recent and remote memory. *Curr Biol, 23*(2), 99-106. doi: 10.1016/j.cub.2012.11.019

Thomas, A., Lee, P. J., Dalton, J. E., Nomie, K. J., Stoica, L., Costa-Mattioli, M., . . . Dierick, H. A. (2012). A versatile method for cell-specific profiling of translated mRNAs in Drosophila. *PLoS One, 7*(7), e40276. doi: 10.1371/journal.pone.0040276

Torre, E. R., & Steward, O. (1992). Demonstration of local protein synthesis within dendrites using a new cell culture system that permits the isolation of living axons and dendrites from their cell bodies. *J Neurosci, 12*(3), 762-772.

Tryon, R. C., Pisat, N., Johnson, S. L., & Dougherty, J. D. (2013). Development of translating ribosome affinity purification for zebrafish. *Genesis, 51*(3), 187-192. doi: 10.1002/dvg.22363

Tsai, K. L., Tomomori-Sato, C., Sato, S., Conaway, R. C., Conaway, J. W., & Asturias, F. J. (2014). Subunit architecture and functional modular rearrangements of the transcriptional mediator complex. *Cell, 157*(6), 1430-1444. doi: 10.1016/j.cell.2014.05.015

Upadhya, S. C., Smith, T. K., & Hegde, A. N. (2004). Ubiquitin-proteasome-mediated CREB repressor degradation during induction of long-term facilitation. *J Neurochem, 91*(1), 210-219. doi: 10.1111/j.1471-4159.2004.02707.x

Wang, Z., Gerstein, M., & Snyder, M. (2009). RNA-Seq: a revolutionary tool for transcriptomics. *Nature Reviews Genetics, 10*(1), 57-63.

Weiler, I. J., & Greenough, W. T. (1991). Potassium ion stimulation triggers protein translation in synaptoneurosomal polyribosomes. *Mol Cell Neurosci, 2*(4), 305-314.

Weiler, I. J., & Greenough, W. T. (1993). Metabotropic glutamate receptors trigger postsynaptic protein synthesis. *Proc Natl Acad Sci U S A, 90*(15), 7168-7171.

Wilkins, B. J., Gong, W., & Pack, M. (2014). A novel keratin18 promoter that drives reporter gene expression in the intrahepatic and extrahepatic biliary system allows isolation of cell-type specific transcripts from zebrafish liver. *Gene Expr Patterns, 14*(2), 62-68. doi: 10.1016/j.gep.2013.12.002

Zhou, P., Zhang, Y., Ma, Q., Gu, F., Day, D. S., He, A., . . . Pu, W. T. (2013). Interrogating translational efficiency and lineage-specific transcriptomes using ribosome affinity purification. *Proc Natl Acad Sci U S A, 110*(38), 15395-15400. doi: 10.1073/pnas.1304124110

Zuccotti, P., & Modelska, A. (2016). Studying the Translatome with Polysome Profiling. *Methods Mol Biol, 1358*, 59-69. doi: 10.1007/978-1-4939-3067-8_4

Zukin, R. S., Richter, J. D., & Bagni, C. (2009). Signals, synapses, and synthesis: how new proteins control plasticity. *Front Neural Circuits, 3*, 14. doi: 10.3389/neuro.04.014.2009